弱束缚原子核^{6}Li引起的反应机制和核结构研究

张高龙
zgl@buaa.edu.cn

北京航空航天大学

2022年10月28日

内容

- 弱束缚原子核熔合反应
- 实验方法
- 开展的研究
- 总结

弱束缚原子核熔合反应

^{6}Li, ^{7}Li, ^{9}Be

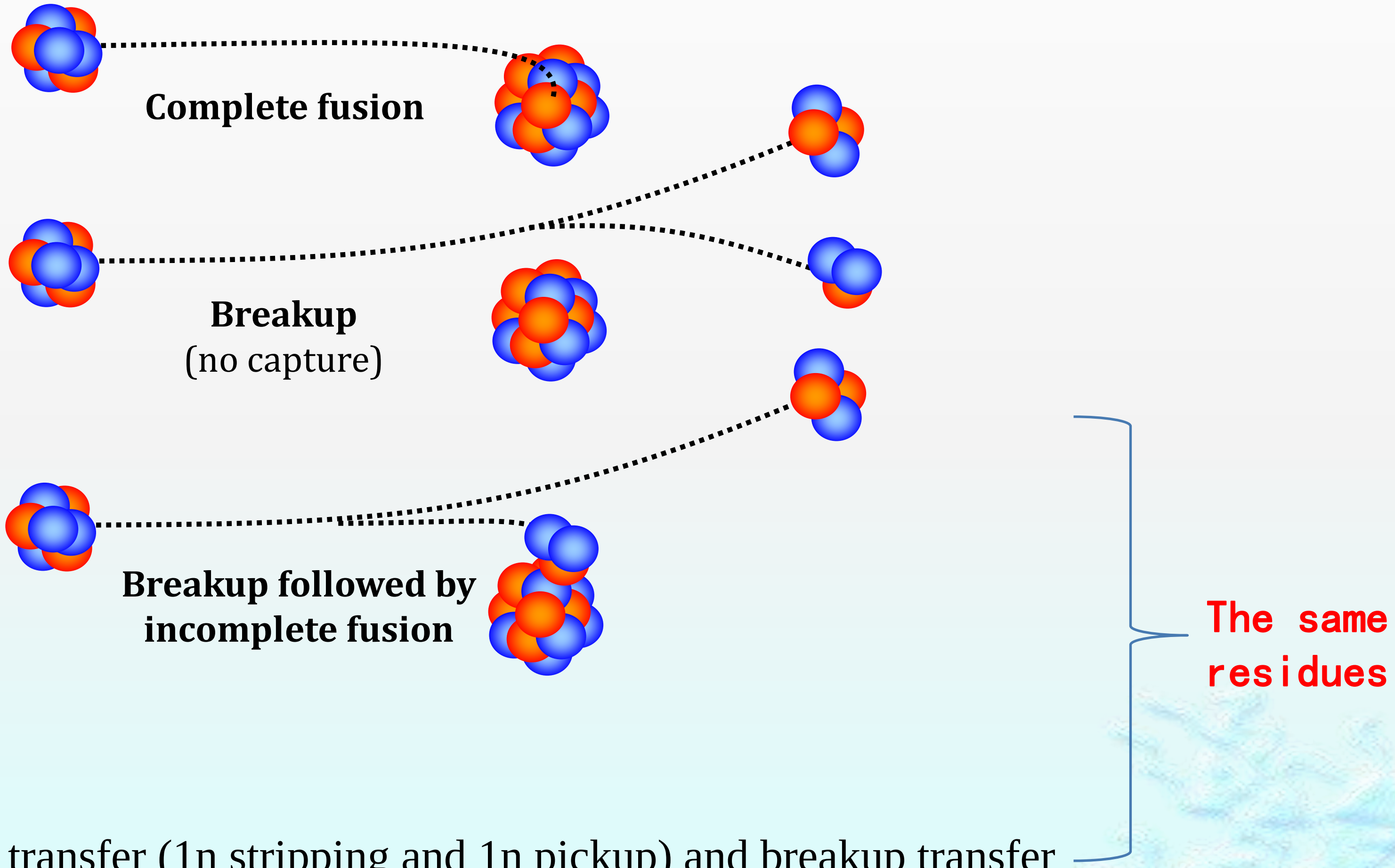

Transfer: direct transfer (1n stripping and 1n pickup) and breakup transfer

实验方法

- γ射线测量方法
  1、在线γ射线测量方法
  2、离线γ射线测量方法
- 带电粒子测量方法
  1、在线带电粒子测量方法
  2、离线带电粒子测量方法
- 带电粒子-γ射线符合测量方法

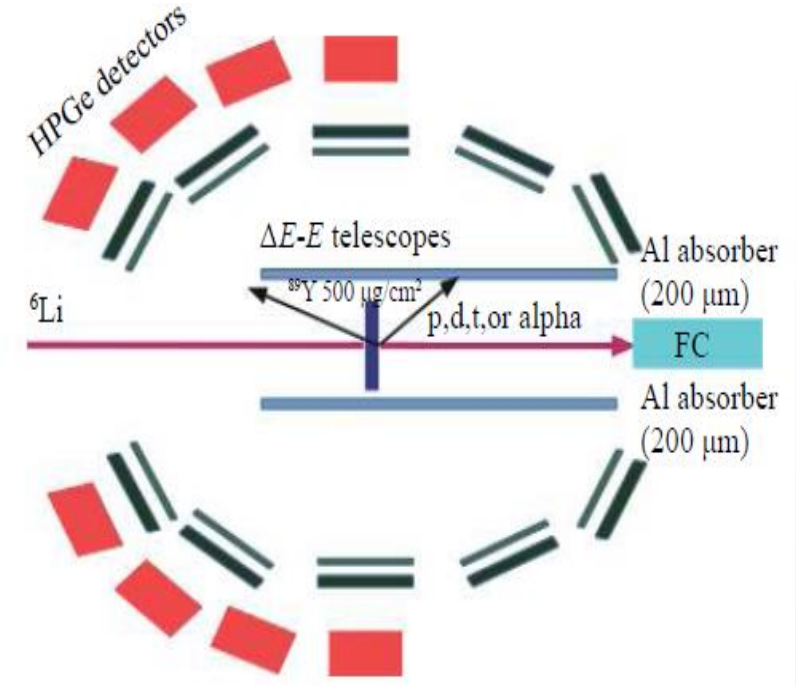

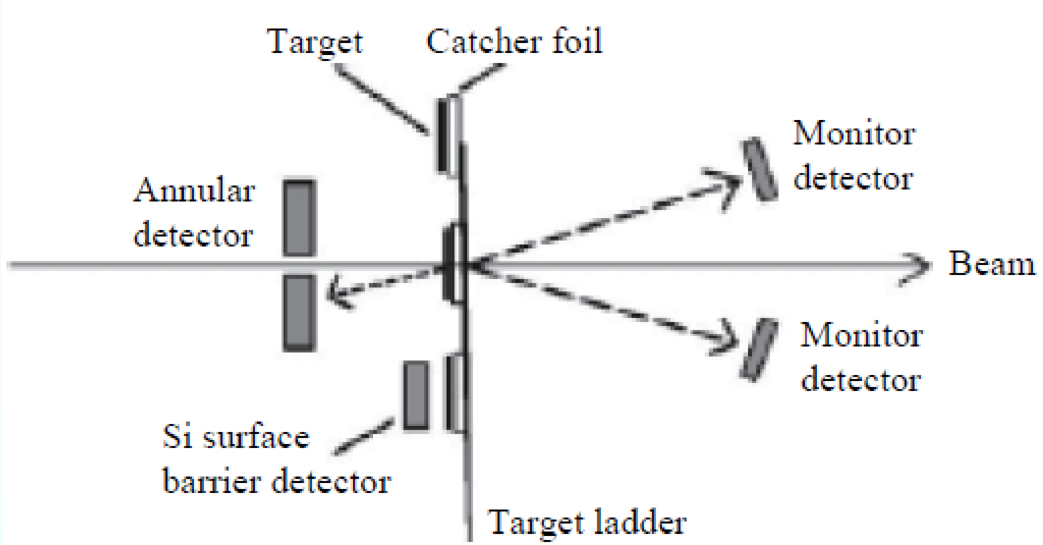

苏学斗等，原子核物理评论87(2) (2020) 120

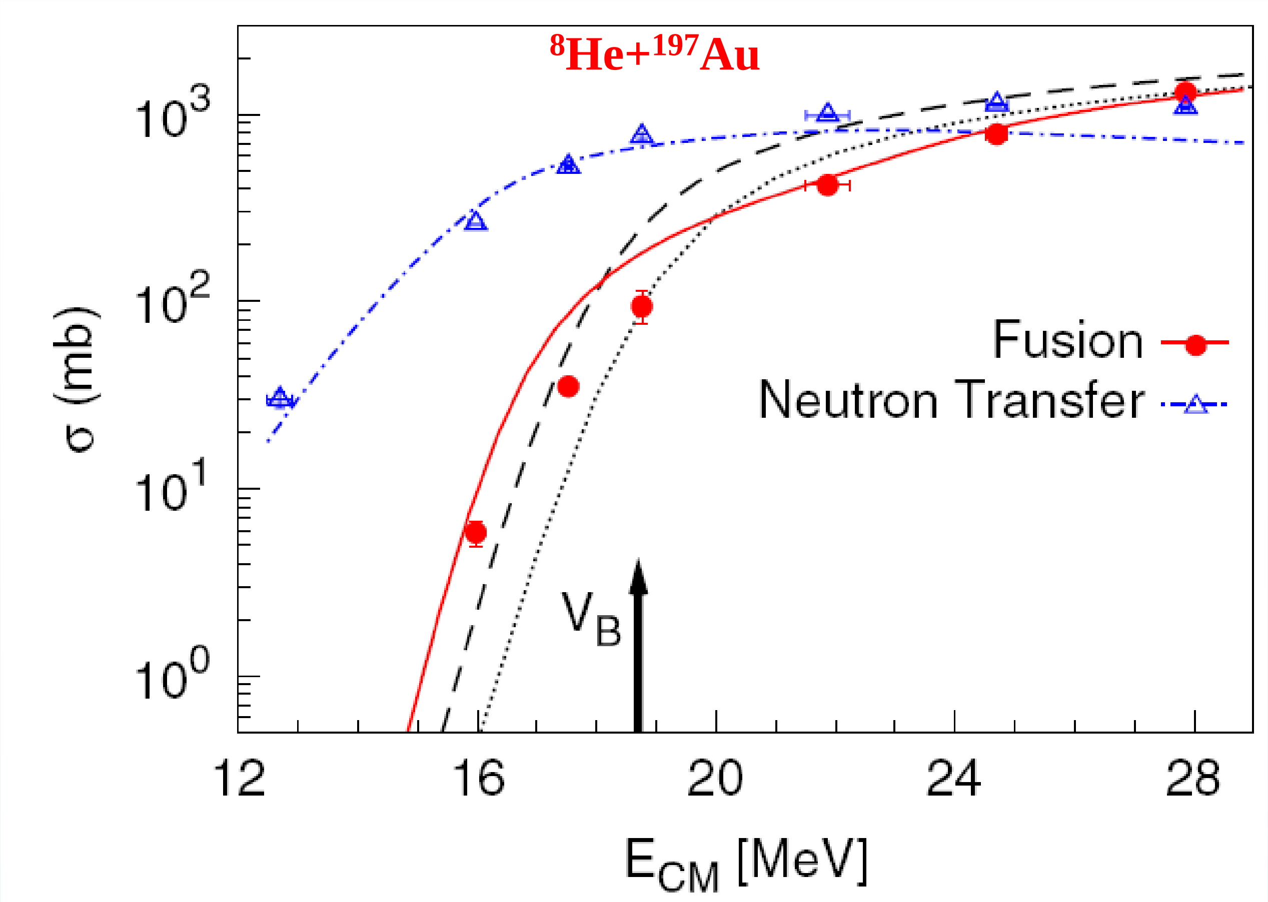

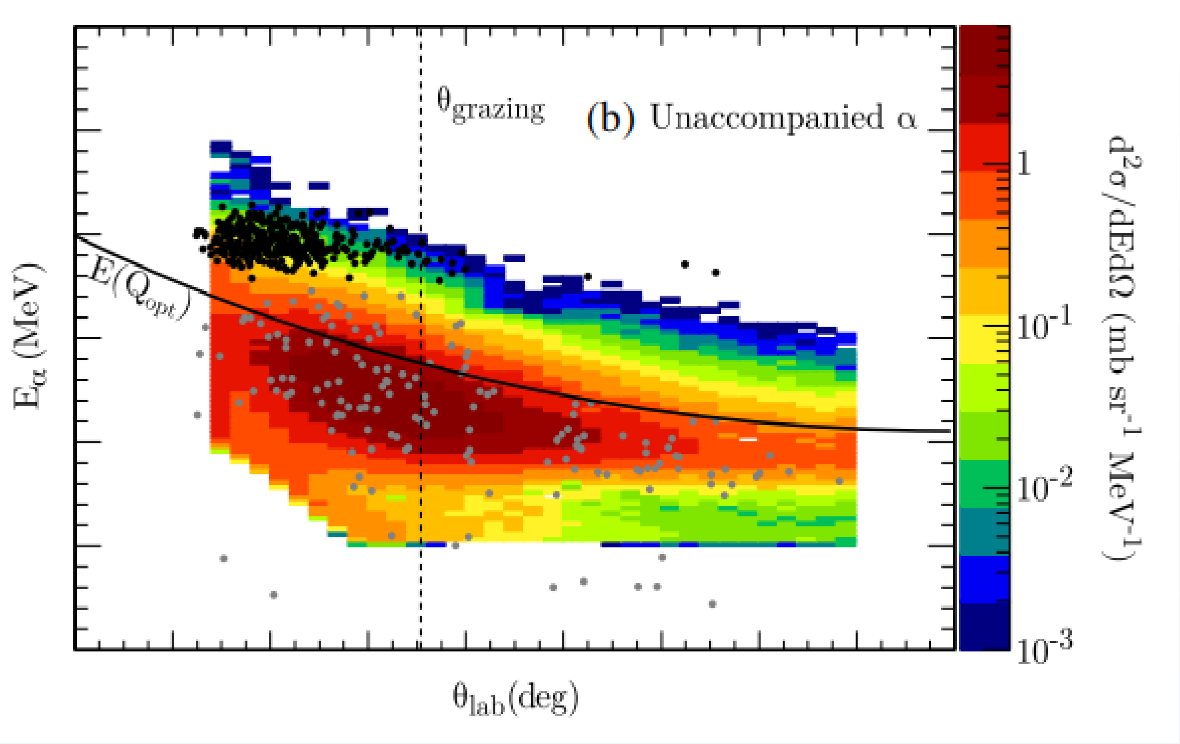

^{7}Li+^{209}Bi无伴随α粒子的双微分截面

A. Lemasson *et al.*, Phys. Rev. Lett. 103, 232701 (2009).

K. J. Cook, E. C. Simpson, L. T. Bezzina, et al. Phys. Rev. Lett. 122, 102501 (2019).

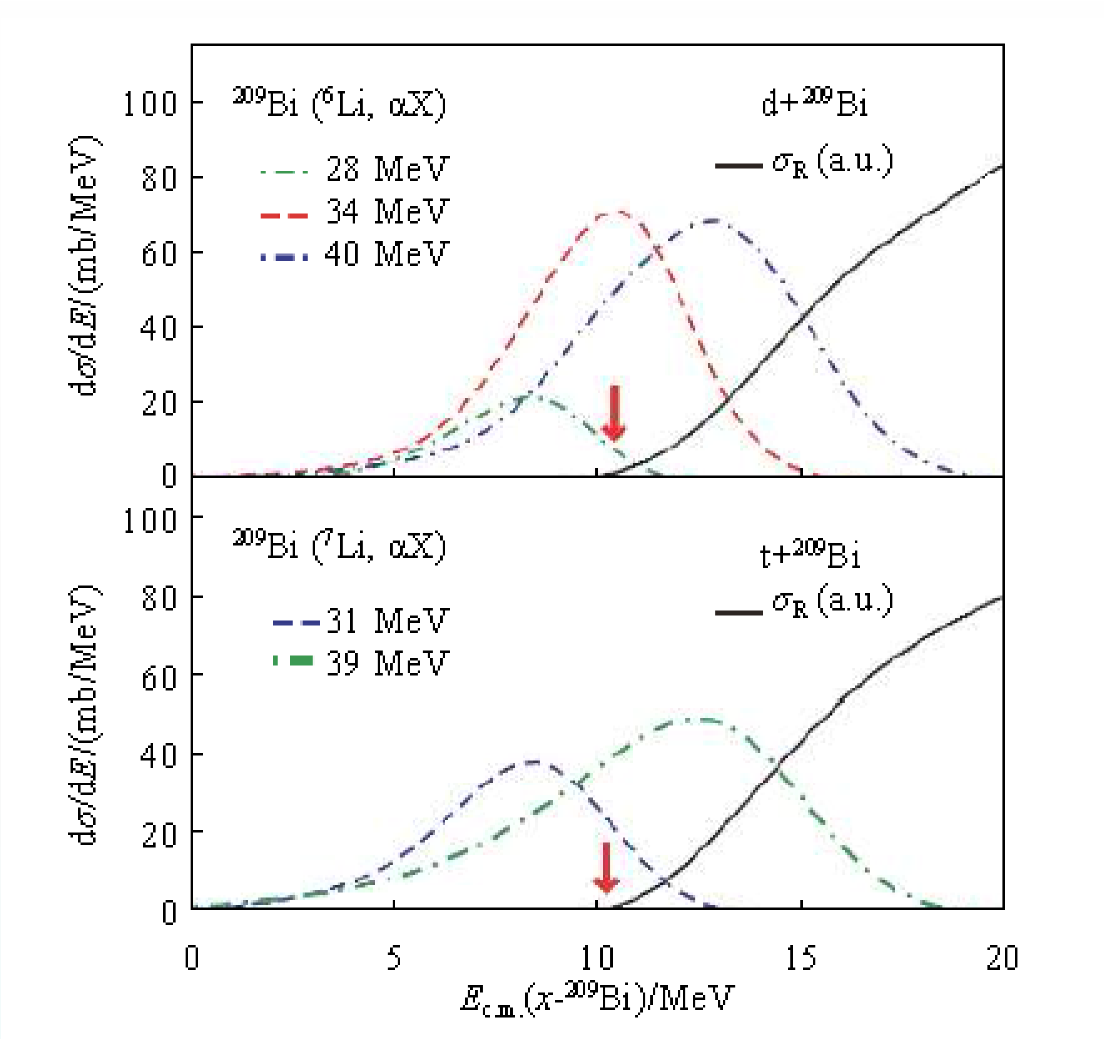

^{209}Bi(^{6,7}Li, αX) 反应截面随能量的分布

JIN L, MORO A M. Phys Rev Lett, 2019, 122: 042503.

- 两体反应过程：截面随着入射能量的减小而逐渐减小，到库仑位垒附近截面几乎为零；
- 三体反应过程：即使入射能量比库仑位垒小很多，反应截面依然很大；
- 特洛伊木马方法：炮弹^{6,7}Li将d、t集团带进了库仑位垒里；
- 实验上观察到的大的α产额，说明完全熔合截面压低主要是由NEB过程的反应机制引起的。

■ Coincident measurements of gamma with charged particles

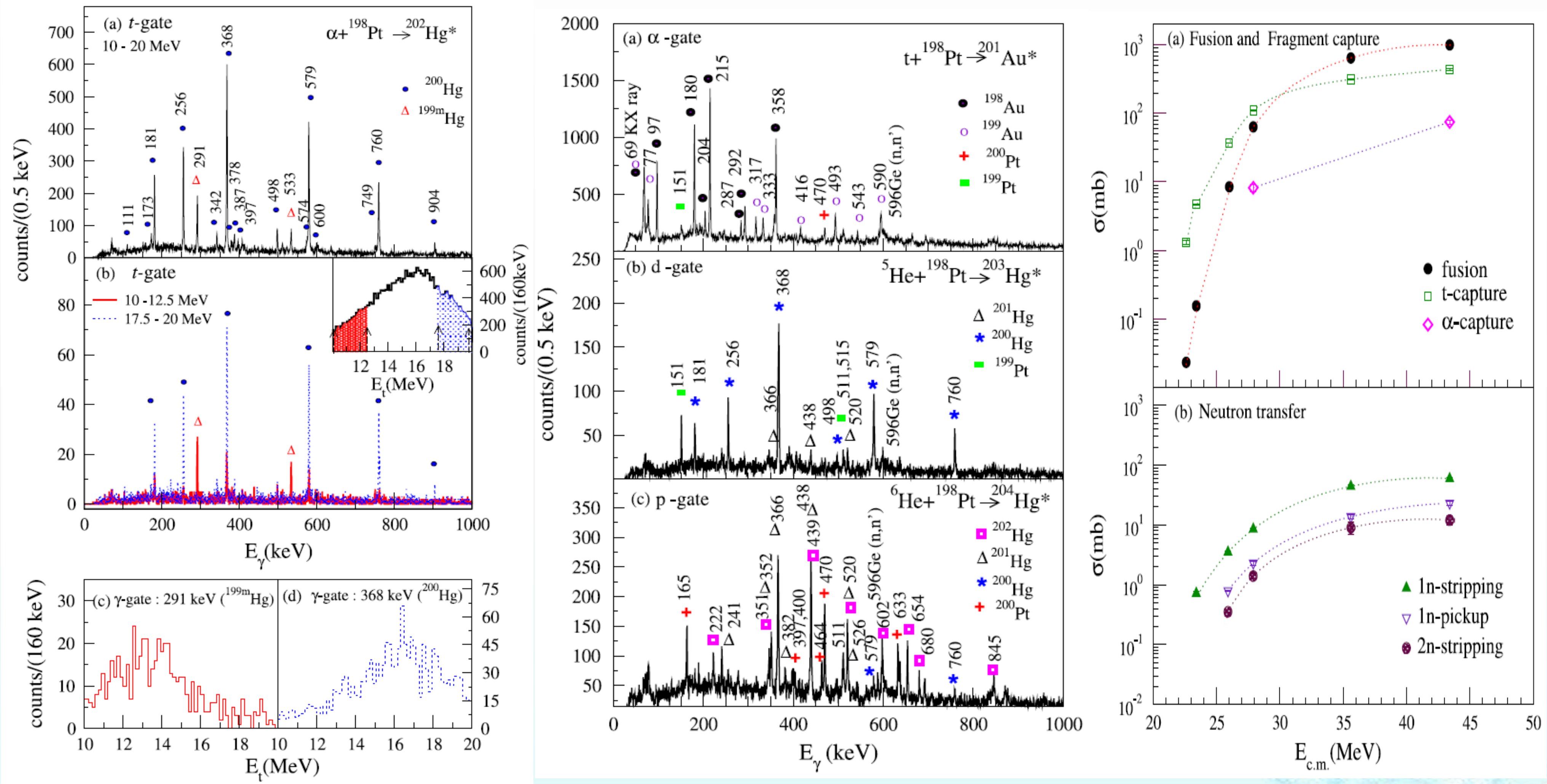

The α-capture cross sections were measured employing in-beam γ method by exclusive measurements of prompt γ-rays from the heavy-residues with various light charged particles (α, t, d and p).

A. Shrivastava *et al.*, Phys. Lett. B 718 (2013) 931.

实验研究

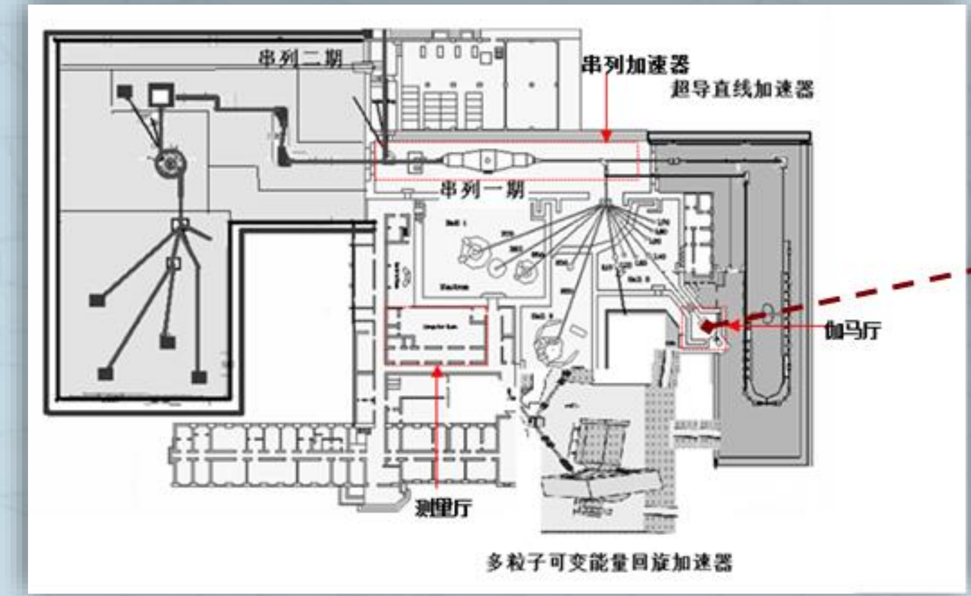

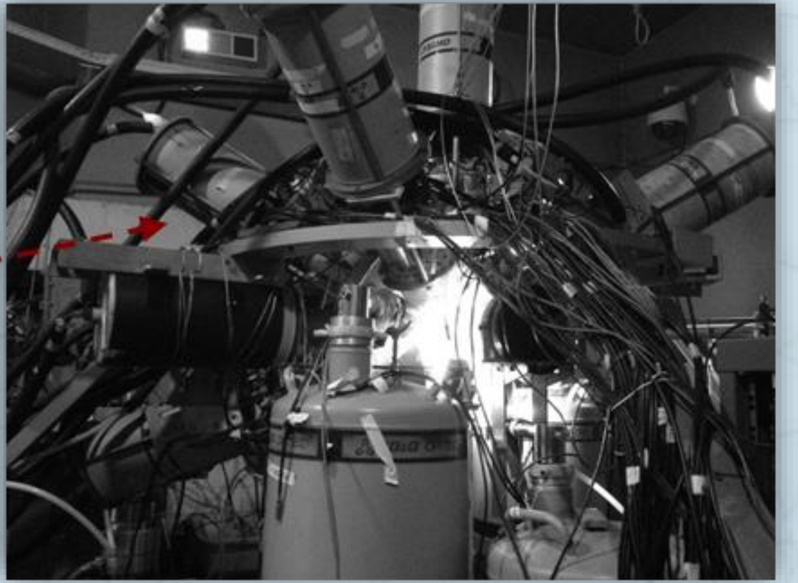

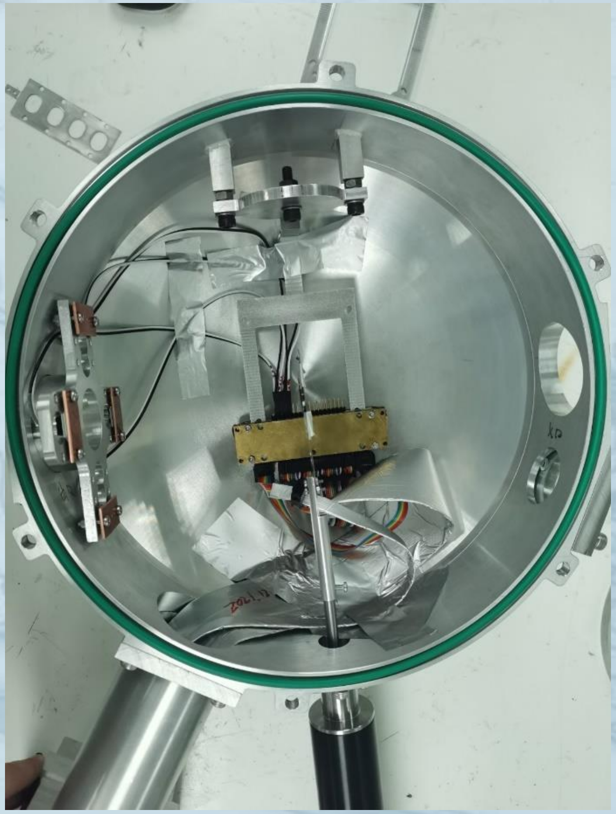

$^{6}Li+^{94}Zr$

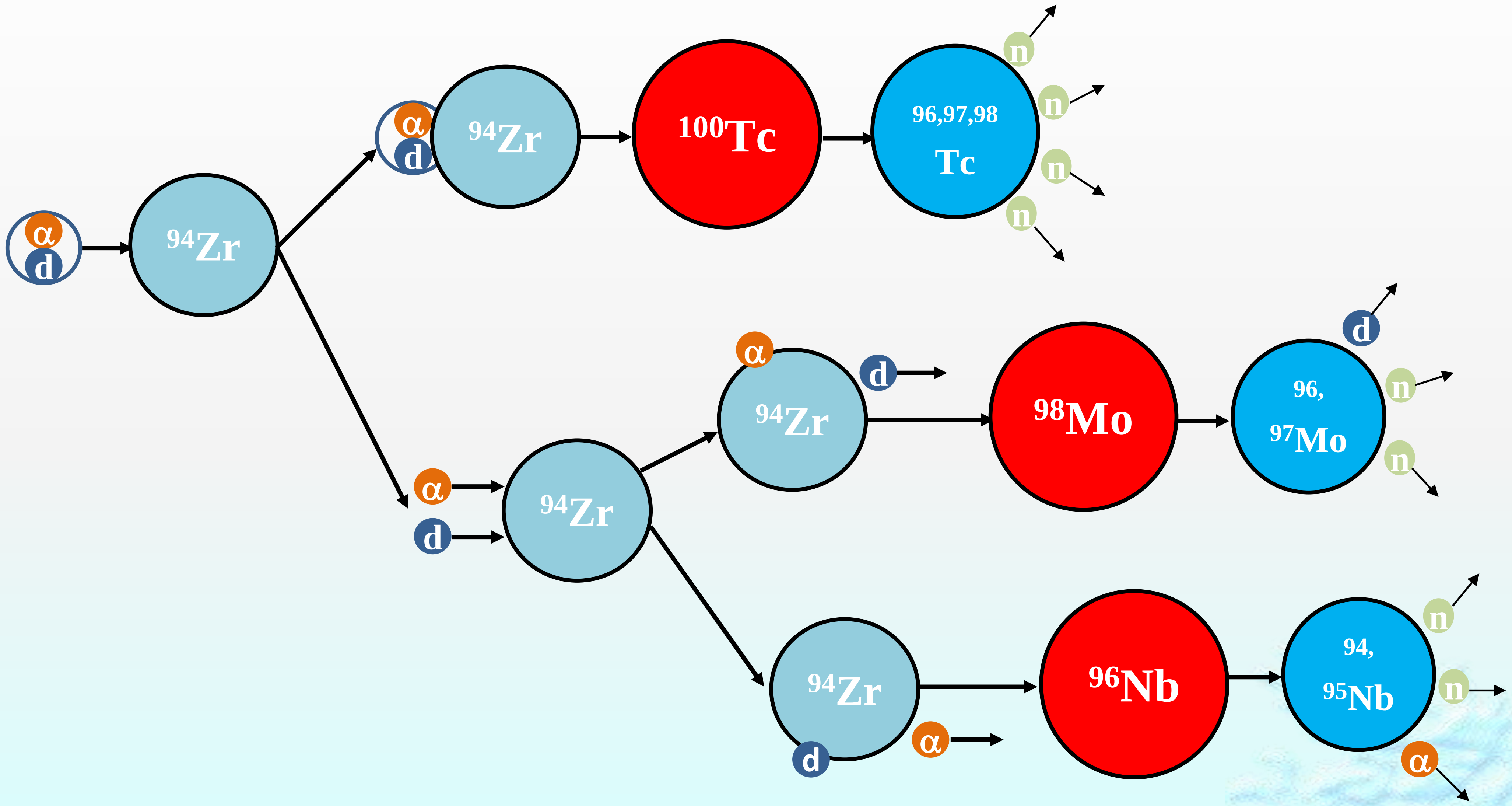

$^{6}Li+^{94}Zr$系统熔合反应示意图

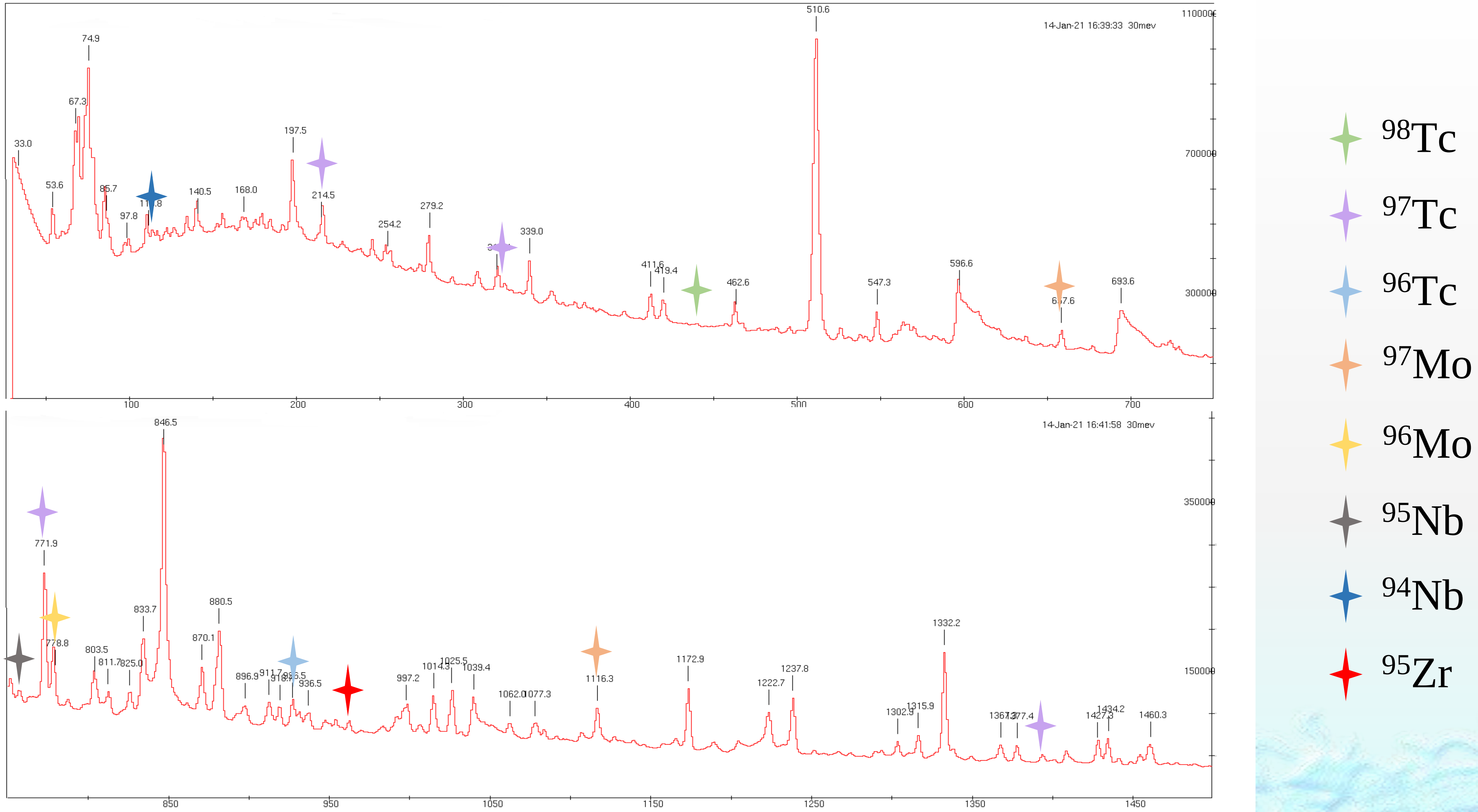

30MeV^{6}Li时的γ射线单谱

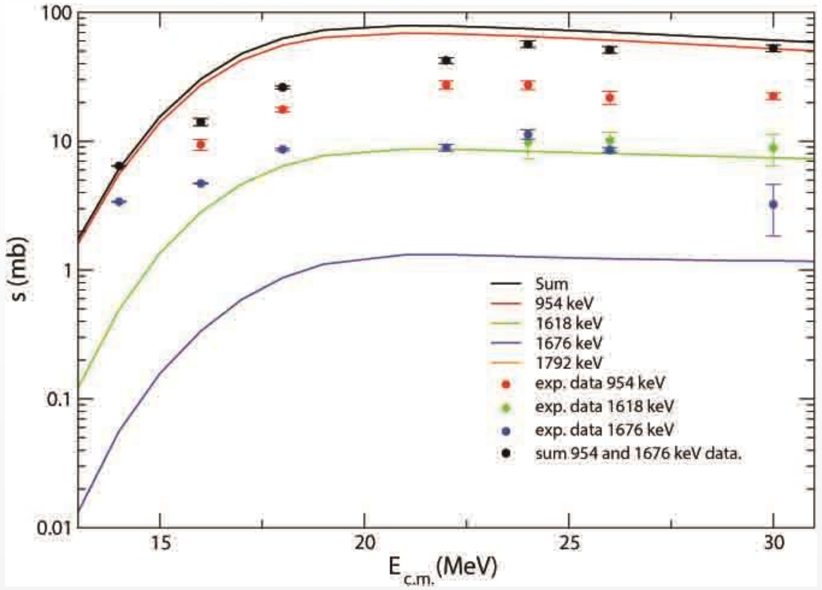

^{6}Li+^{94}Zr1n转移反应截面与耦合反应道计算结果比较

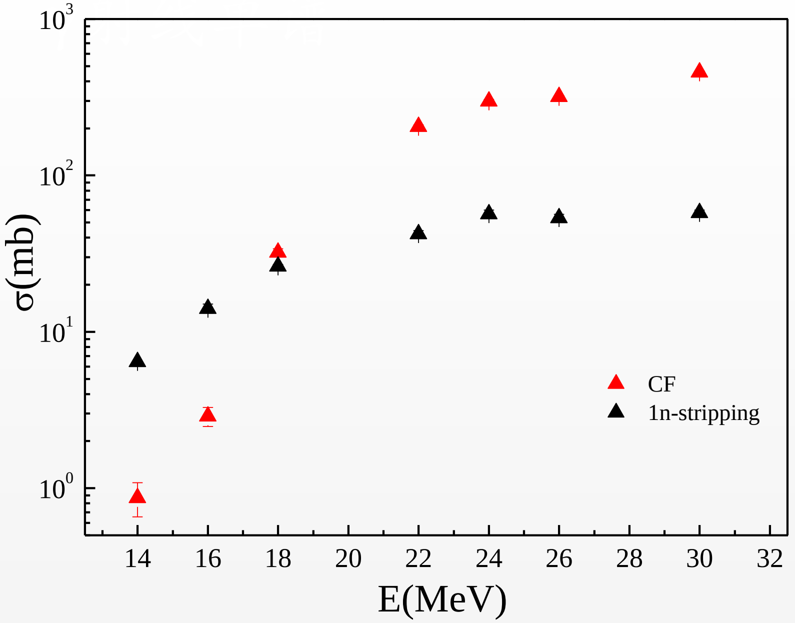

^{6}Li+^{94}Zr完全熔合与1n转移反应截面比较

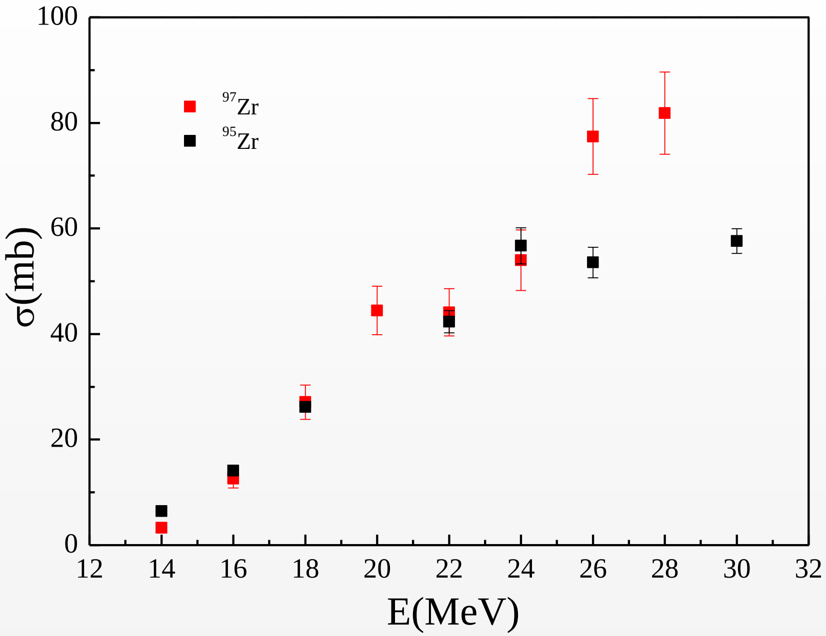

^{6}Li+^{94}Zr与^{6}Li+^{96}Zr1n转移反应截面比较

- 实验与理论计算结果：初步得到^{6}Li+^{94}Zr系统完全熔合截面压低因子为~32%；
- 转移反应激发函数比完全熔合激发函数变化缓慢，
  近垒能区转移与CF截面具有相同的数量级，垒下能区转移反应占主要贡献；
- ^{6}Li+^{94}Zr与^{6}Li+^{96}Zr 1n转移反应激发函数相似。

S. P. Hu *et al.*, Phys. Rev. C 93, 014621 (2016).

$^{6}Li+^{12}C$

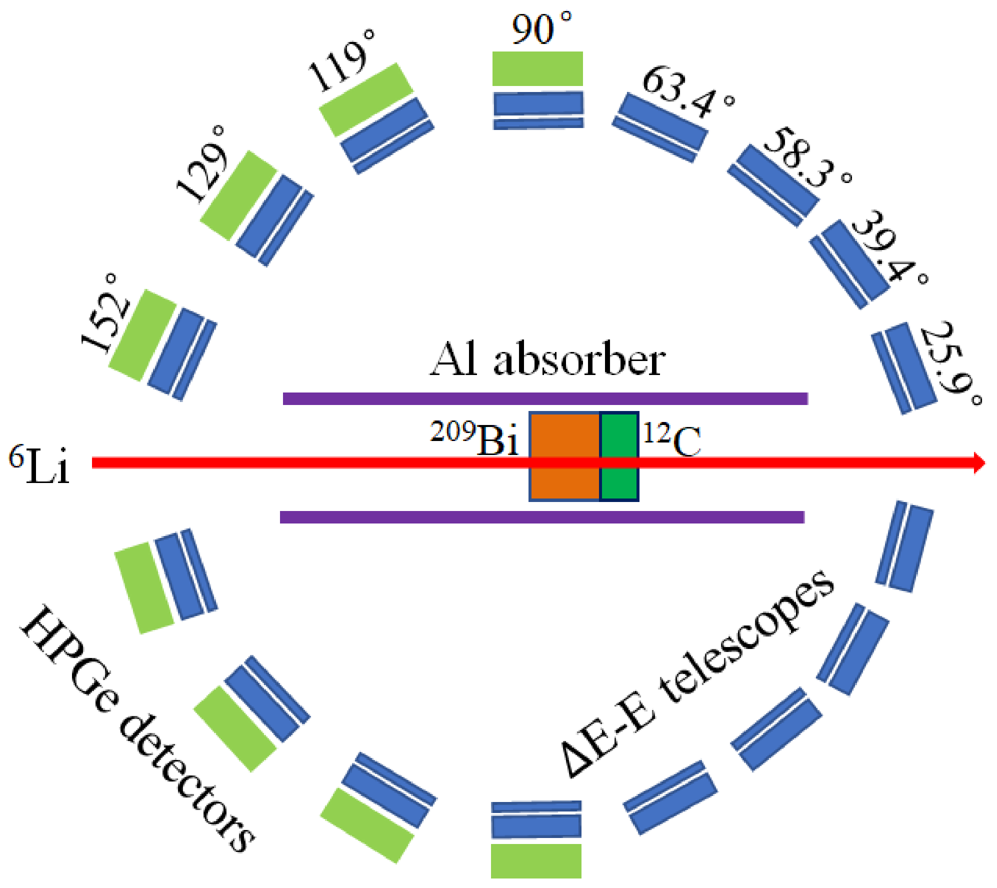

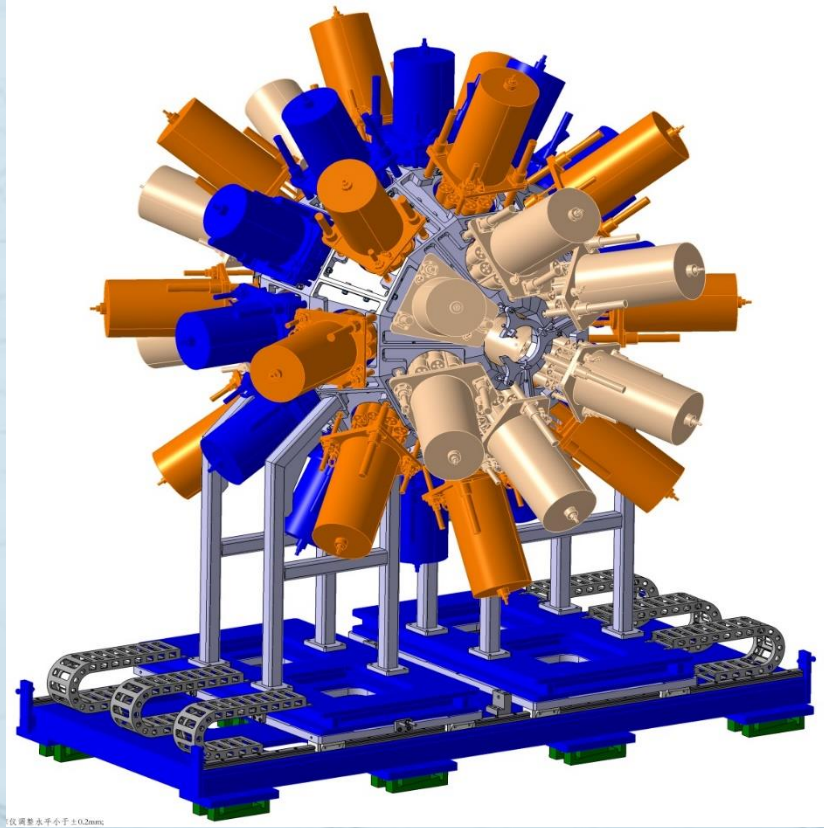

- **带电粒子-γ符合方法**
- **$^{6}Li^{3+}$：** 34, 30, 28MeV
- **靶：** ^{209}Bi (550μg/cm^{2})
- **衬底：** ^{12}C (100μg/cm^{2})
- **γ探测器：** 25个BGO-HPGe
- **带电粒子探测器：** 40个ΔE-E

- **在线γ测量方法**
- **$^{6}Li^{3+}$：** 34, 30, 28, 15MeV
- **靶：** ^{12}C (142μg/cm^{2})
- **衬底：** ^{197}Au (5.2mg/cm^{2})
- **探测器：** BGO-HPGe, Clover
- **角度：** 30°, 60°, 90°, 120°, 150°

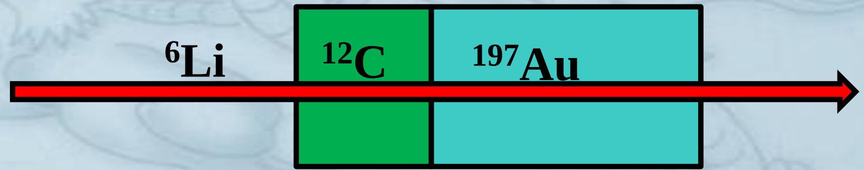

反应产物鉴别

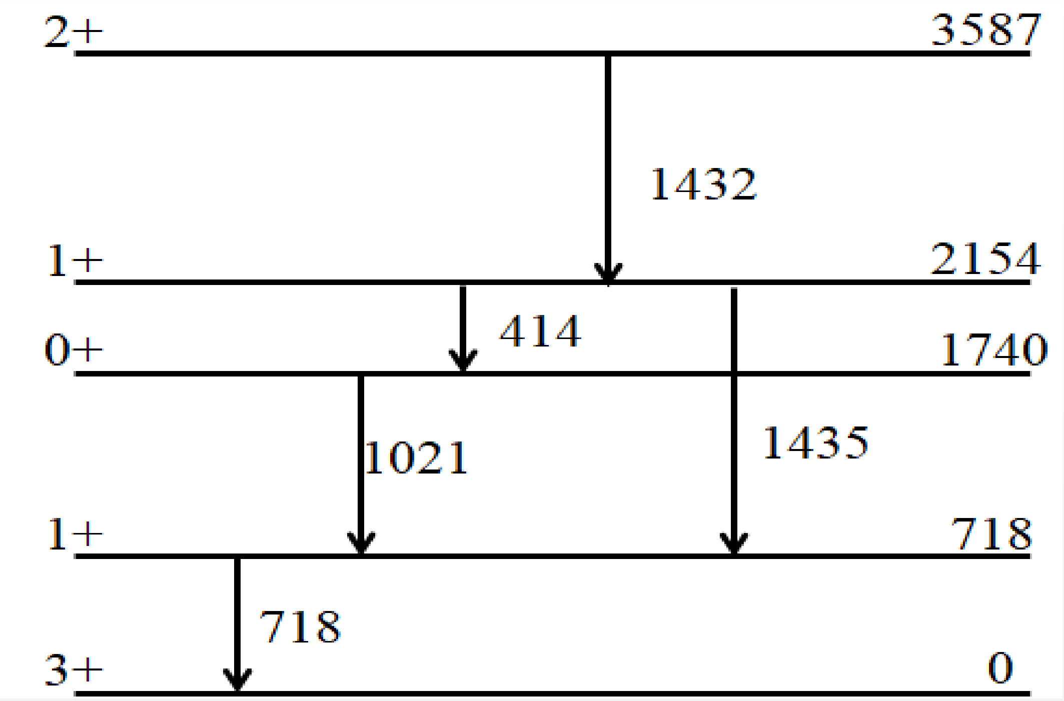

^{10}B的部分能级纲图

是否存在其它产物

每个产物发射哪些γ射线

提取每个产物的截面

γ-γ符合方法

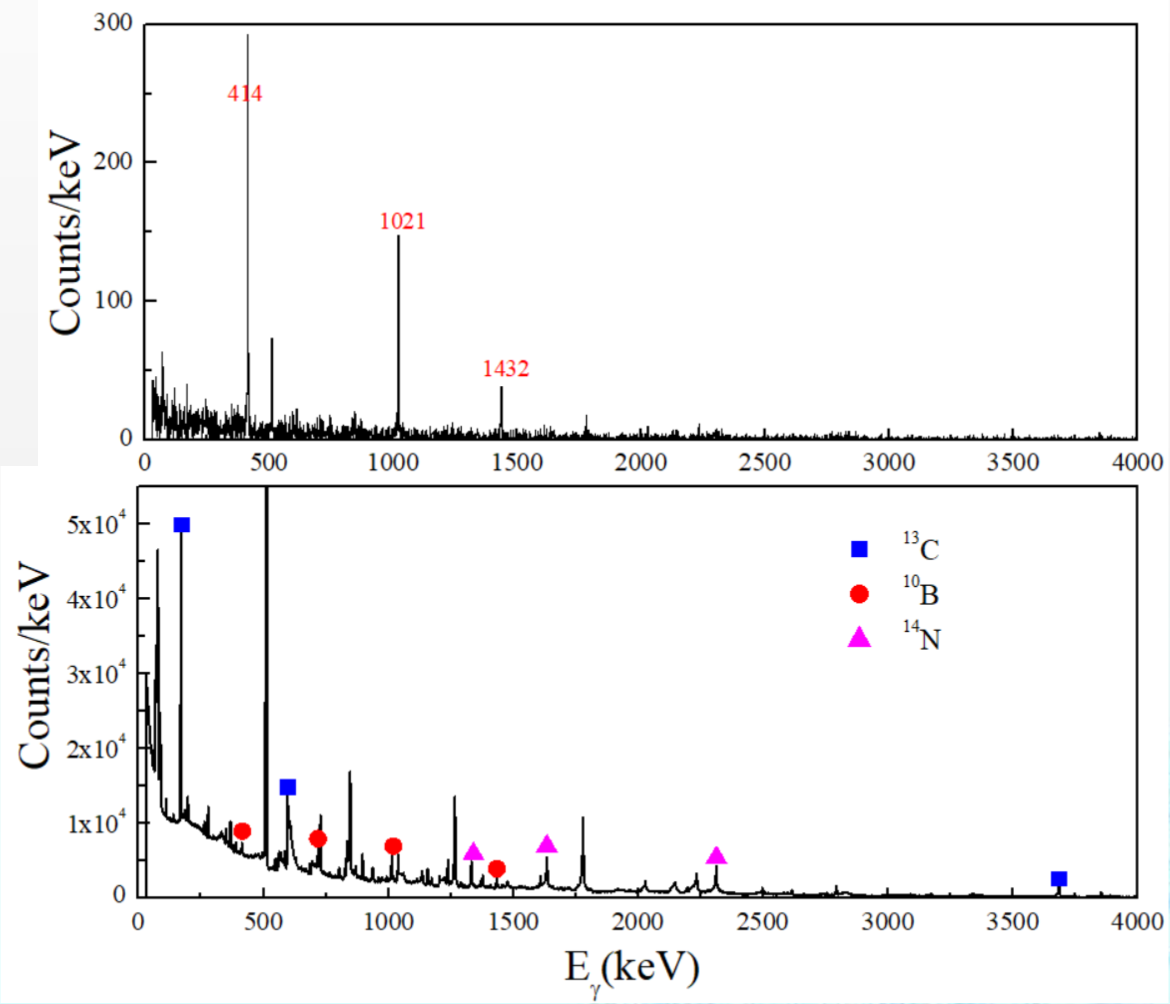

^{6}Li+^{12}C γ 射线投影谱和718keV γ 射线开窗谱

研究内容-反应道鉴别

反应产物的可能来源

没有^{10}B!

统计蒸发模型计算的产物									
^{17}F	^{17}O	^{16}O	^{15}O	^{14}N	^{13}C	^{13}N	^{12}C	^{9}B	^{9}Be
?	?	?	?	✓	✓	?	?	?	?

^{10}B可能的来源

熔合蒸发反应 ?

$\cancel{^{6}\mathrm{Li}+{}^{12}\mathrm{C}\rightarrow{}^{18}\mathrm{F}\rightarrow{}^{10}\mathrm{B}+2\alpha}$

削裂反应

$^{6}\mathrm{Li}+\mathrm{d}\rightarrow{}^{8}\mathrm{Be}\rightarrow 2\alpha$

$^{12}\mathrm{C}\text{-}\mathrm{d}\rightarrow{}^{10}\mathrm{B}$ 类靶产物

拾取反应

$^{12}\mathrm{C}\text{-}\alpha\rightarrow{}^{8}\mathrm{Be}\rightarrow 2\alpha$

$^{6}\mathrm{Li}+\alpha\rightarrow{}^{10}\mathrm{B}$ 类弹产物

^{14}N可能的来源

熔合蒸发反应

$^{6}\mathrm{Li}+{}^{12}\mathrm{C}\rightarrow{}^{18}\mathrm{F}\rightarrow{}^{14}\mathrm{N}+\alpha$

削裂反应

$^{6}\mathrm{Li}\text{-}\mathrm{d}\rightarrow\alpha$

$^{12}\mathrm{C}+\mathrm{d}\rightarrow{}^{14}\mathrm{N}$

^{13}C可能的来源

熔合蒸发反应

$^{6}\mathrm{Li}+{}^{12}\mathrm{C}\rightarrow{}^{18}\mathrm{F}\rightarrow{}^{13}\mathrm{C}+\alpha+\mathrm{p}$

削裂反应

$^{6}\mathrm{Li}\text{-}\mathrm{n}\rightarrow{}^{5}\mathrm{Li}\rightarrow\alpha+\mathrm{p}$

$^{12}\mathrm{C}+\mathrm{n}\rightarrow{}^{13}\mathrm{C}$

J. T. Li *et al.*, Nucl. Sci. Tech. 31, 49 (2020).

$^{6}Li+^{89}Y$

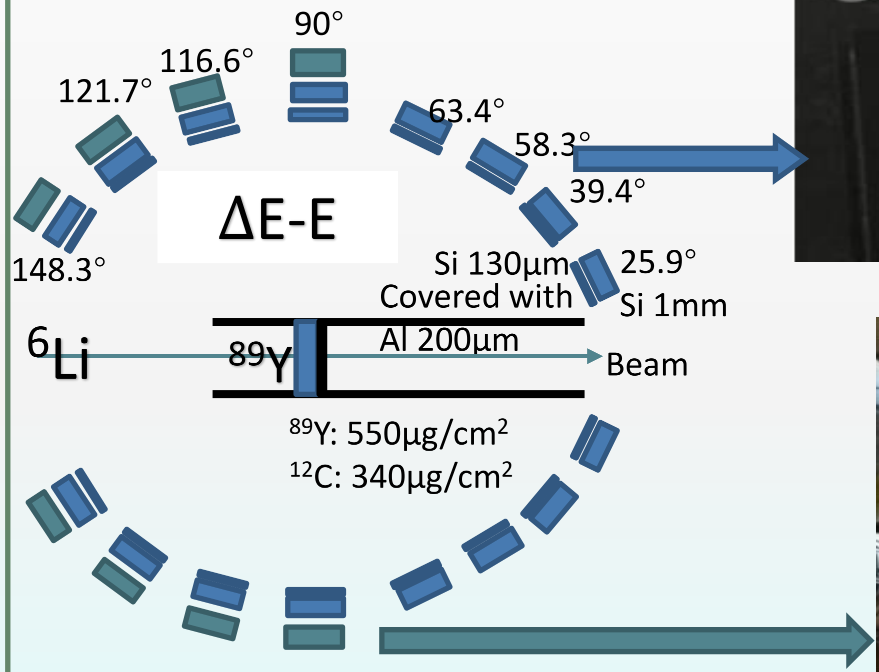

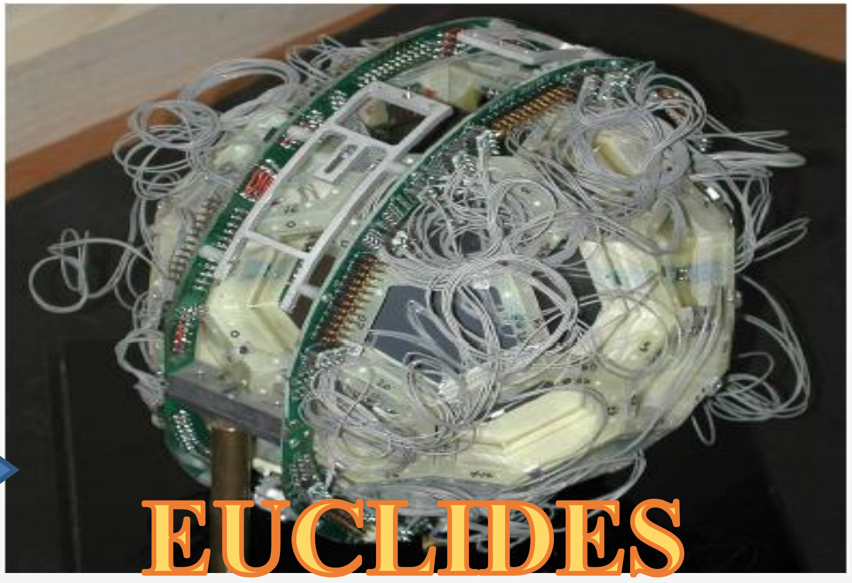

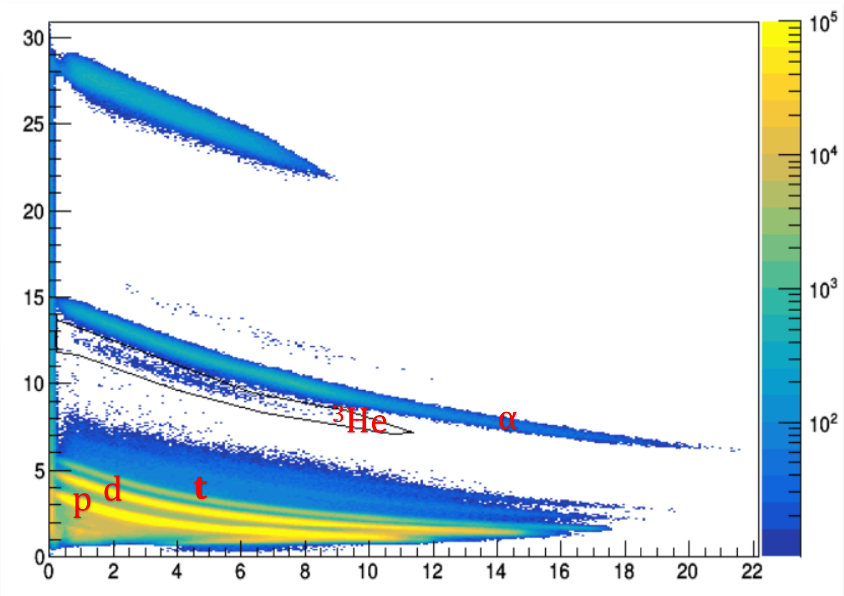

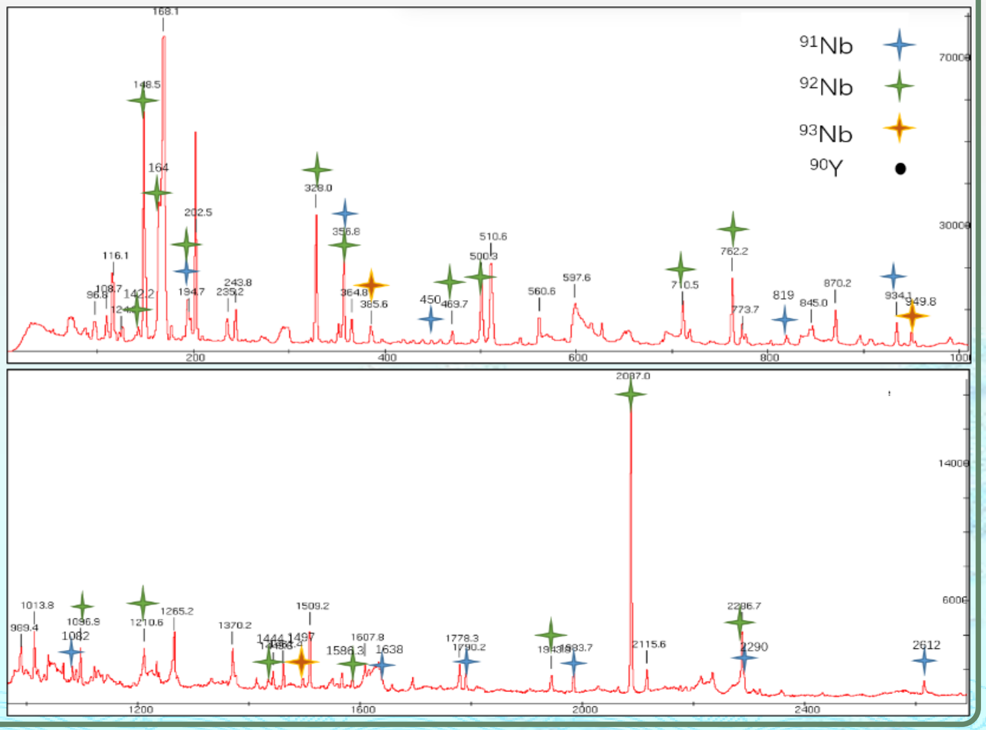

铝桶作用：

- 阻挡弹性散射的粒子以保护硅探测器；
- 筛选覆盖区域里较高能量的带电粒子；

■ Gamma coincidence with α particles

S. P. Hu *et al.*, Nucl. Instru. Method 93, 014621 (2019).

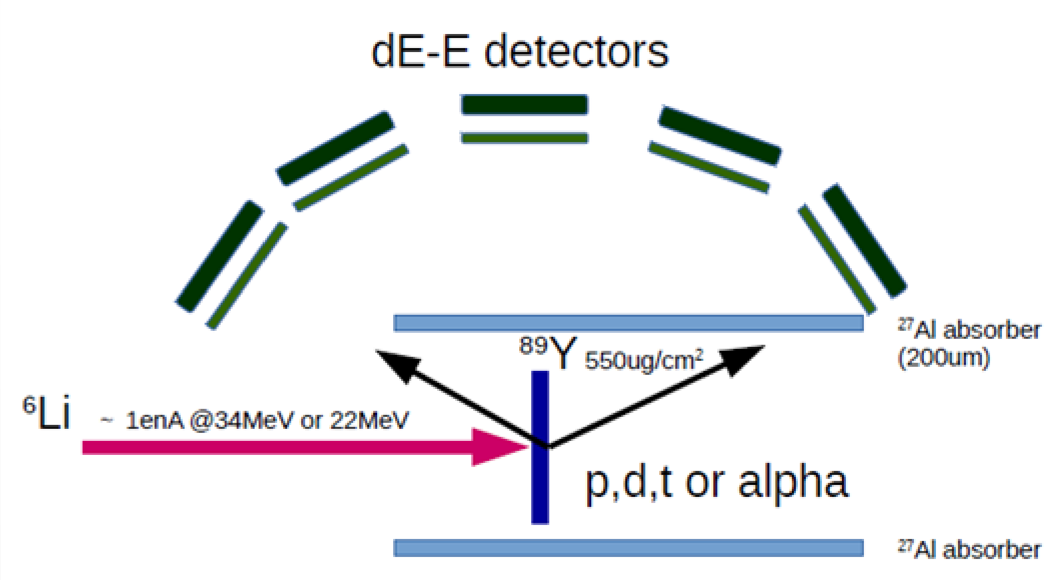

CF process $\quad {}^{6}Li + {}^{89}Y \rightarrow {}^{95}Mo \rightarrow {}^{90}Zr + \alpha + n,$

ICF process $\quad {}^{2}H + {}^{89}Y \rightarrow {}^{91}Zr \rightarrow {}^{90}Zr + n, \alpha$

Transfer process:

1n stripping: $\quad {}^{6}Li + {}^{89}Y \rightarrow {}^{90}Y + {}^{5}Li + 1.19\,MeV;$

$\quad {}^{5}Li \rightarrow \alpha + p$

1p stripping: $\quad {}^{6}Li + {}^{89}Y \rightarrow {}^{90}Zr + \alpha + n + 3.92\,MeV$

1d stripping: $\quad {}^{6}Li + {}^{89}Y \rightarrow {}^{91}Zr + \alpha + 11.85\,MeV$

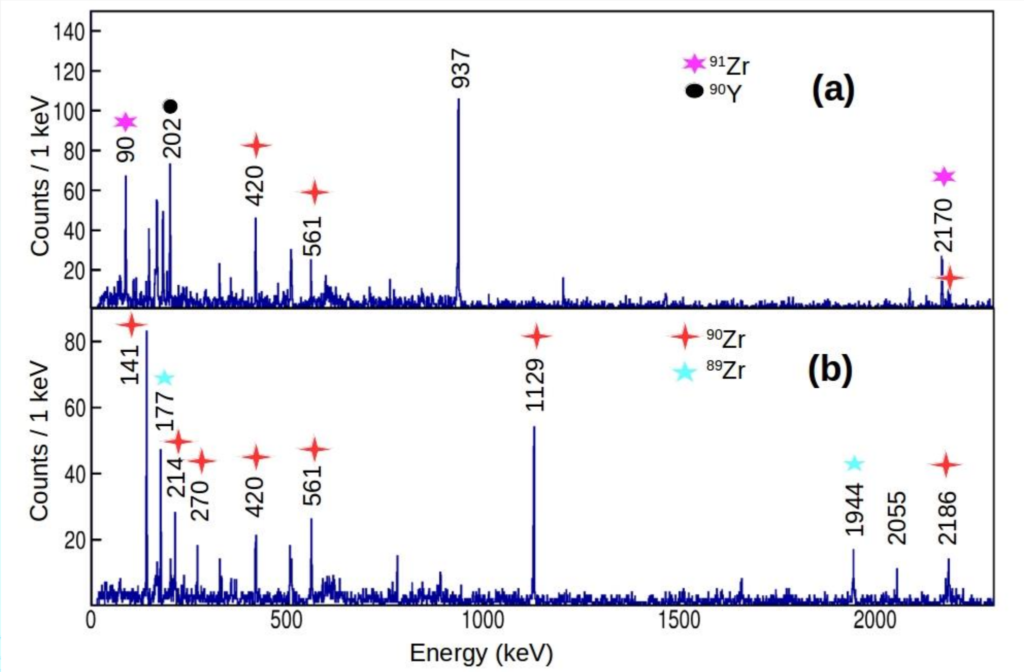

Transfer process

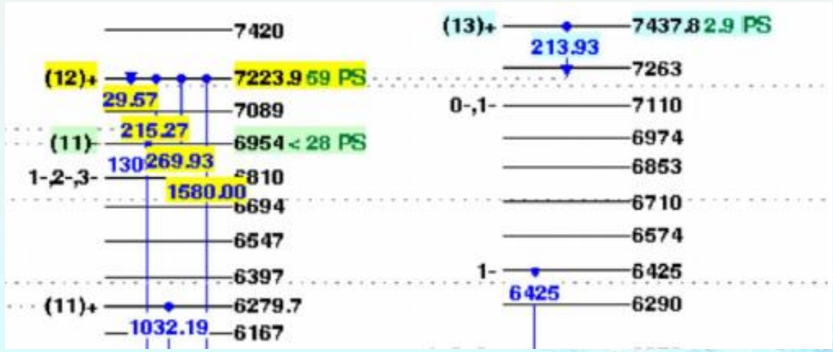

CF: $\quad {}^{6}Li + {}^{89}Y \rightarrow {}^{95}Mo \rightarrow {}^{90}Zr + \alpha + n$

$\qquad\qquad\qquad\qquad \rightarrow {}^{89}Zr + \alpha + 2n$

p-γ符合分析

CF:

$^{6}Li+^{89}Y$——>$(^{95}Mo)^*$——>$^{93}Nb+n+$**p**

$^{6}Li+^{89}Y$——>$(^{95}Mo)^*$——>$^{92}Nb+2n+$**p**

$^{6}Li+^{89}Y$——>$(^{95}Mo)^*$——>$^{91}Nb+3n+$**p**

1n stripping : $^{6}Li + ^{89}Y \rightarrow ^{90}Y + ^{5}Li + 1.19$ MeV , $^{5}Li \rightarrow \alpha +$ **p**

If ICF ? ✗

breakup	Separation energy(MeV)
^{6}Li——>d+α	1.47
^{6}Li——>p+$^{5}He(n+\alpha)$	4.43
^{6}Li——>n+$^{5}Li(\alpha+p)$	5.66
d——>p+n	2.224
^{6}Li——>t+^{3}He	15.79

理论计算

(1) $E_\alpha \approx 2/3E_{6Li} \approx 23$ MeV，而$E_d \approx 1/3E_{6Li} \approx 11$ MeV，所以$E_p \approx 4$ MeV（ p能量大于6.8 MeV才能通过铝膜并且被探测到）;

(2) 相比于^{6}Li破裂为α和d, 可忽略^{6}Li破裂为p和^{5}He以及n和^{5}Li(破裂能较大)。

p-γ符合分析

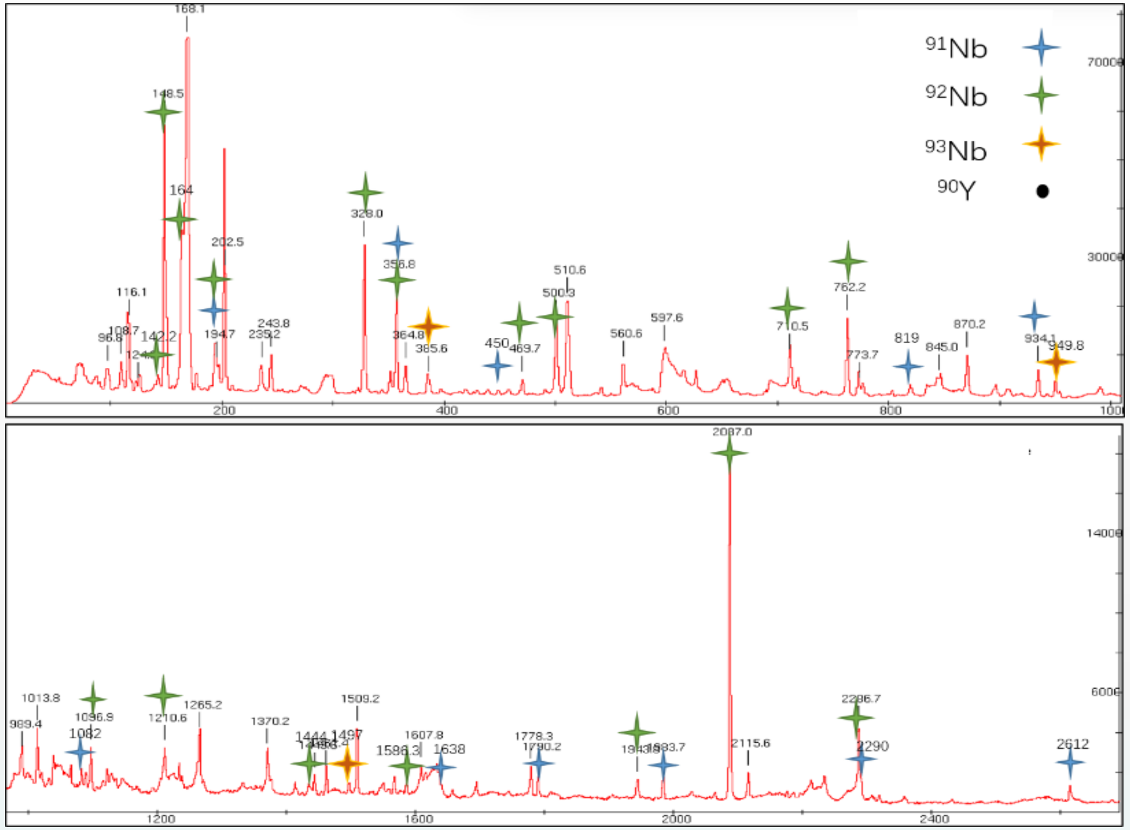

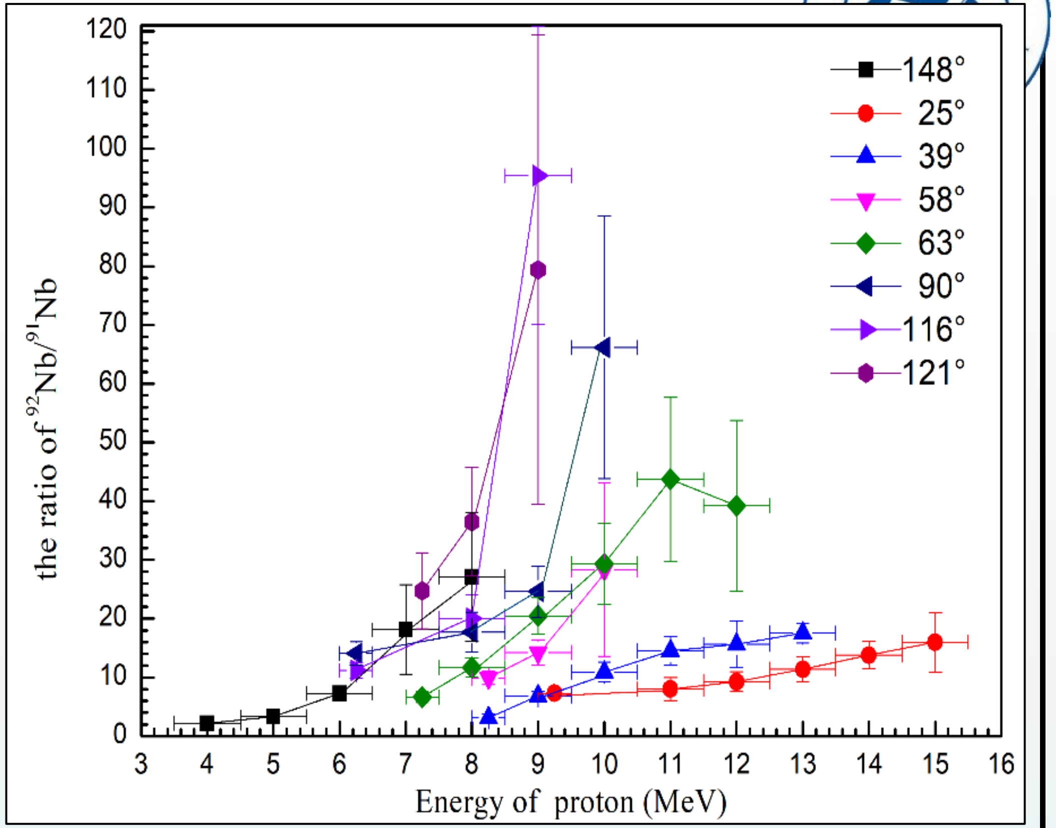

（1）对应于不同的角度，p的能量范围不同。明显前角区p的能量较高；

（2）在同一角度下，^{92}Nb/^{91}Nb比例随着p能量的增加而增加。对应于高的p的能量，复合核的激发能越小，越难实现蒸发更多中子的反应道，故产生^{91}Nb的几率会减少。

实验现象和理论蒸发模型的结果比较一致，故可验证^{91}Nb，^{92}Nb来自于完全熔合过程。

p-γ符合分析

Covered angles

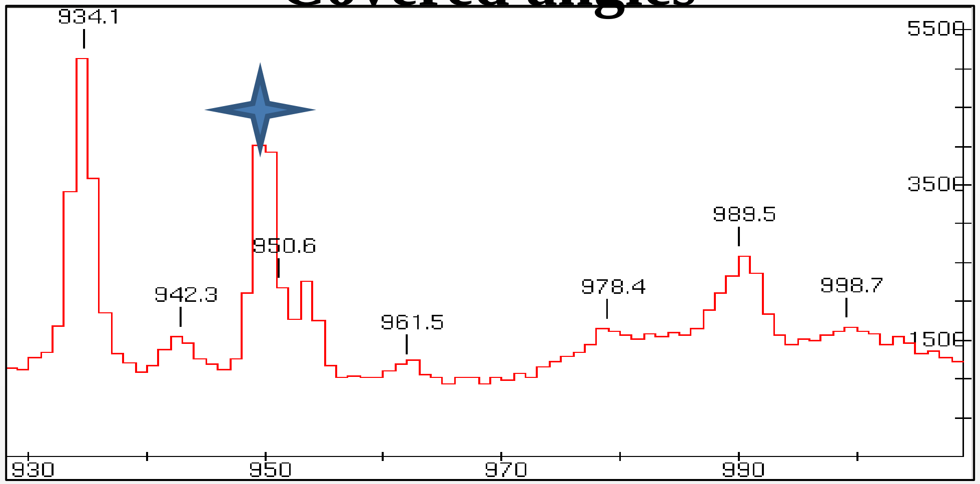

Uncovered angle

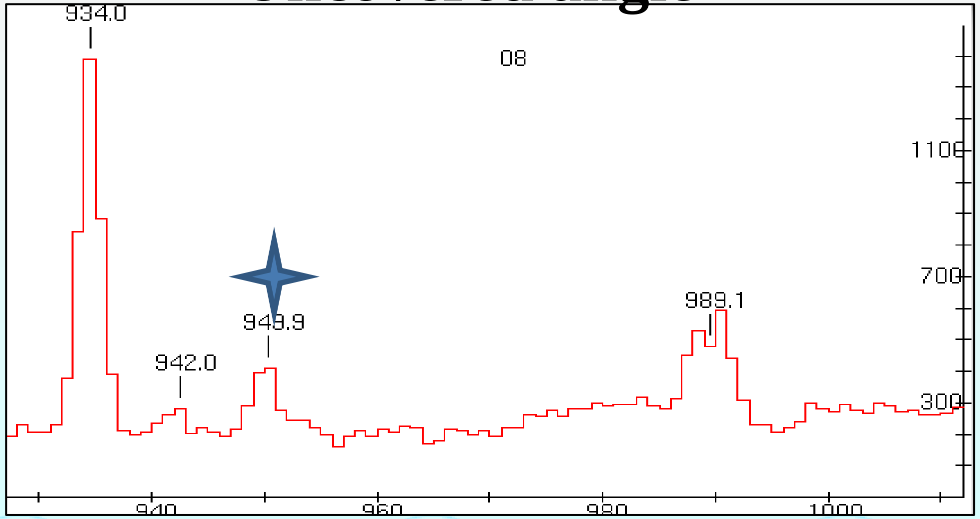

^{93}Nb

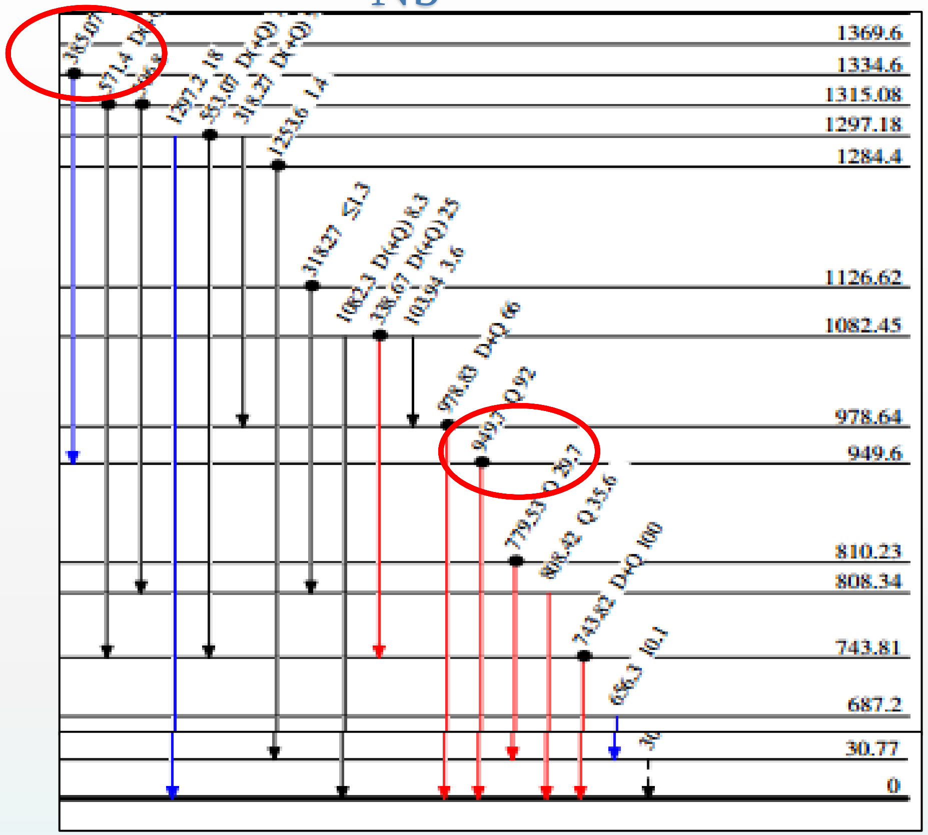

Complete fusion:

^{6}Li+^{89}Y——>(^{95}Mo)*——>^{93}Nb+ n +**p**

^{6}Li+^{89}Y——>(^{95}Mo)*——>^{92}Nb+2n+**p**

^{6}Li+^{89}Y——>(^{95}Mo)*——>^{91}Nb+3n+**p**

p-γ符合分析

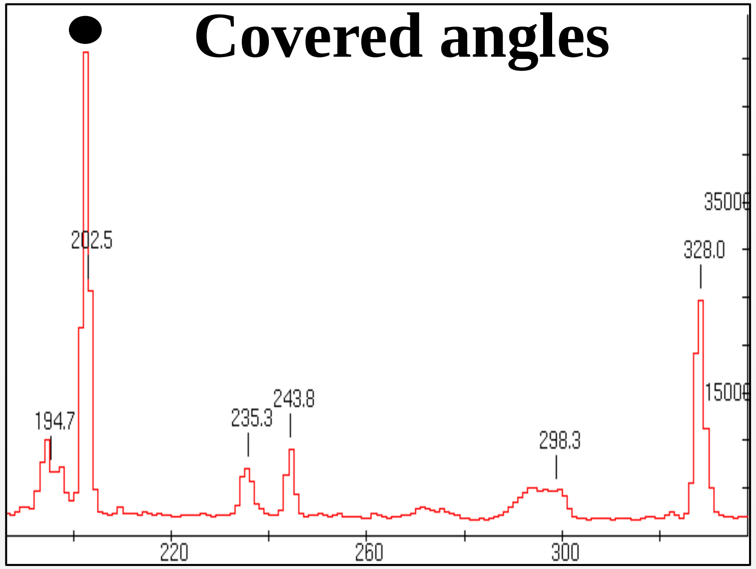

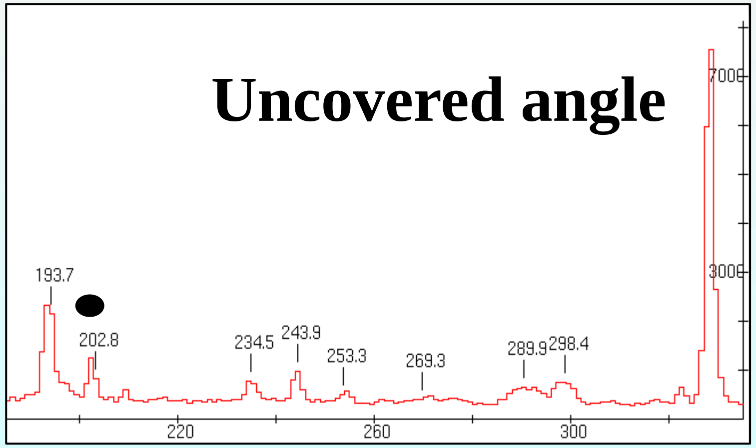

^{90}Y

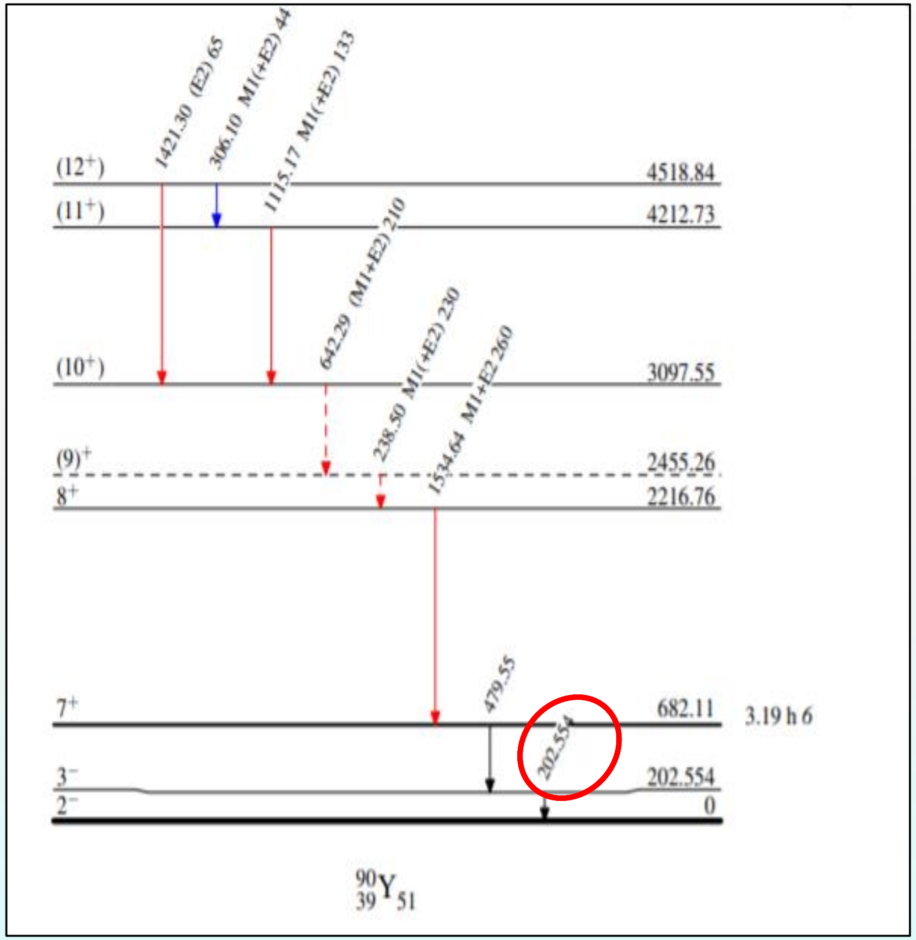

（1）有铝膜覆盖的区域明显，无铝膜覆盖的区域几乎没有；

（2）α开窗文献已经证明，对不同能量的α开窗。

（3）熔合蒸发计算中很少。

G. L. Zhang *et al.*, Phys. Rev. C 97, 044618 (2018).

^{89}Y+^{6}Li——>^{90}Y+（^{5}Li）*——>^{90}Y+α+p+3158 keV

^{3}He-γ符合分析

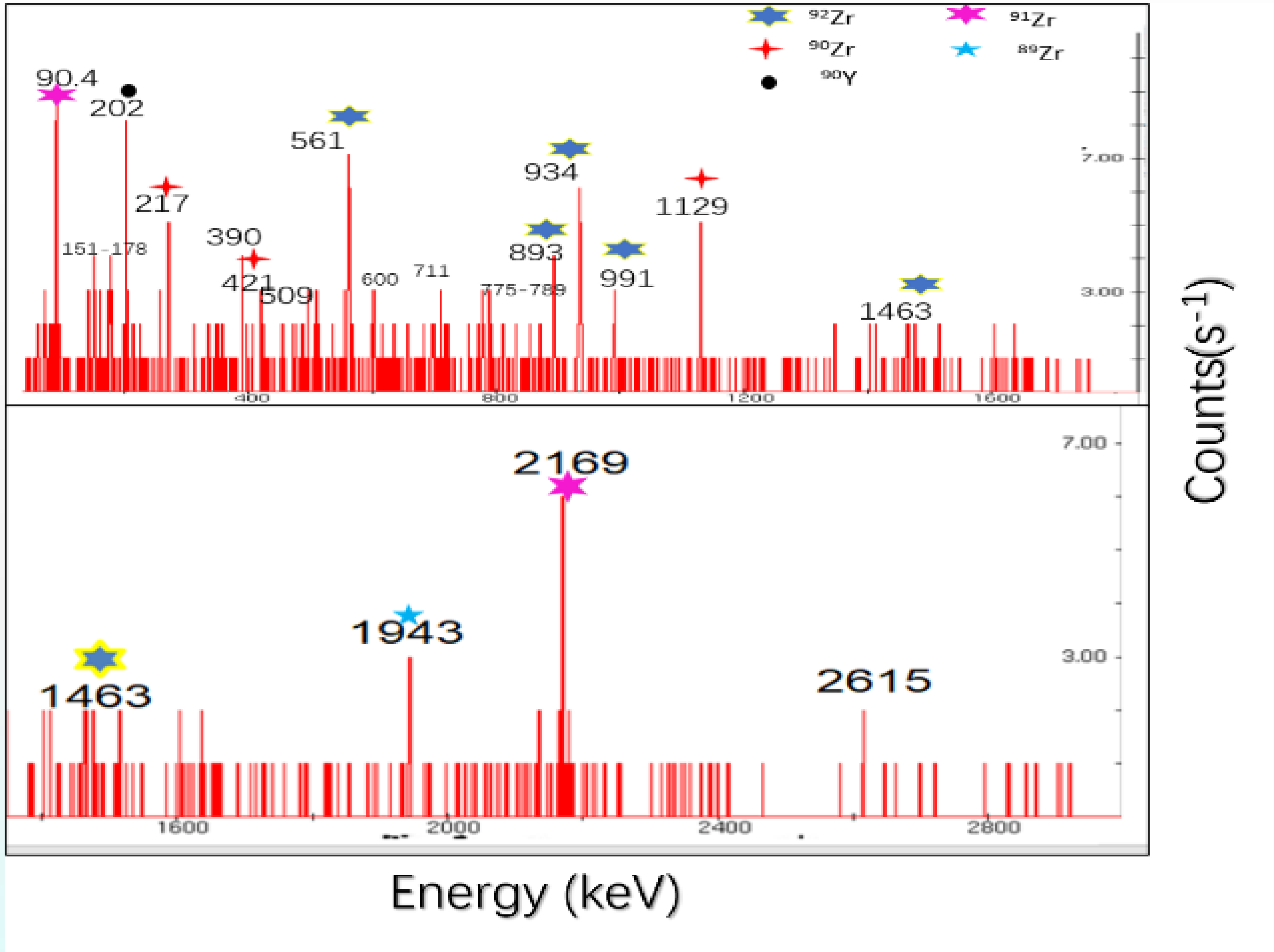

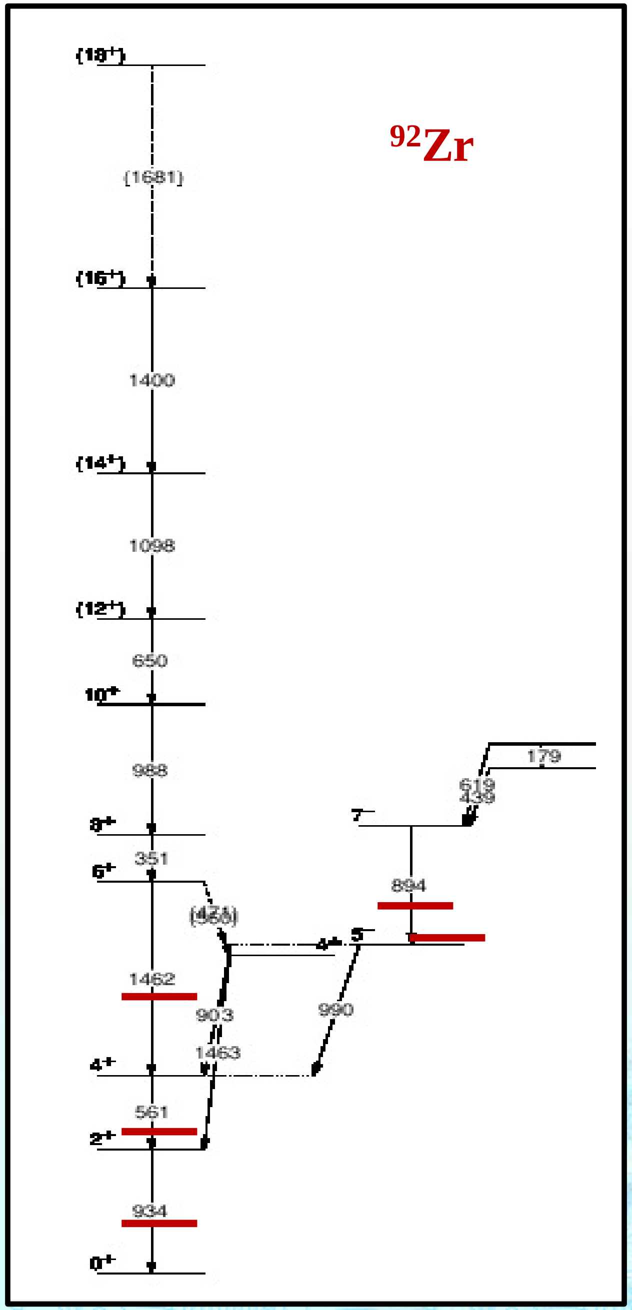

t stripping reaction: ^{6}Li+^{89}Y—> ^{3}He+ ^{92}Zr+ (-0.9 MeV)

t-γ符合分析

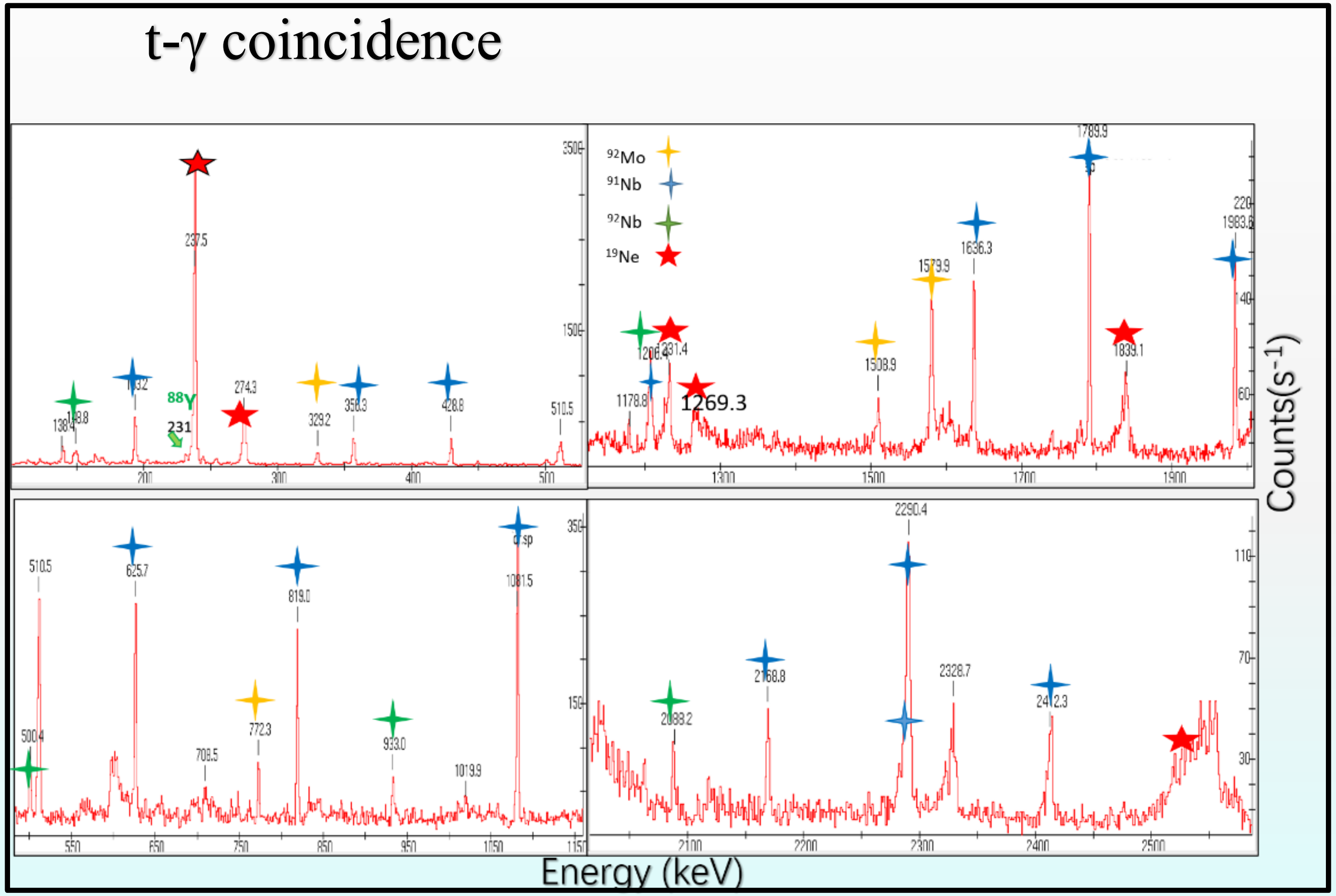

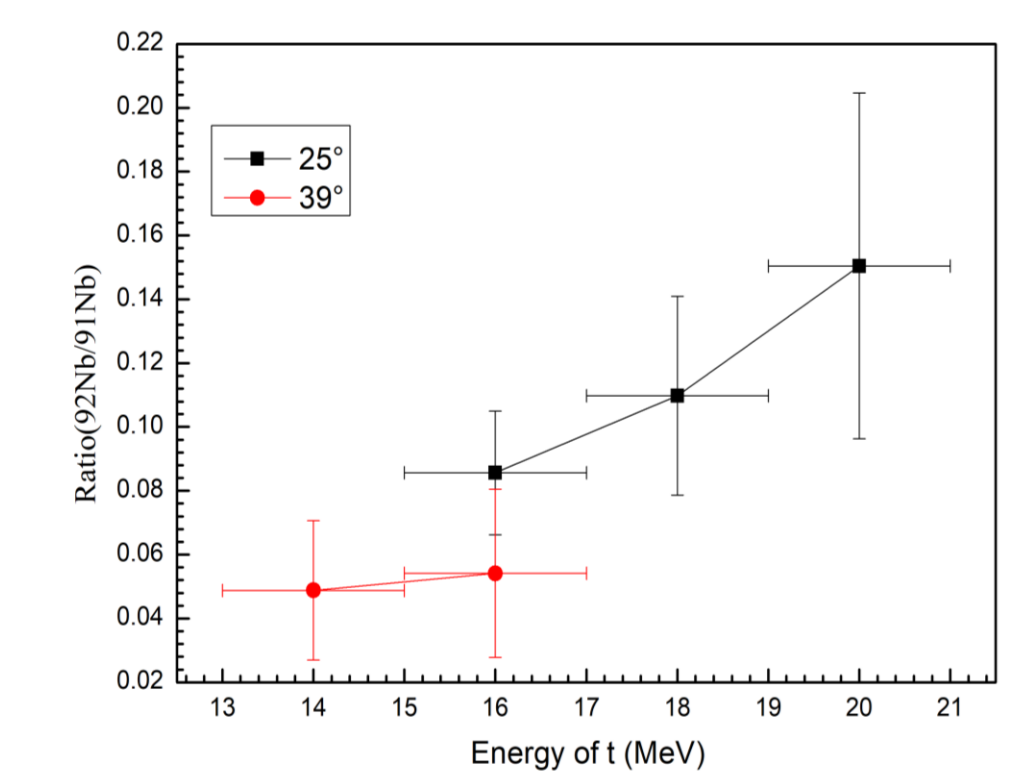

对探测到的t已经进行了铝膜修正，观察到在同一个角度下，其比例也是随着出射的t的能量的增加而增加的。

t-γ符合分析

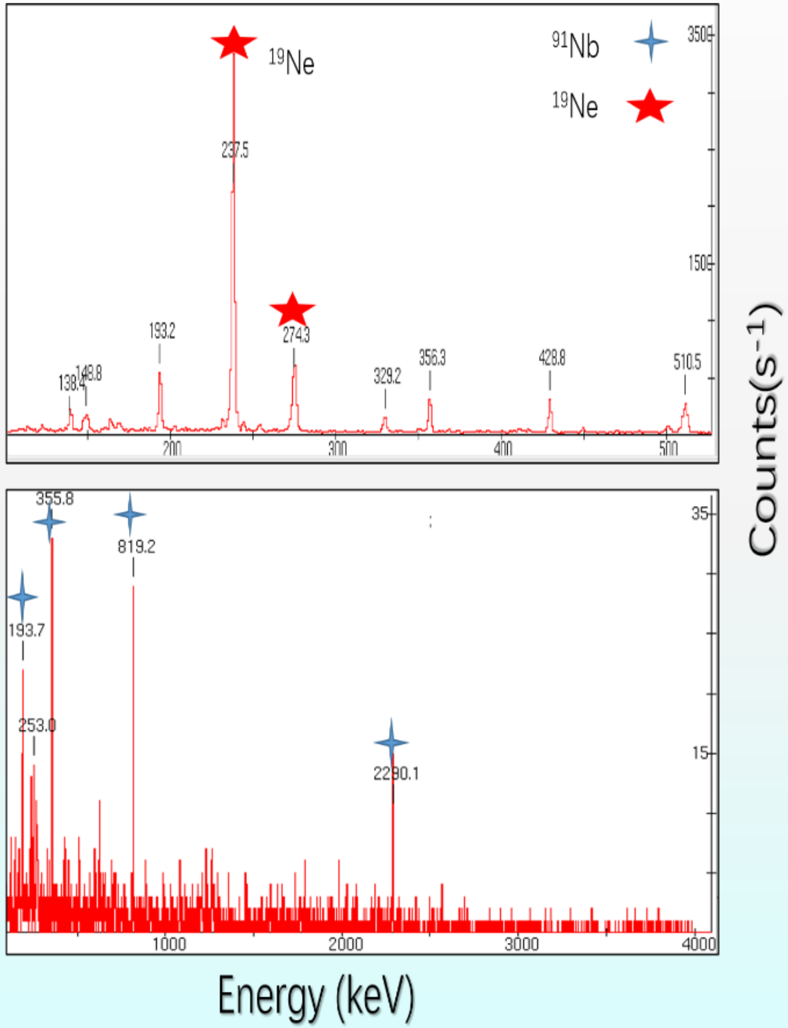

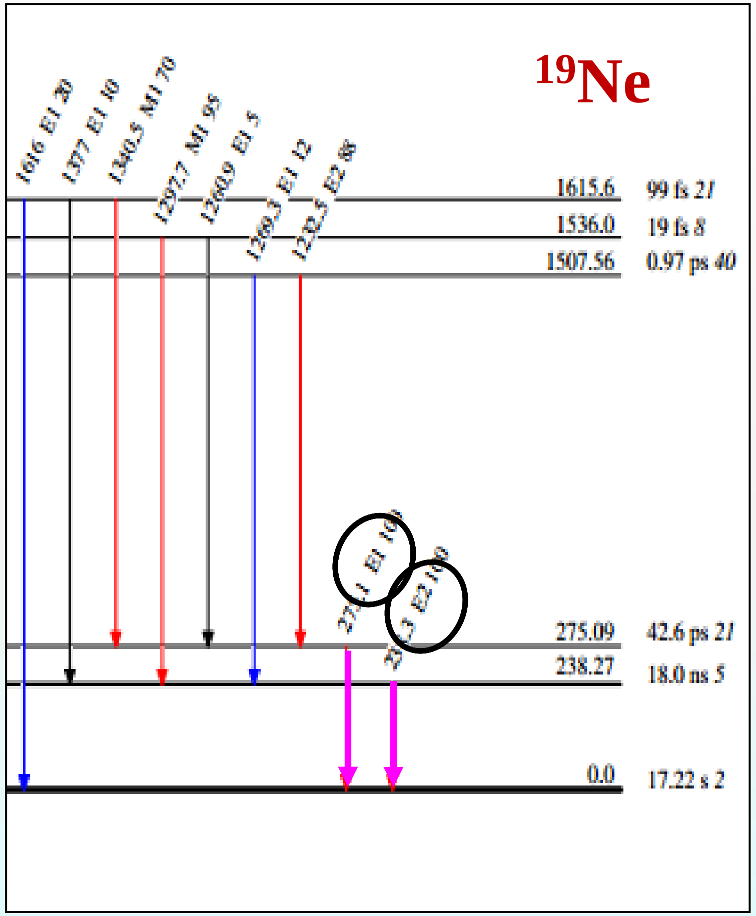

M. Martz *et al.*, Phys. Rev. C 20, 1340 (1979).

（1）在t开窗符合中，在有铝膜覆盖的区域（t>12 MeV）^{19}Ne的特征γ射线可以很清楚地看见，但是在无铝膜覆盖的区域看不见。

(2) 根据统计蒸发模型，^{6}Li和^{16}O的完全熔合反应，主要产物是^{20}Ne不是^{19}Ne。

^{3}He stripping reaction: ^{6}Li+^{16}O——>^{19}Ne+t+(-7.35 MeV)

t-γ符合分析

^{3}He stripping :

$^{6}Li+^{89}Y$——>**t**+ ^{92}Nb+(-2.12 MeV)	(1) E_t≈ 25~30.5 MeV
$^{6}Li+^{16}O$——>^{19}Ne+**t**+(-7.35 MeV)	(2) E_t≈ 8~24 MeV

1n pick up: ✗

$^{6}Li+^{89}Y$——>α +**t** + ^{88}Y+(-6.697 MeV) ^{7}Li ——> α +**t** +(-2.47 MeV) α + ^{89}Y——>$^{93}Nb_{51}$ (^{91}Nb+2n) +**t**	(1) E_{7Li}≈21.7~29.4 MeV, Eα ≈12.82~17.95 MeV, E_t≈ 6.41~8.97 MeV, 所以，t 可能穿过Al(10.57 MeV）

综上所述，^{3}He 的转移反应存在。

$^{6}Li+^{209}Bi$

α衰变方式测量^{6}Li、^{7}Li与重核的熔合反应截面

- **实验特点：**
- ✓ 环形探测器(Annular detector) 探测由半衰期较短的剩余核(110 ns~23.1 min) 衰变产生的α粒子；
- ✓ Si 面垒探测器探测半衰期较长的剩余核(23.1 min~138 d)衰变产生的α粒子；
- ✓ Monitor归一入射束流；
- ✓ 通过鉴别特征α粒子的能量和半衰期来区分不同产物；
- ✓ 产物的α衰变半衰期分布在110ns到138d之间。
- **实验不足：**
- ✓ 无法测量长寿命α衰变核；
- ✓ 无法区分转移和熔合反应道；
- ✓ 个别α衰变产物无法区分；

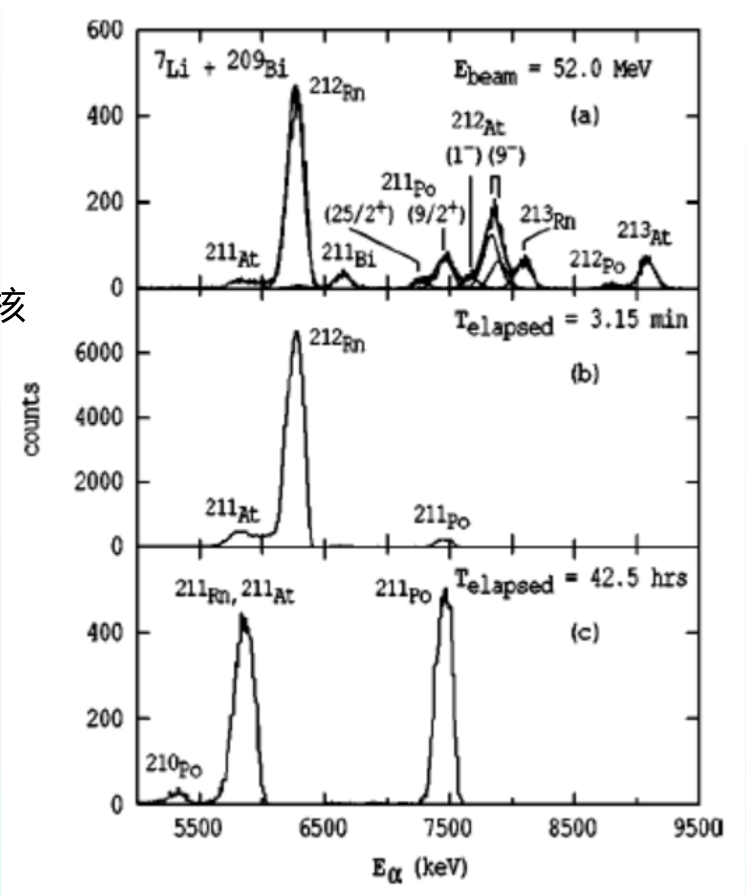

^{7}Li +^{209}Bi反应在束流能量为52MeV时典型的α能谱。(a)在辐照过程中获取;(b)在辐照结束3.2 min后开始离线测量;(c)在辐照42.5 h后开始离线测量。

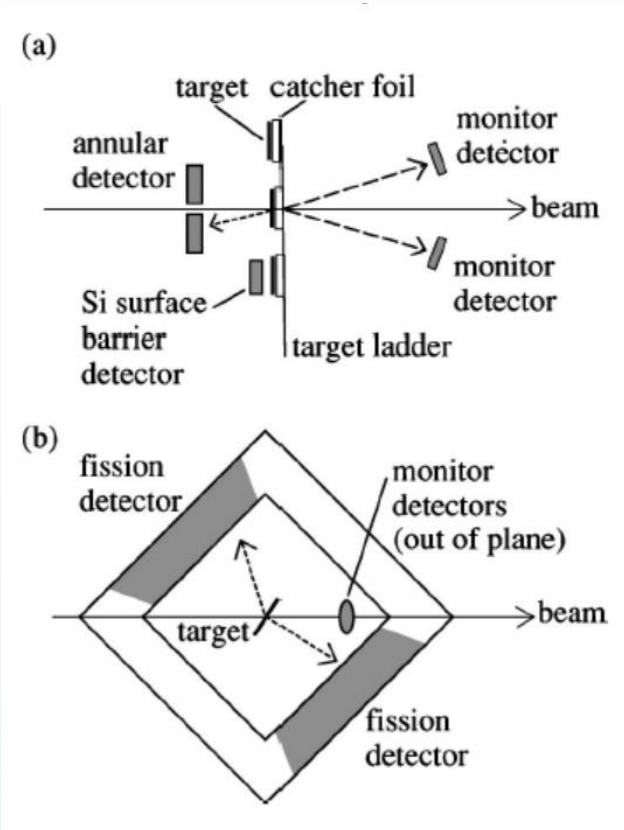

实验测量装置

Dasgupta M , Hinde D J , Hagino K , et al. Phys. Rev. C, 2002, 66(4).

✈ 熔合反应

✈ 转移反应

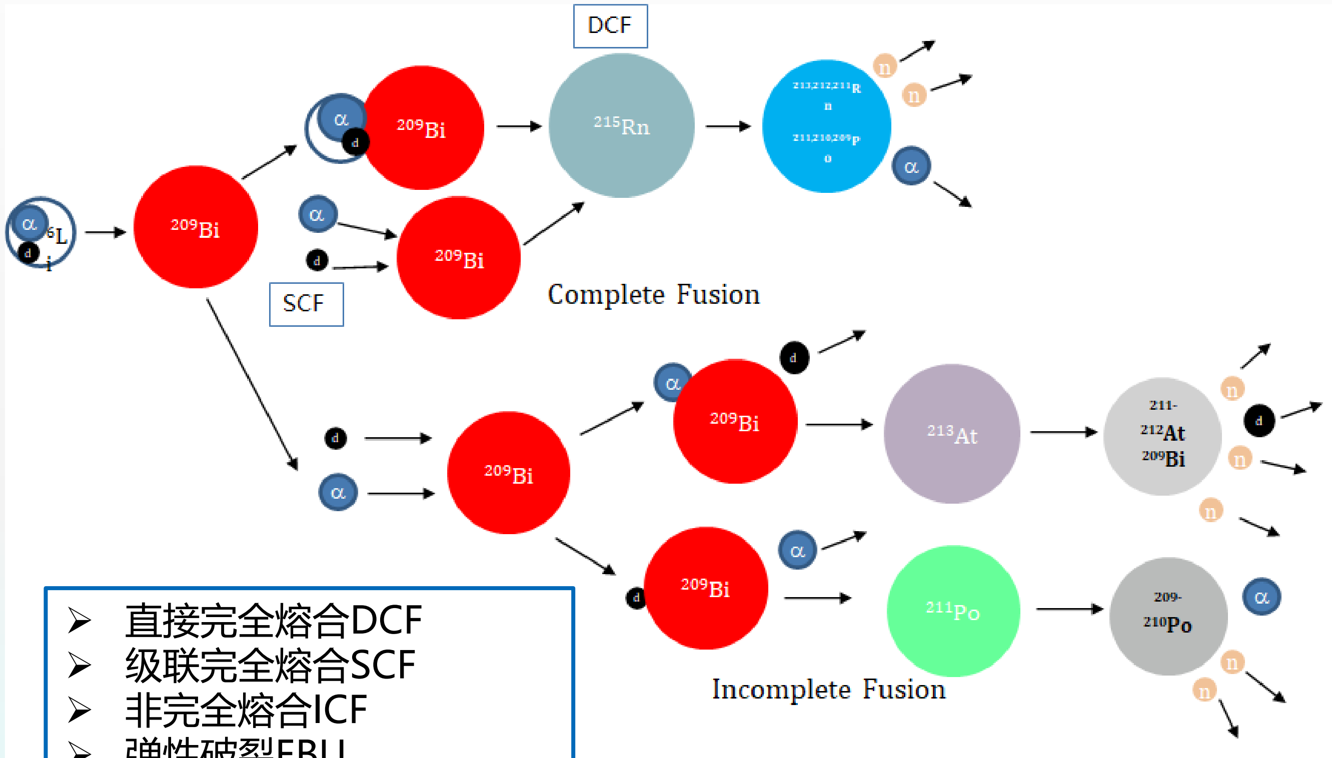

- 直接完全熔合DCF
- 级联完全熔合SCF
- 非完全熔合ICF
- 弹性破裂EBU

$^{6}Li+^{209}Bi$ 熔合反应示意图

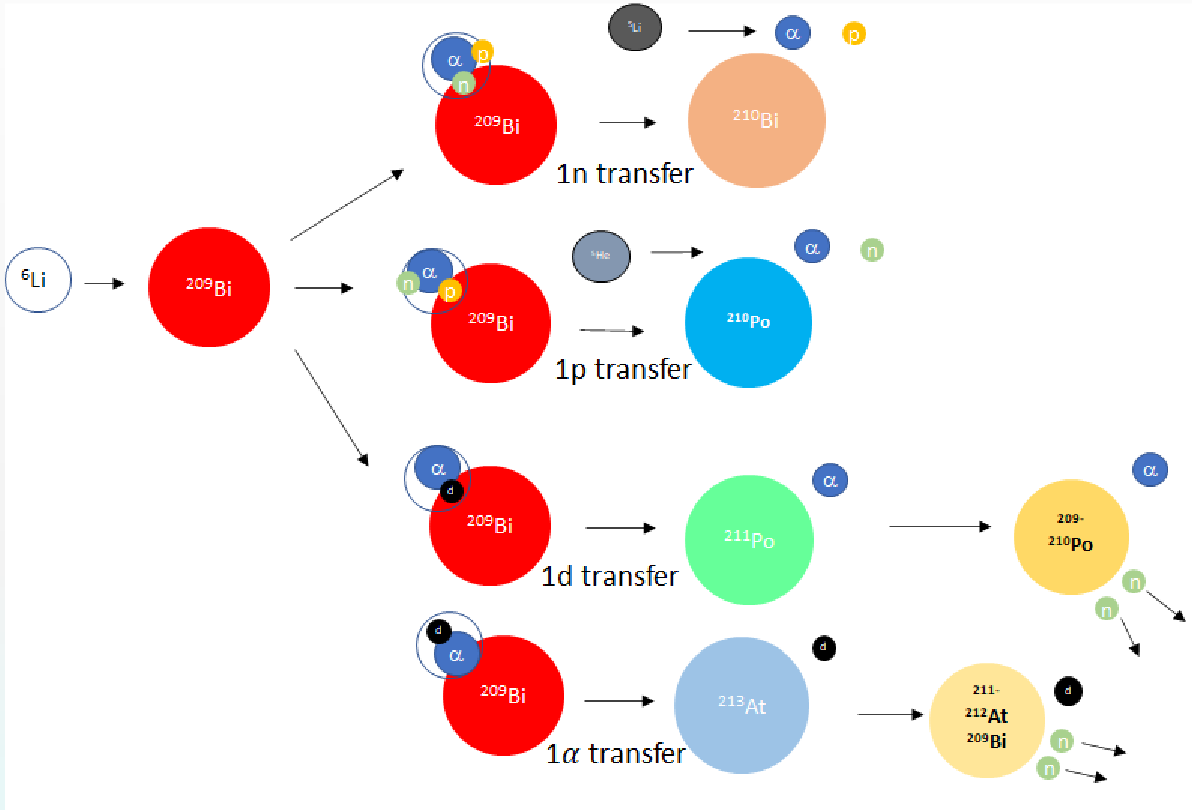

$^{6}Li+^{209}Bi$ 转移反应示意图

$$\sigma_{CF}=\sigma_{DCF}+\sigma_{SCF}$$

$$\sigma_{ICF}=\sigma_{ICF1}+\sigma_{ICF2}$$

1n transfer reaction

$^{6}Li+209Bi \rightarrow ^{210}Bi+p+\alpha$

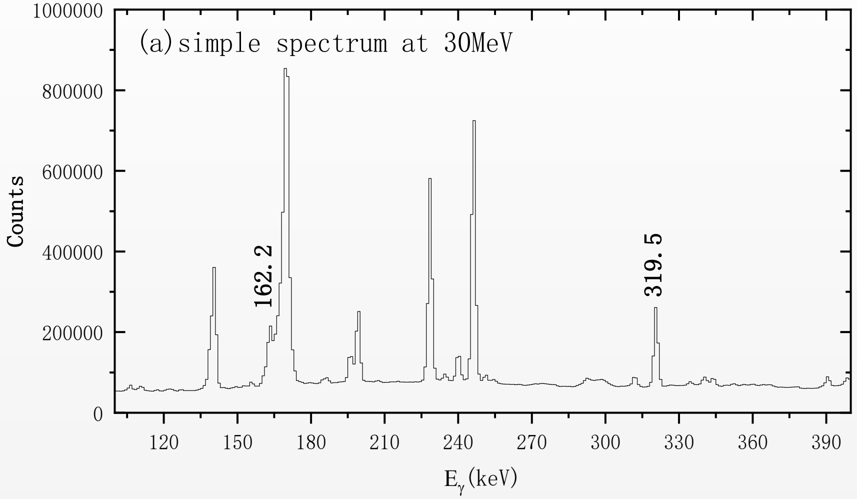

Characteristic γ rays of 210Bi

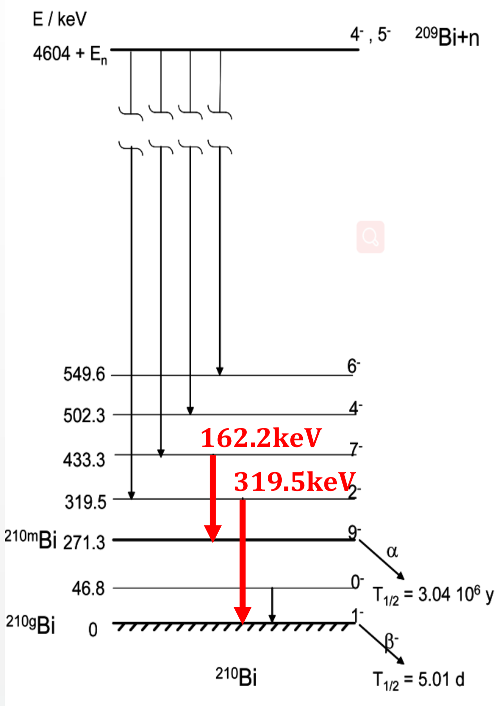

The partial level scheme of ^{210}Bi

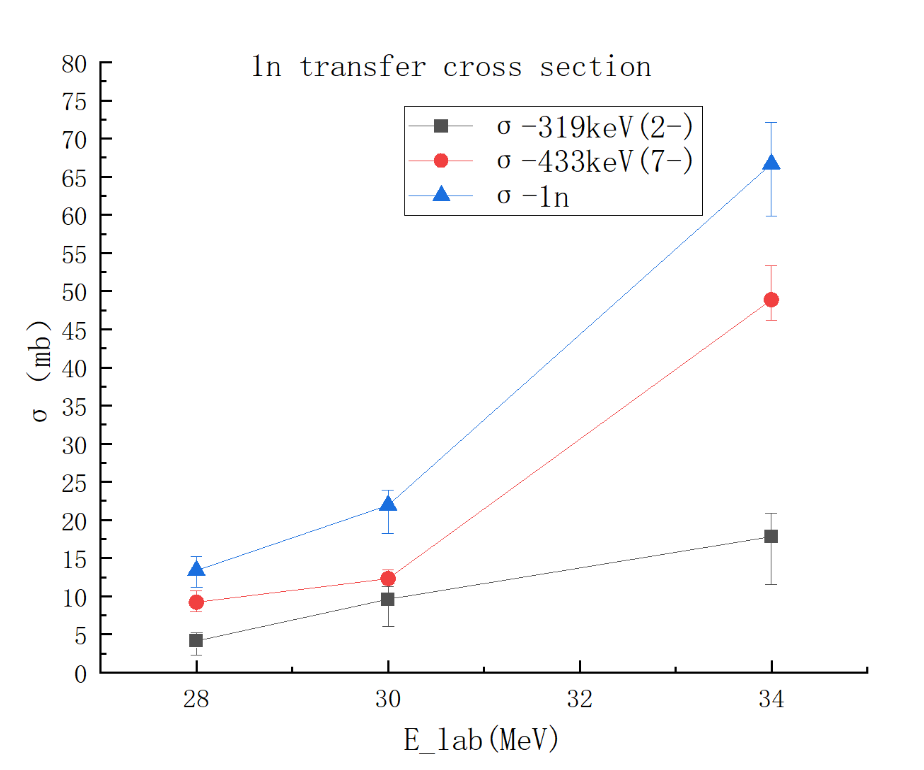

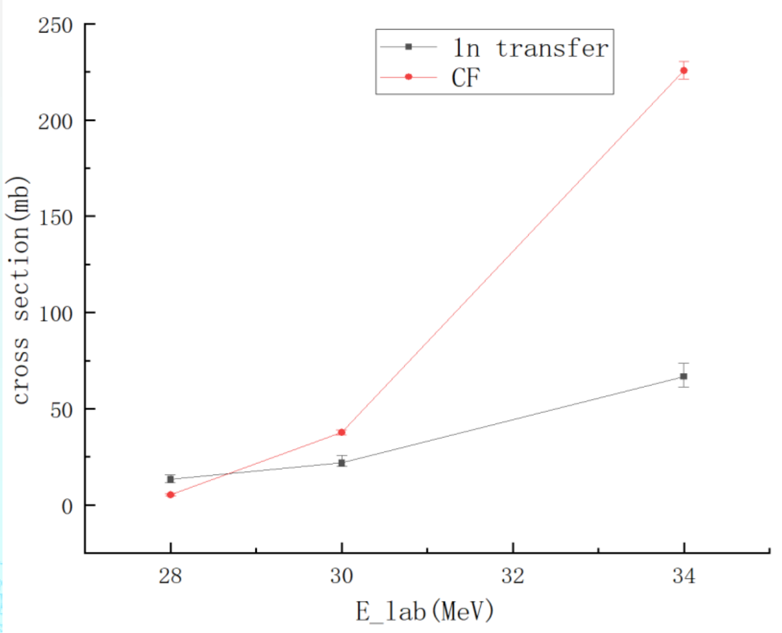

Theoretical

E lab MeV	28	30	34
cs_319 keV (mb)	6.88	14.73	24.92
cs_433 keV (mb)	7.45	15.89	26.84

CF and ICF reaction

Experimental Results

Reaction	CF radon		d-ICF polonium						α-ICF astatine					
Energy_lab(MeV)	σ_211Rn (mb)	error	σ_210Po (mb)	error	σ_209Po (mb)	error	sum	error	σ_212At (mb)	error	σ_211At (mb)	error	sum	error
28	/	/	15.38	2.09	15.49	2.10	30.87	2.96	/	/	/	/	/	/
30	/	/	42.04	2.42	65.33	3.77	107.37	4.48	2.74	0.09	0.60	0.05	3.34	0.10
34	30.01	1.54	52.58	2.66	155.05	7.85	207.63	8.29	10.52	0.37	23.05	1.14	33.57	1.20

EXP_ous VS EXP_AUS VS Theory

beam (MeV)	E_c.m. (MeV)	exp_aus(mb) [1]			theory(mb) [2]			exp_our(mb)		
		ICF	alpha-ICF	d-ICF	ICF	alpha-ICF	d-ICF	ICF	alpha-ICF	d-ICF
28	27.11	/	1.62	/	37.01	9.408	31.915	/	/	30.87
30	29.08	72.3	11.09	/	133.03	37.218	99.684	110.71	3.34	107.37
34	32.96	130.1	60.99	/	360.46	110.513	249.437	241.2	33.57	207.63

- The experimental results of d-ICF agree well with the theoretical calculation
- Our alpha-ICF cross section result is small, perhaps for two reasons:
  - 1st: The yields of some rays are too small to count.
  - 2nd: The rays directly populated to the ground state cannot be counted.

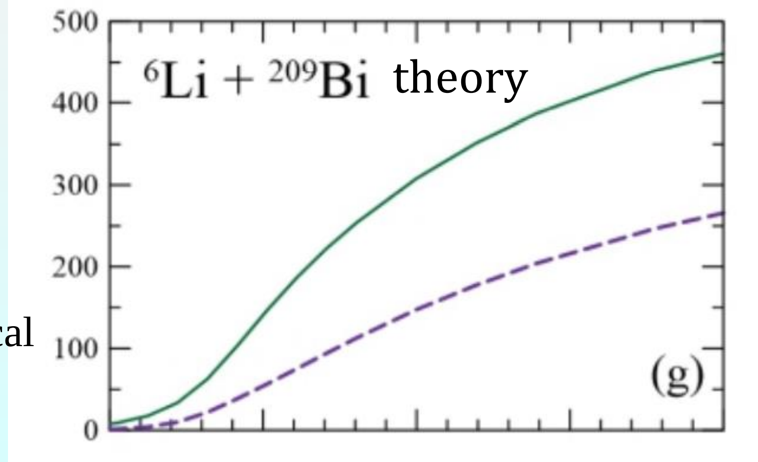

[1] M. Dasgupta, et al, Effect of breakup on the fusion ofLi6,Li7, andBe9with heavy nuclei, Physical Review C, 70 (2004).

[2] J. Lubian ,et al, Study of fusion processes in collisions of 6Li beams on heavy targets

$^{6,7}Li+^{209}Bi$破裂反应机制研究

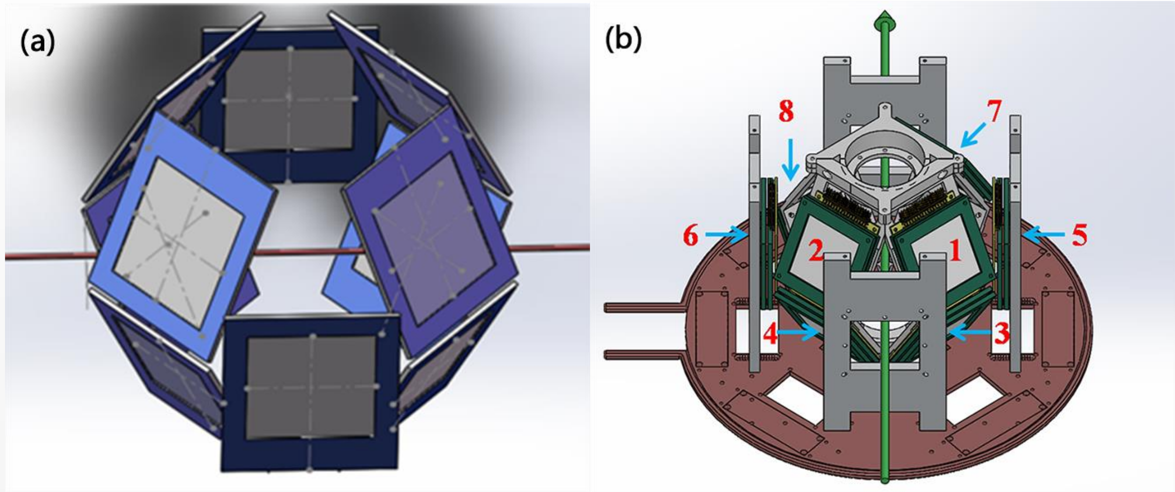

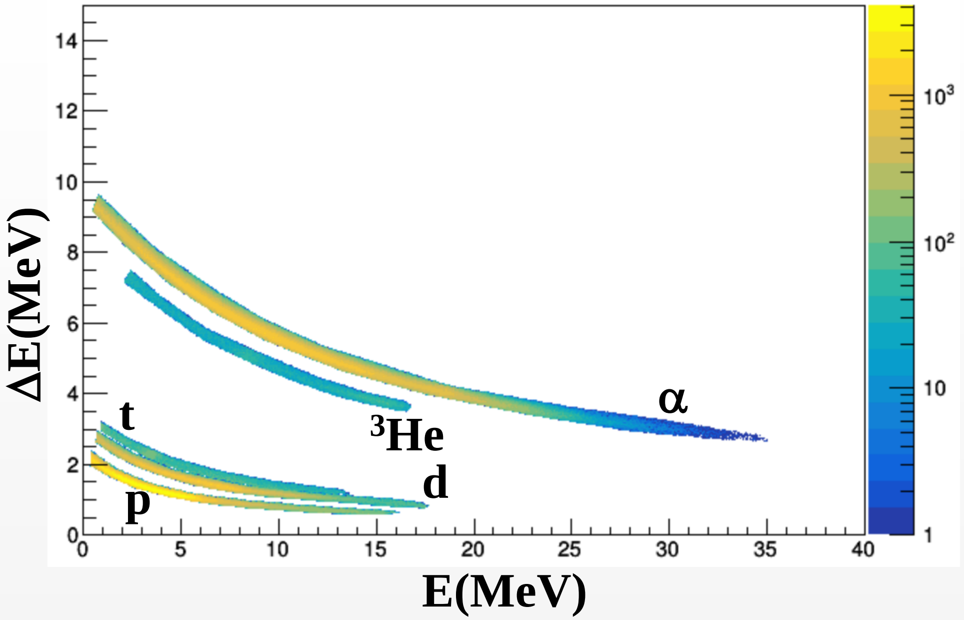

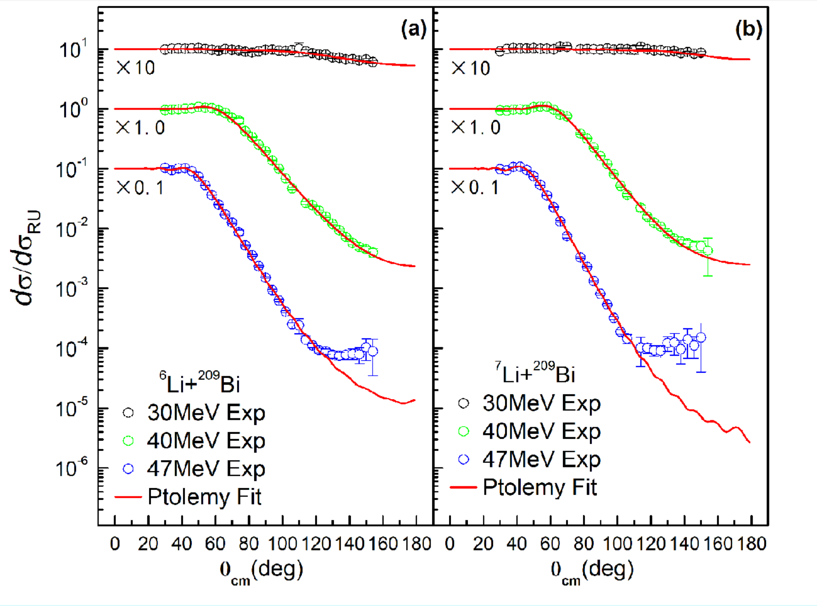

	E_{beam} (MeV)	^{6}Li				^{7}Li		
		α + α	α + t	α + d	α + p	α + α	α + t	α + d
a	30.0	2.2%	0.4%	57.2%	40.2%	50.2%	30.1%	19.7%
	40.0	4.6%	2.7%	50.6%	42.1%	44.8%	33.7%	21.5%
	47.0	2.9%	4.0%	60.5%	32.6%	38.7%	32.1%	29.2%
b	30.0	2.4%	0.4%	49.4%	47.8%	48.5%	31.6%	19.9%
	40.0	5.3%	2.6%	41.5%	50.7%	53.3%	35.0%	11.7%
	47.0	4.0%	4.8%	44.2%	47.0%	55.2%	34.9%	9.9%

1、首次得到近垒和垒上各破裂道的百分比
2、在垒上，转移引起的破裂扮演重要作用

Yao Yongjin et al, Nucl. Sci. Tech 32 (2021) 14.
Yao Yongjin et al., Chin. Phys. C 45 (2021) 054104.

构建反应Q值谱

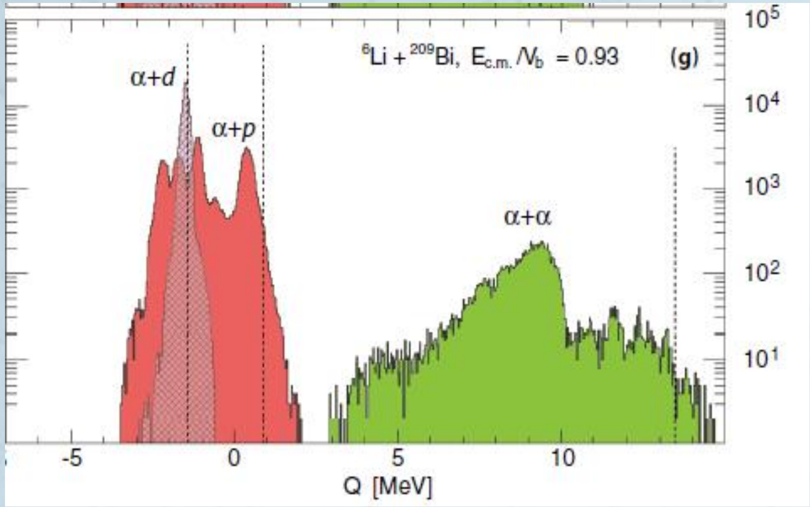

D. H. Luong,et al., Phys. Rev. C 88, 034609 (2013)

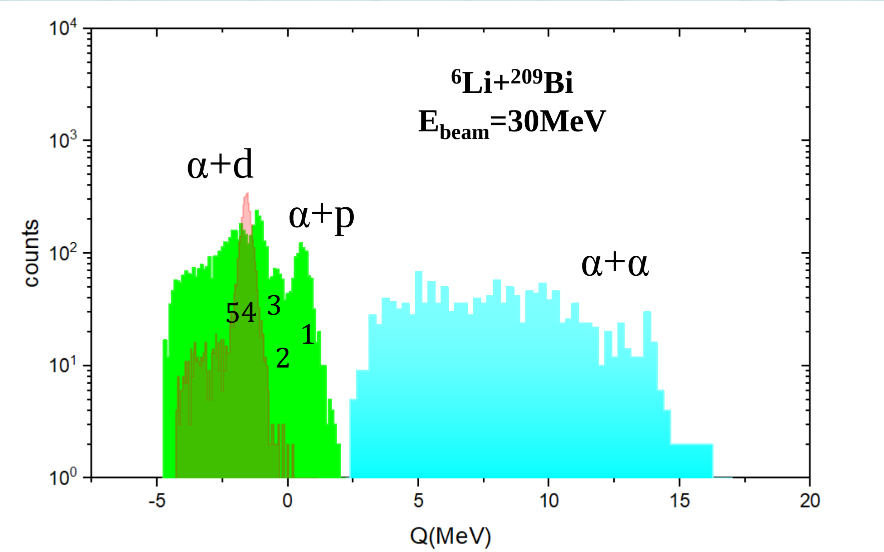

<table>
<tr><th colspan="5">α+p (^{210}Bi)</th><th colspan="2">α+d (^{209}Bi)</th><th colspan="2">α+α (^{207}Pb)</th></tr>
<tr><td colspan="4">理论Qgg:0.906MeV</td><td>210Bi激发能</td><td colspan="2">理论Qgg：-1.473MeV</td><td>理论Qgg</td><td>13.57MeV</td></tr>
<tr><td>峰1-文献Aus</td><td>0.380MeV</td><td>峰1-exp</td><td>0.466MeV(σ=0.3)</td><td>440keV左右</td><td>文献Aus</td><td>-1.545MeV</td><td>文献Aus</td><td>无明显峰型</td></tr>
<tr><td>峰2-文献Aus</td><td>-0.581MeV</td><td>峰2-exp</td><td>-0.489MeV(σ=0.28)</td><td>1395keV左右</td><td>exp</td><td>-1.609MeV(σ=0.22)</td><td>exp</td><td>无明显峰型</td></tr>
<tr><td>峰3-文献Aus</td><td>-1.152MeV</td><td>峰3-exp</td><td>-1.214MeV(σ=0.29)</td><td>2120keV左右</td><td colspan="2" rowspan="3">209Bi基态</td><td colspan="2" rowspan="3">推测可能存在^{207}Pb多个激发态，能量集中在0-10MeV之间</td></tr>
<tr><td>峰4-文献Aus</td><td>-1.722MeV</td><td>峰4-exp</td><td>-1.772MeV(σ=0.17)</td><td>2678keV左右</td></tr>
<tr><td>峰5-文献Aus</td><td>-2.186MeV</td><td>峰5-exp</td><td>-2.105MeV(σ=0.52)</td><td>3011keV左右</td></tr>
</table>

Q:E_{rel}二维谱

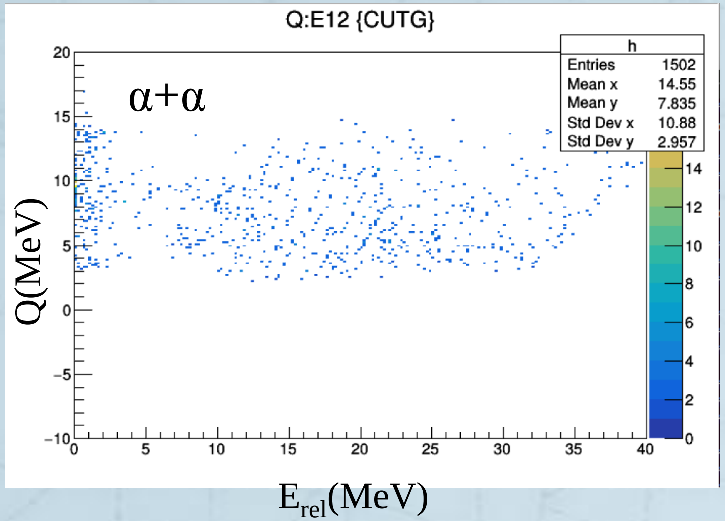

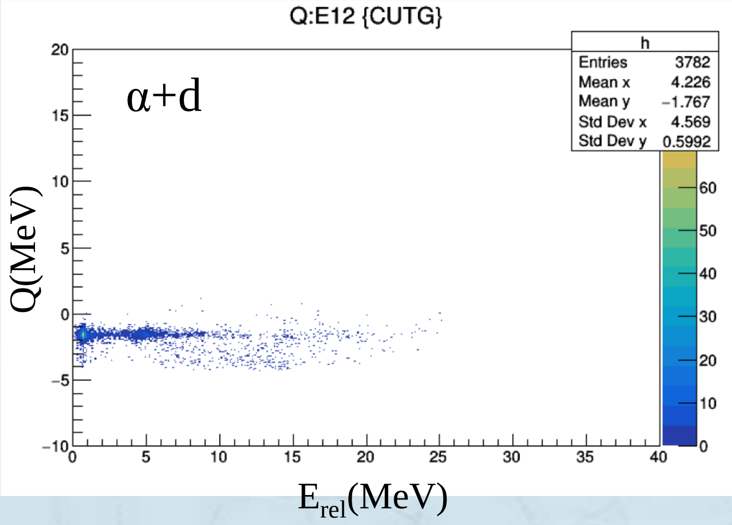

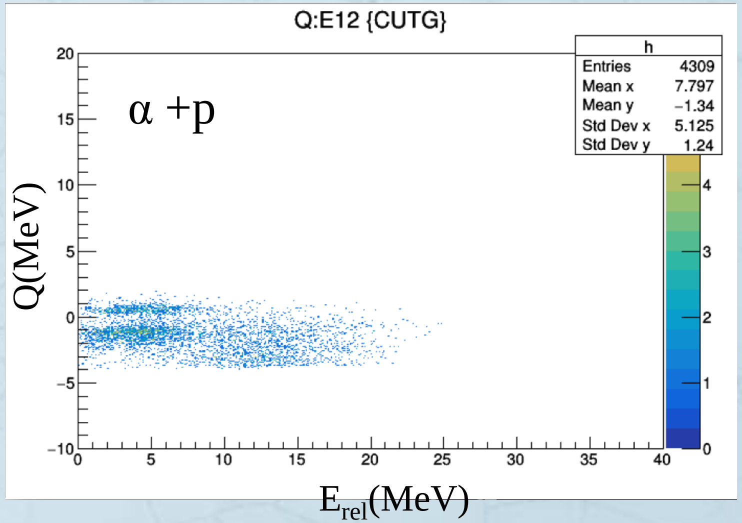

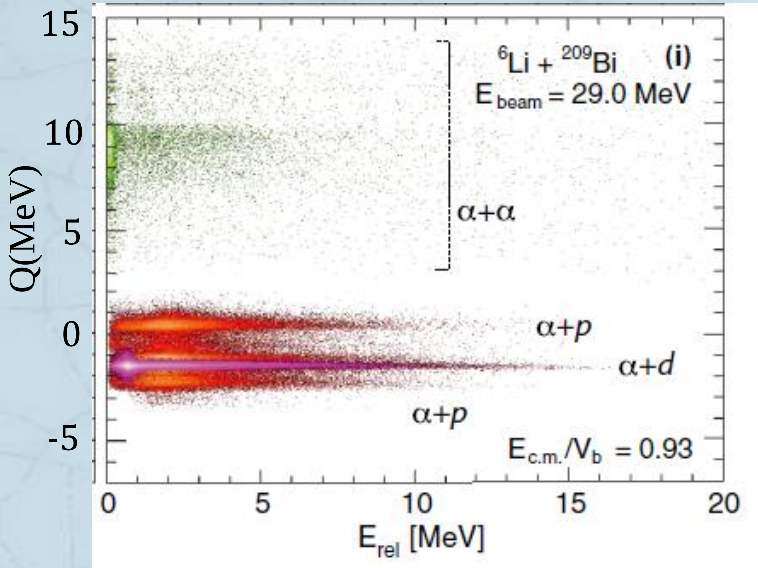

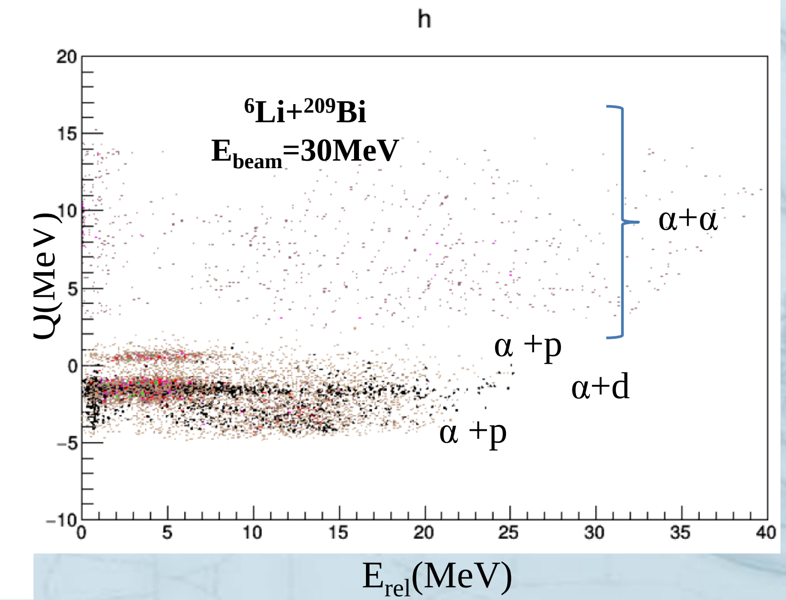

D. H. Luong,et al., Phys. Rev. C 88, 034609 (2013)

- α+α无明显Q值峰， E_{rel}在0MeV附近成峰
- α+d中可以观察一个明显的Q值峰， E_{rel}在0.7MeV附近成峰
- α +p中可以看到多条Q值峰，分布在-3至2MeV之间，在文献中， E_{rel}在2MeV附近成峰，我们的数据中， E_{rel}在2-6MeV之间连续分布，存在多个峰重叠

β : θ_{12}二维谱

^{6}Li+^{209}Bi-30MeV

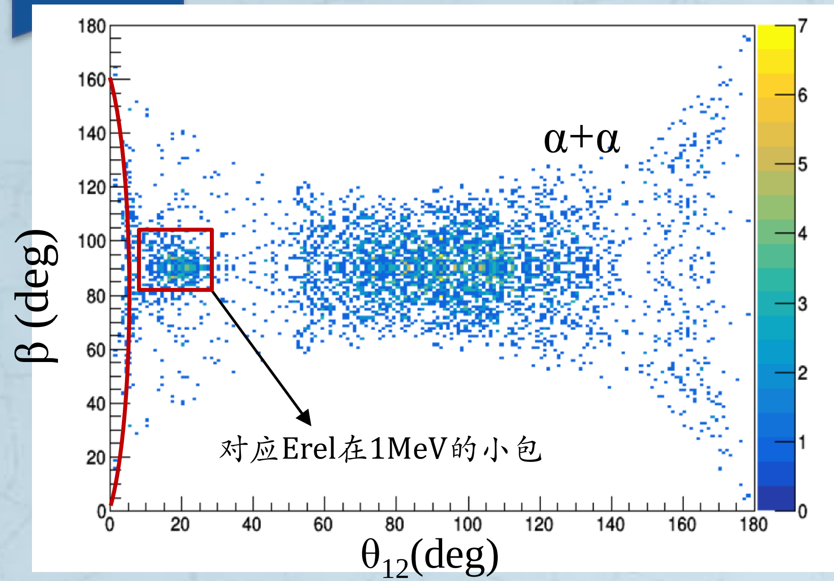

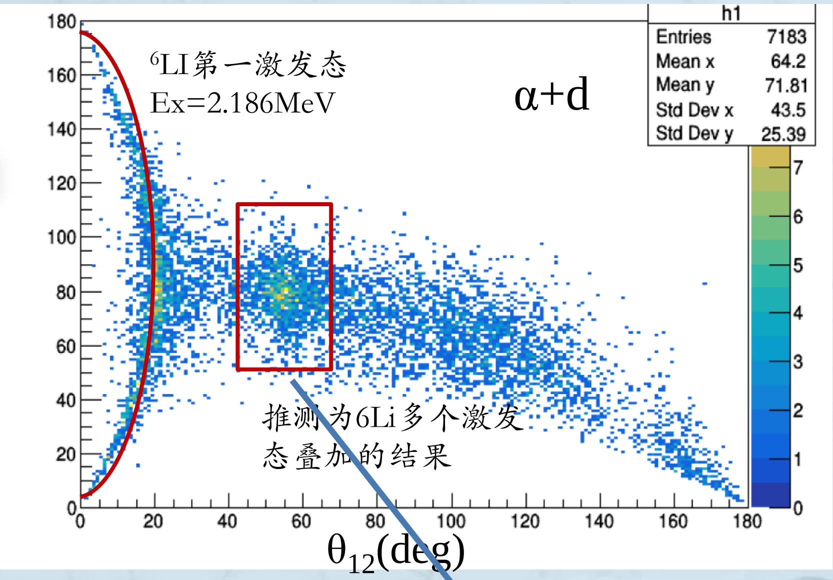

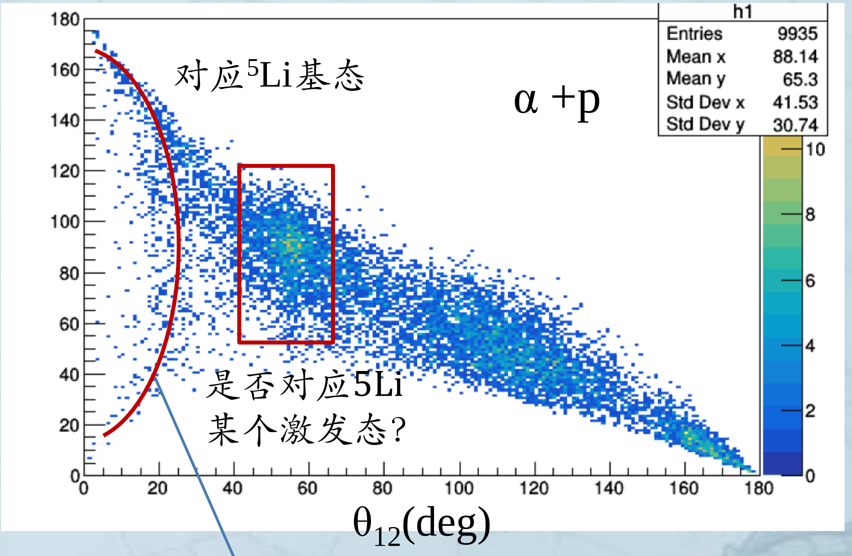

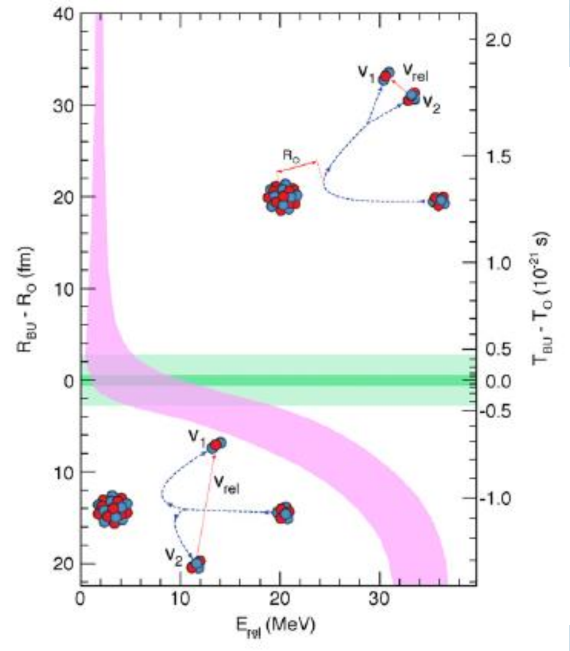

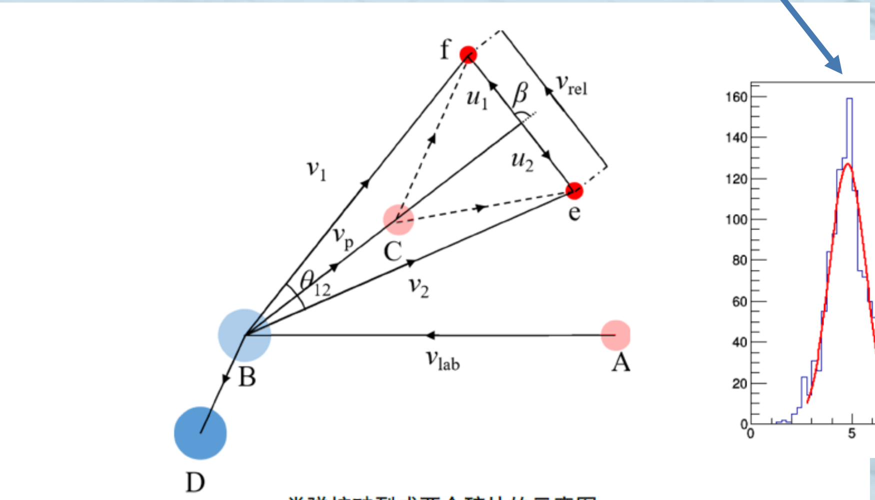

类弹核破裂成两个碎片的示意图。

A 是弹核，B 是靶核，C 是类弹核，D 是类靶核，e 和 f 是类弹核破裂的两个碎片。

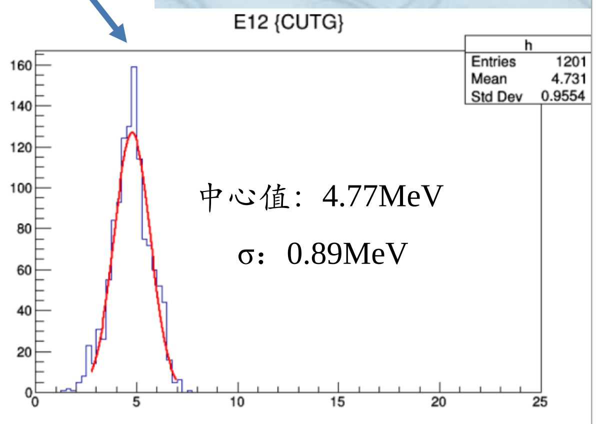

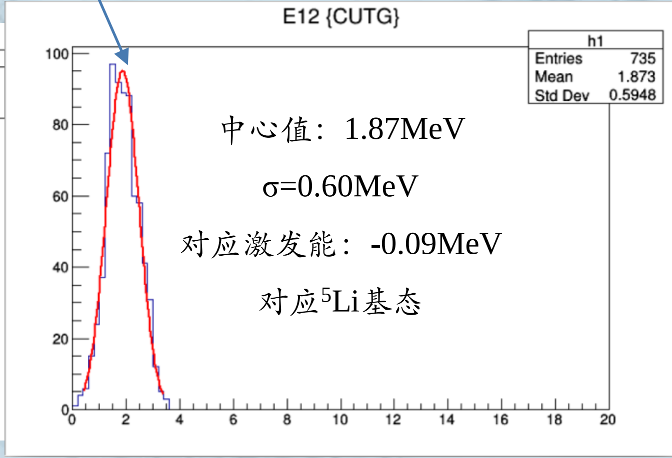

E_{rel}相对能谱（α+d）

$^{6}Li+^{209}Bi$-30MeV

Q_{bu}= -1.47MeV，$E_{rel}=Q_{bu}+E_x$（类弹核激发能）

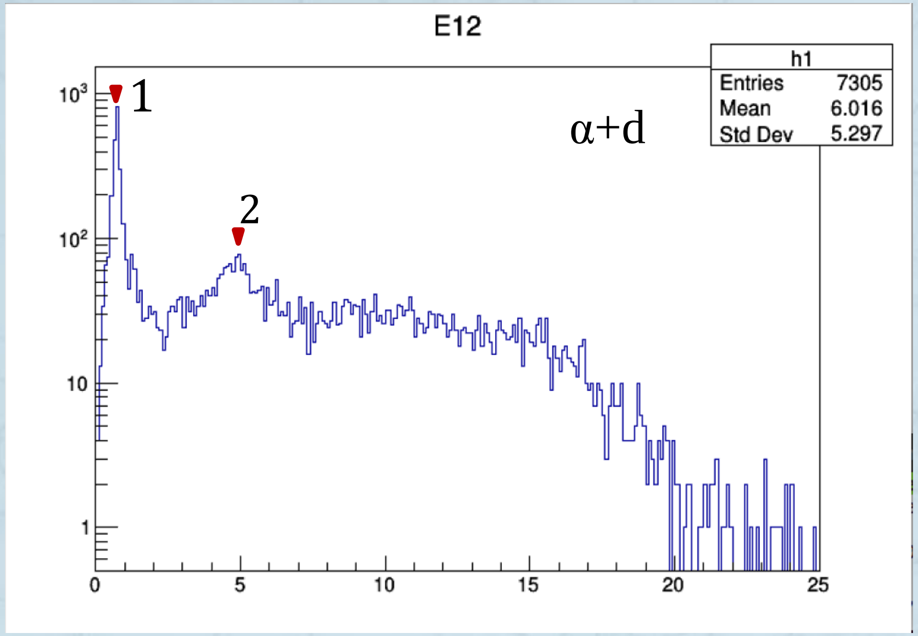

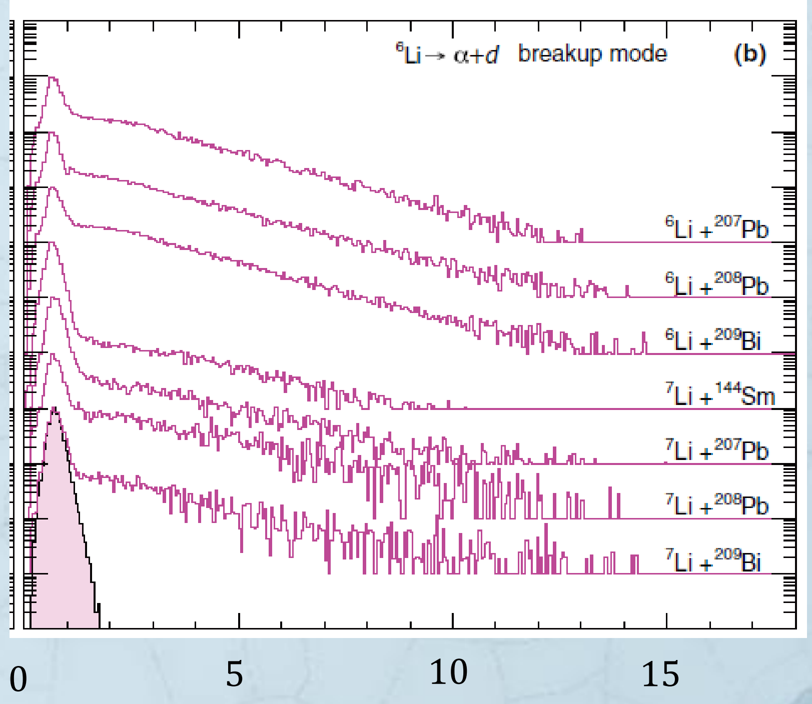

Luong 6,7Li+209Bi（Ebeam=29MeV）

E(level) (keV)	XREF	J^{π}(level)	$T_{1/2}$(level)	E(γ) (keV)	M(γ)
0.0	AB DEFGHIJKLMNO QRSTUVW	1+	STABLE		
2186 *2*	BCDEFGHIJKLMNOPQRSTUV	3+	24 keV *2* % IT = ? % α = ?	2186	E2
3562.88 *10*	B DEFGH J LMNOPQ W	0+	8.2 eV *2* % IT = ?	3561.75	M1
4312 *22*	BCDEFG K MNOP U	2+	1.30 MeV *10* % IT = ? % α = ?	4310	E2
5366 *15*	B D F MNOP R	2+	541 keV *20* % IT = ? % n = ? % p = ? % α = ?	5363	M1
5.65E3 *5*	C F K OP R	1+	1.5 MeV *2* % α = ?		
15.8E3?	B	3+	17.8 MeV *8* % α = ?		

- 峰1中心值为：0.72MeV(σ=0.21)，对应激发能为2.19MeV,对应^{6}Li第一激发态
- 峰2存在一个小包,中心值：4.75MeV（σ=0.76），对应激发能为6.22MeV,推测是^{6}Li多个激发态叠加的结果（4312.22keV、5366.15keV、5650keV）

束流：^{28}Si(138MeV)

靶 ：^{74}Ge(600μg/cm^2)

Ta(10mg/cm^2)

New energy levels of ^{92}Mo

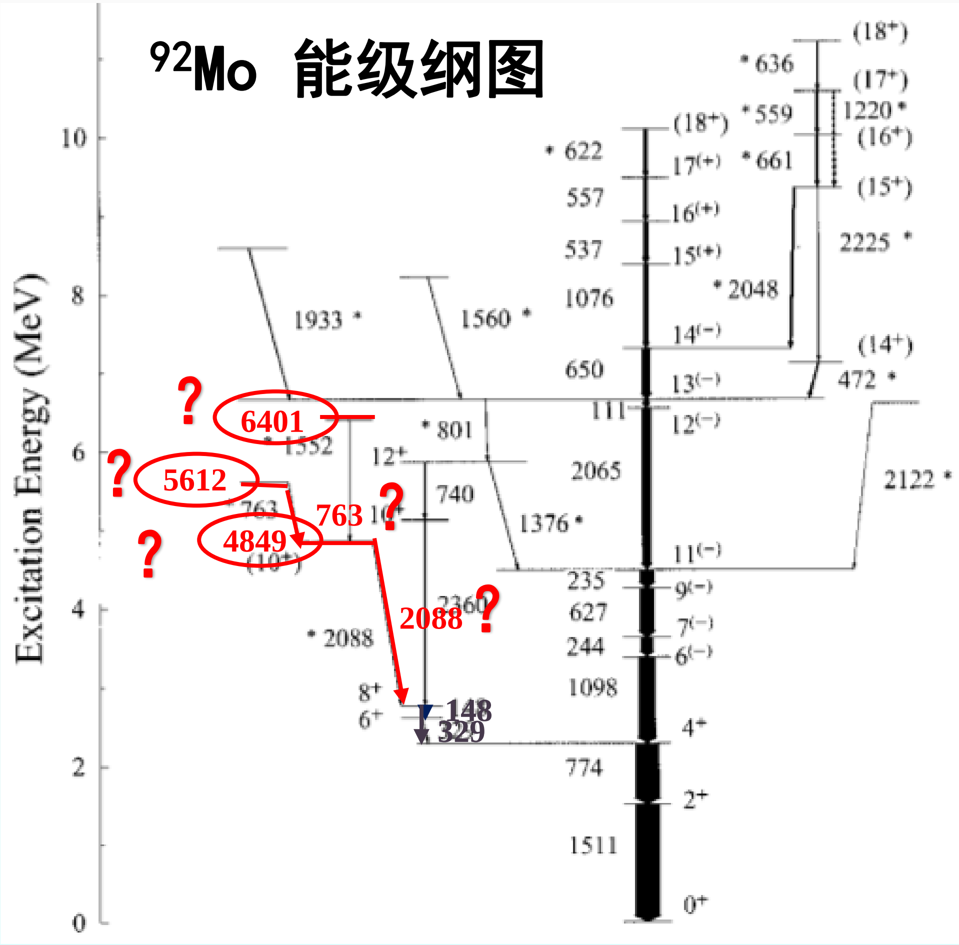

PHYSICAL REVIEW C, VOLUME 65, 044324

Level structure of ^{92}Mo at high angular momentum: Evidence for $Z=38$, $N=50$ core excitation

N. S. Pattabiraman, S. N. Chintalapudi, and S. S. Ghugre

Inter University Consortium For DAE Facilities, Calcutta Centre, Sector III LB-8, Bidhan Nagar, Kolkata 700 098, India

B. V. Tirumala Rao, M. L. N. Raju, and T. Seshi Reddy

Department of Nuclear Physics, Andhra University, Visakhapatnam 530 003, India

P. K. Joshi, R. Palit, and H. C. Jain

Tata Institute of Fundamental Research, Dr Homi Babha Road, Mumbai 400 005, India

(Received 13 July 2001; published 3 April 2002)

疑问：

- 能级6401keV，5612keV，4849keV的放置存在异议。

结论：

- 763keV，2088keV，148keV和329keV这一级联关系不属于^{92}Mo，应该属于^{92}Nb。

N . S. Pattabiraman et al ., Phys. Rev. C65,044324(2002)

- 763keV 和2088keV与148keV有符合，与1510keV无符合。
- 329keV 、763keV、 148keV和2088keV这一级联关系不属于^{92}Mo

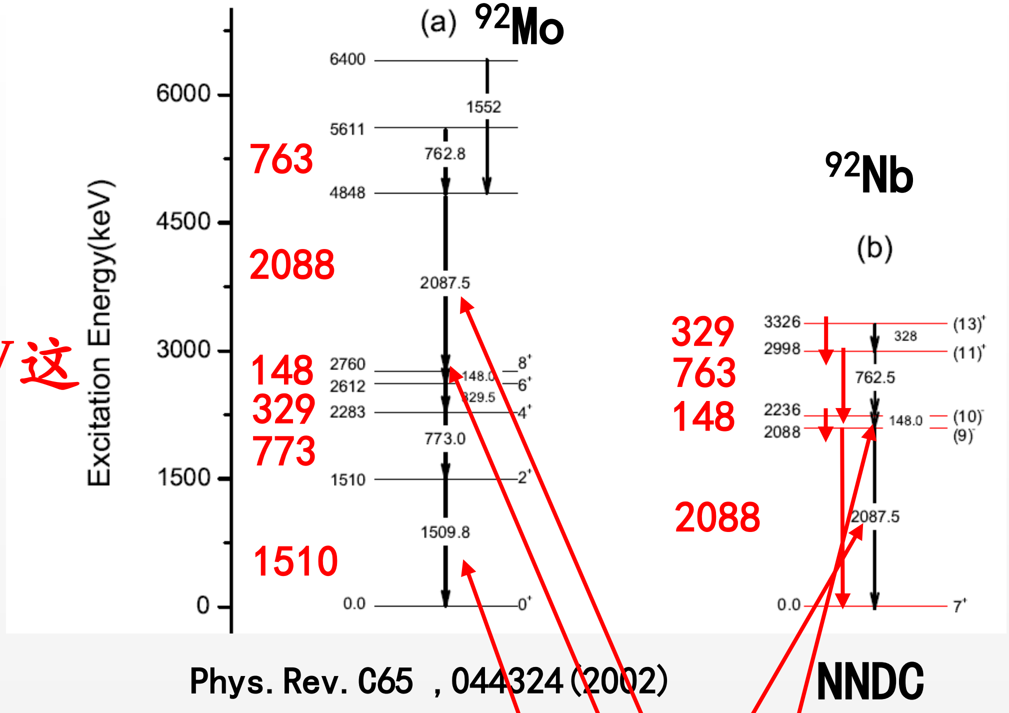

我们的结果

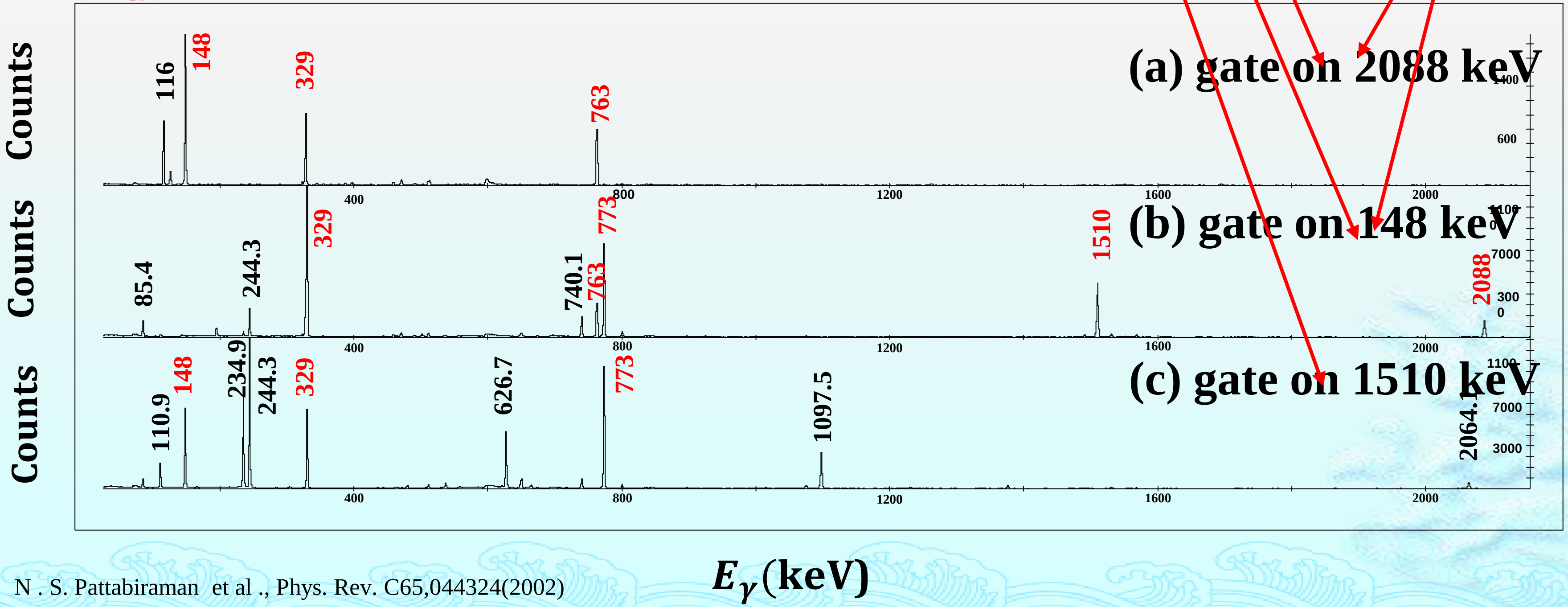

N . S. Pattabiraman et al ., Phys. Rev. C65,044324(2002)

$$^{6}Li + {}^{89}Y \rightarrow {}^{95}Mo \rightarrow \begin{cases} 3n + {}^{92}Mo \\ p + 2n + {}^{92}Nb \end{cases}$$

质子开窗的 γ 能谱

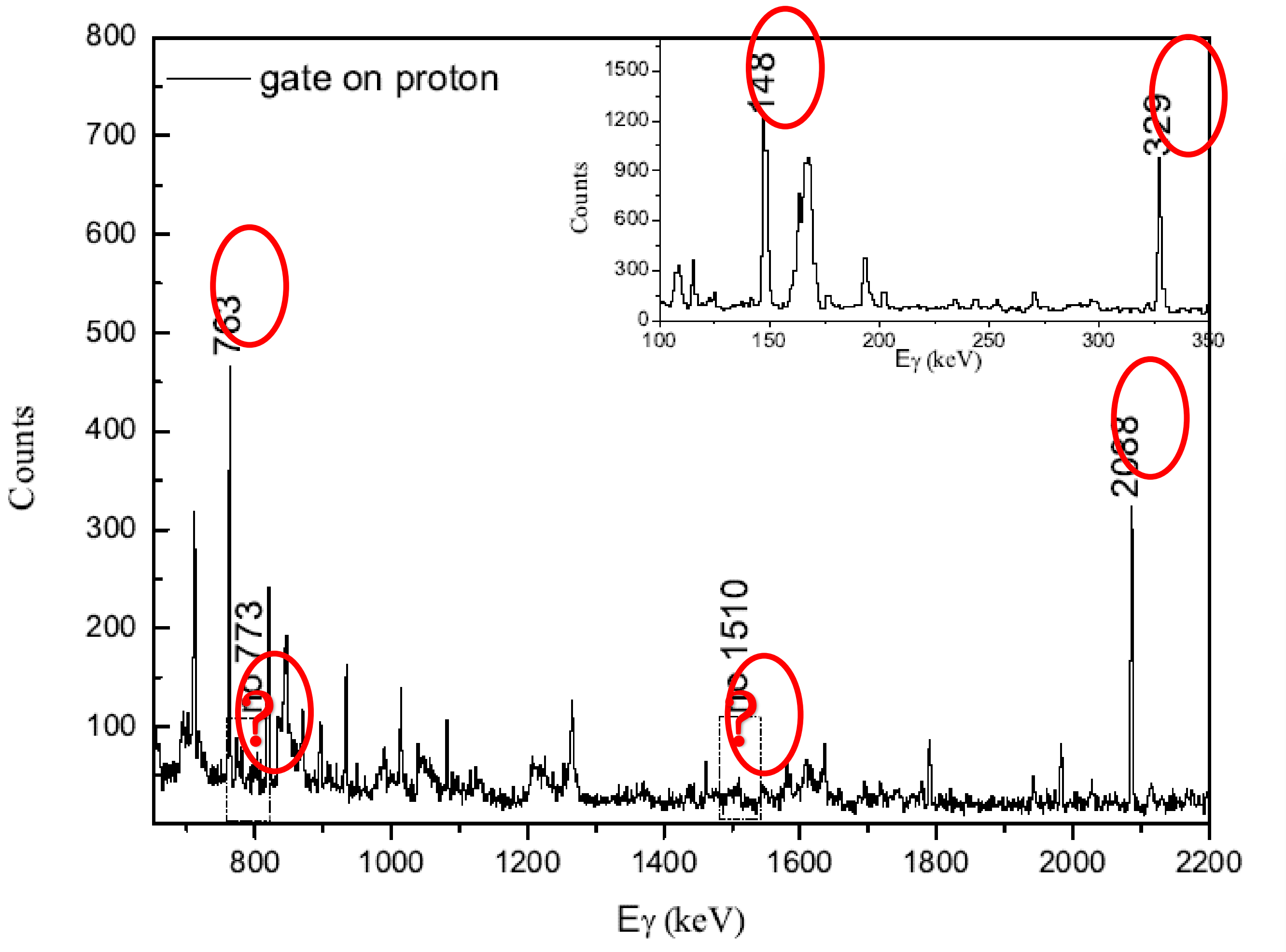

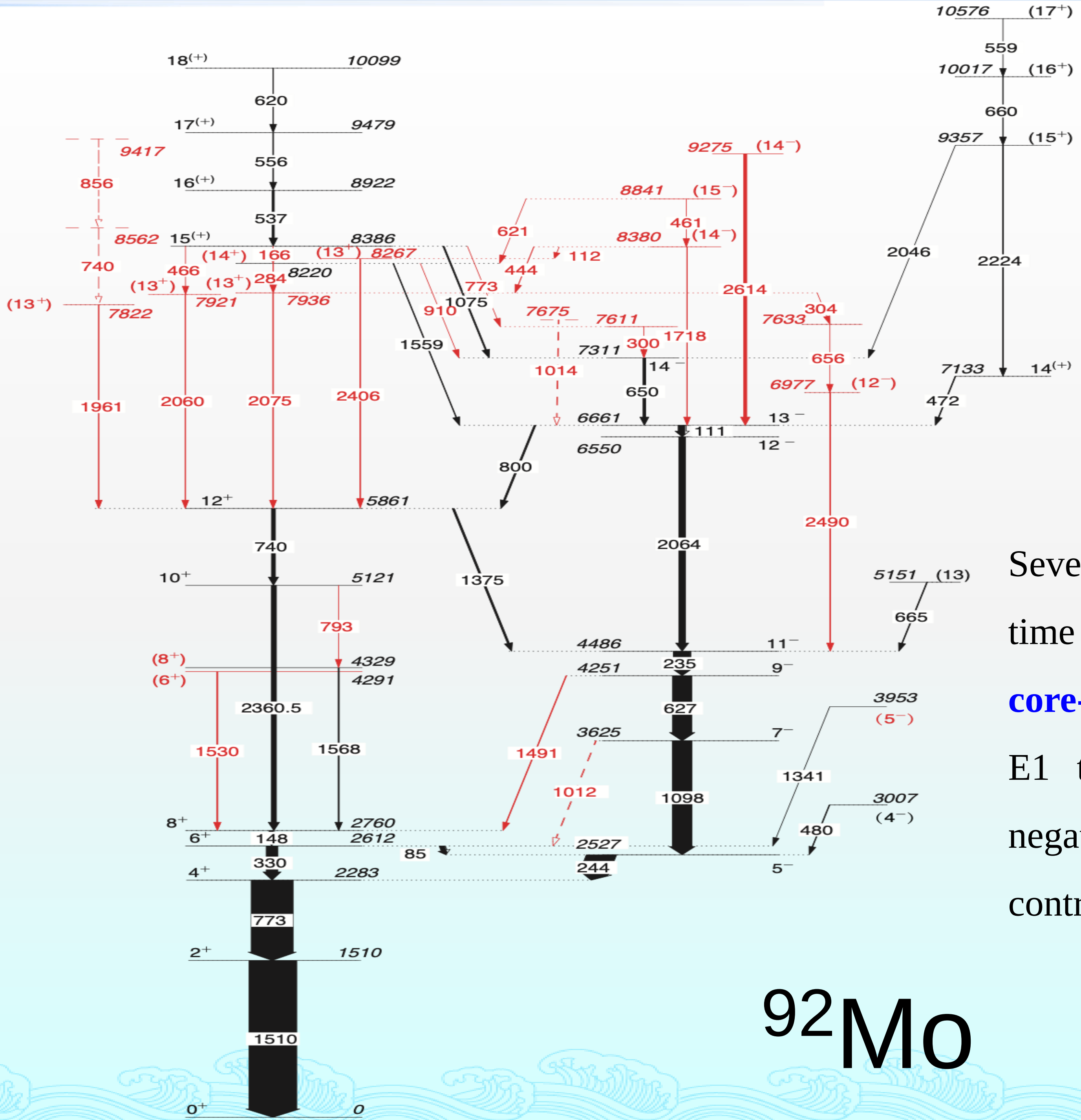

^{92}Mo

✓ 14 new states

✓ 24 new γ-rays

Several ~2 MeV transitions observed for the first time could be a presumable signature of **N=50 core-breaking effect**. The measured strengths of E1 transitions between low-lying positive and negative bands indicates an importance contribution from **Z = 28 proton core-excitation**.

Angular distribution of γ rays emitted by oriented nuclei: the case of ^{92}Mo

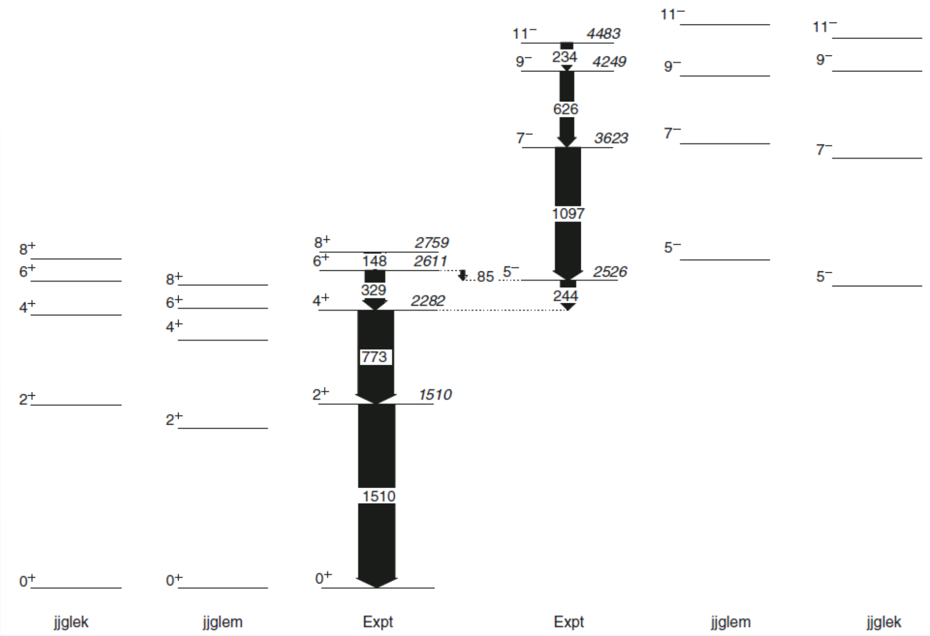

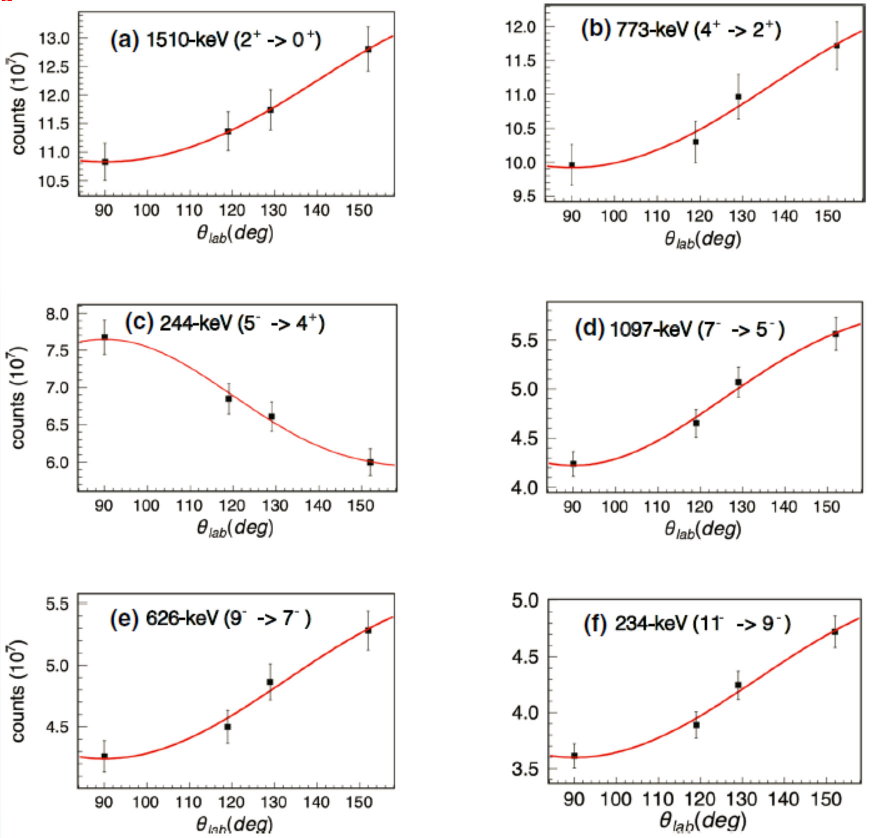

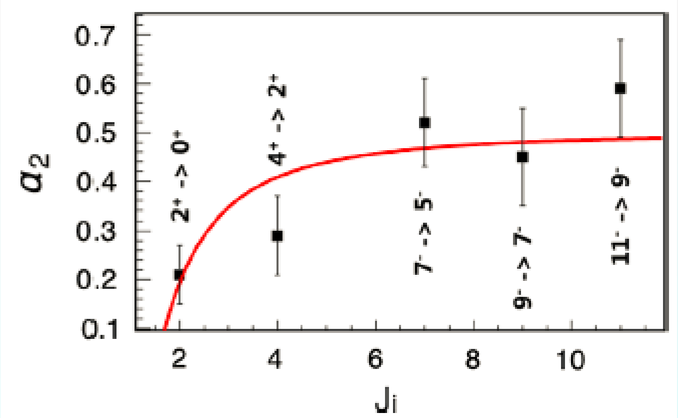

$$\alpha_2 = D\left(1 - \frac{3\sigma^2}{J_i(J_i+1)}\right)$$

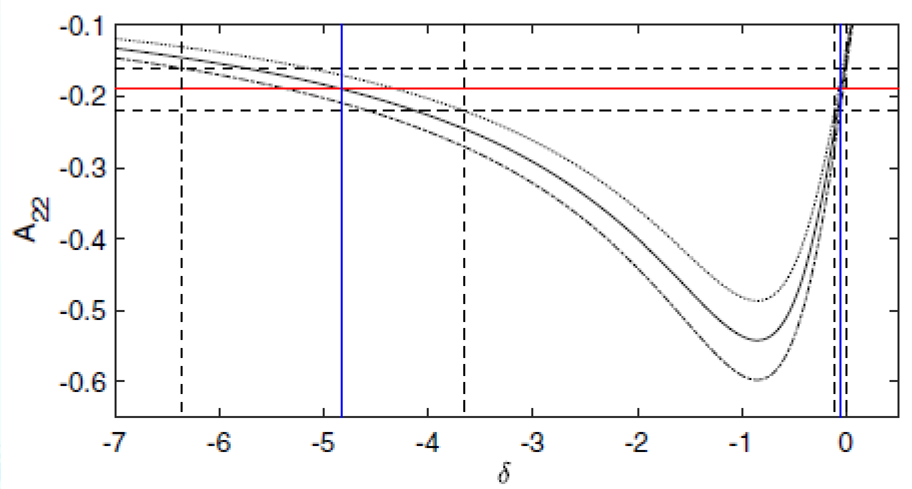

Z. Huang et al., Eur. Phys. J. A57 (2021) 137

^{91}Mo level scheme

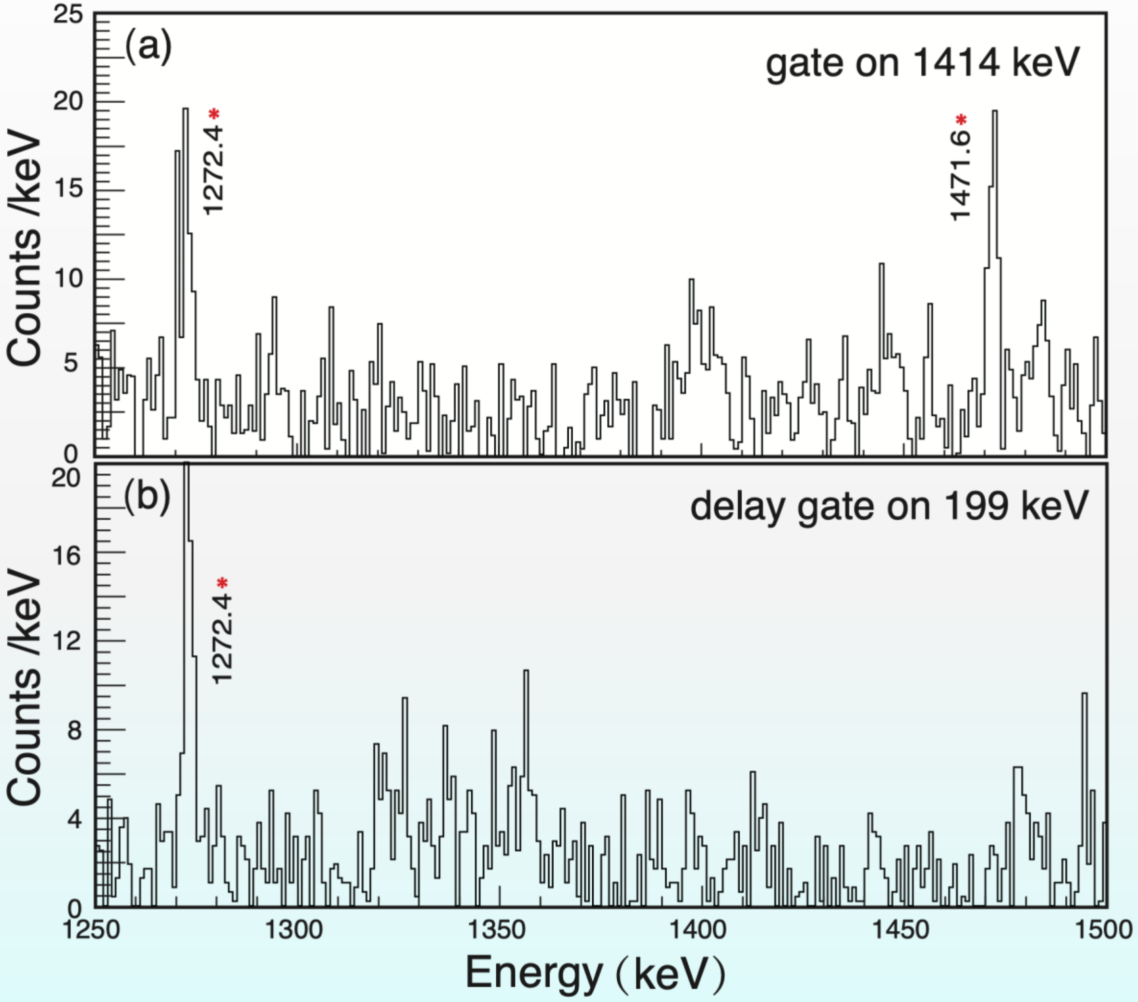

-500~-60 ns   197-201 keV

Background:170-180 keV

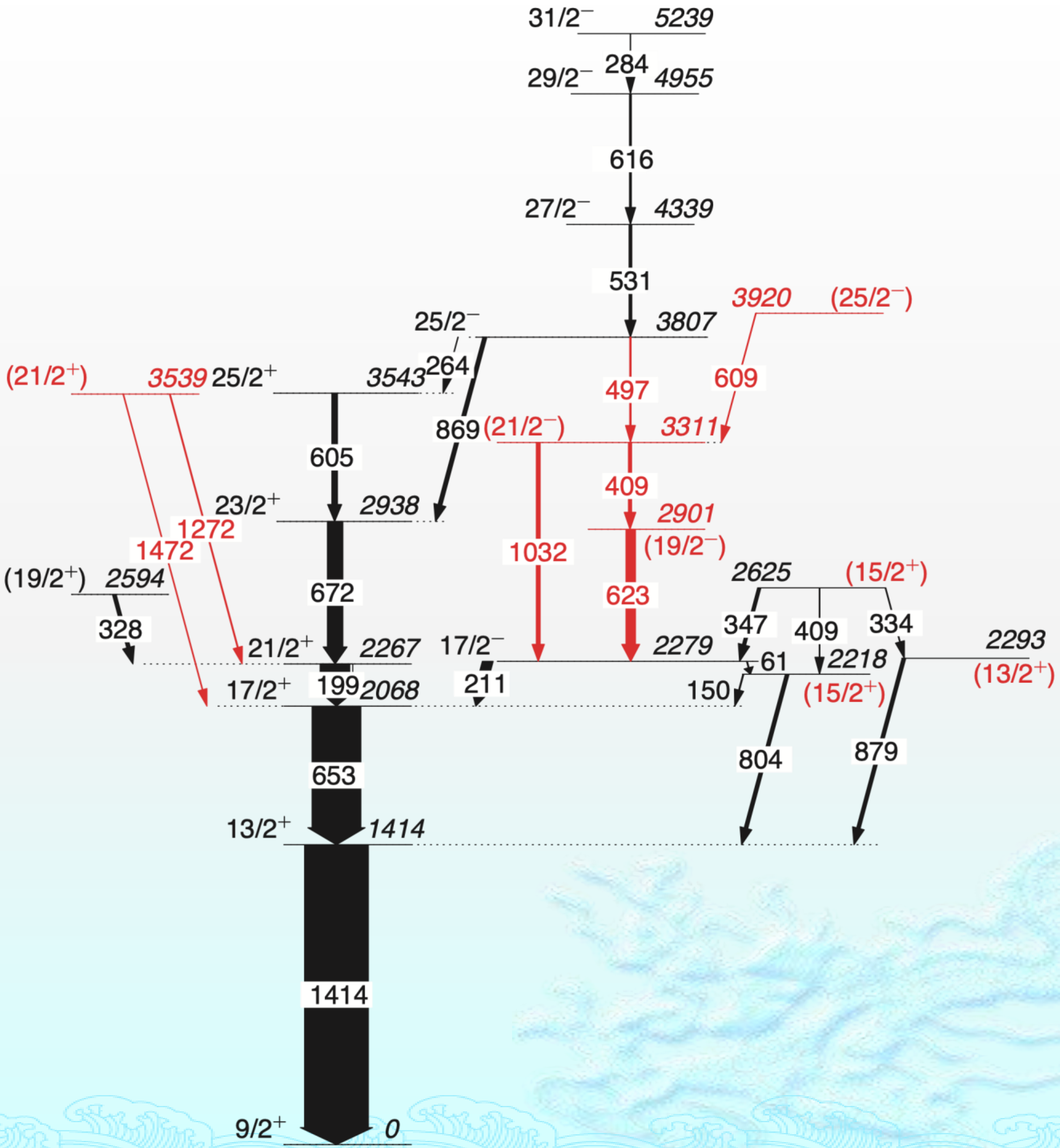

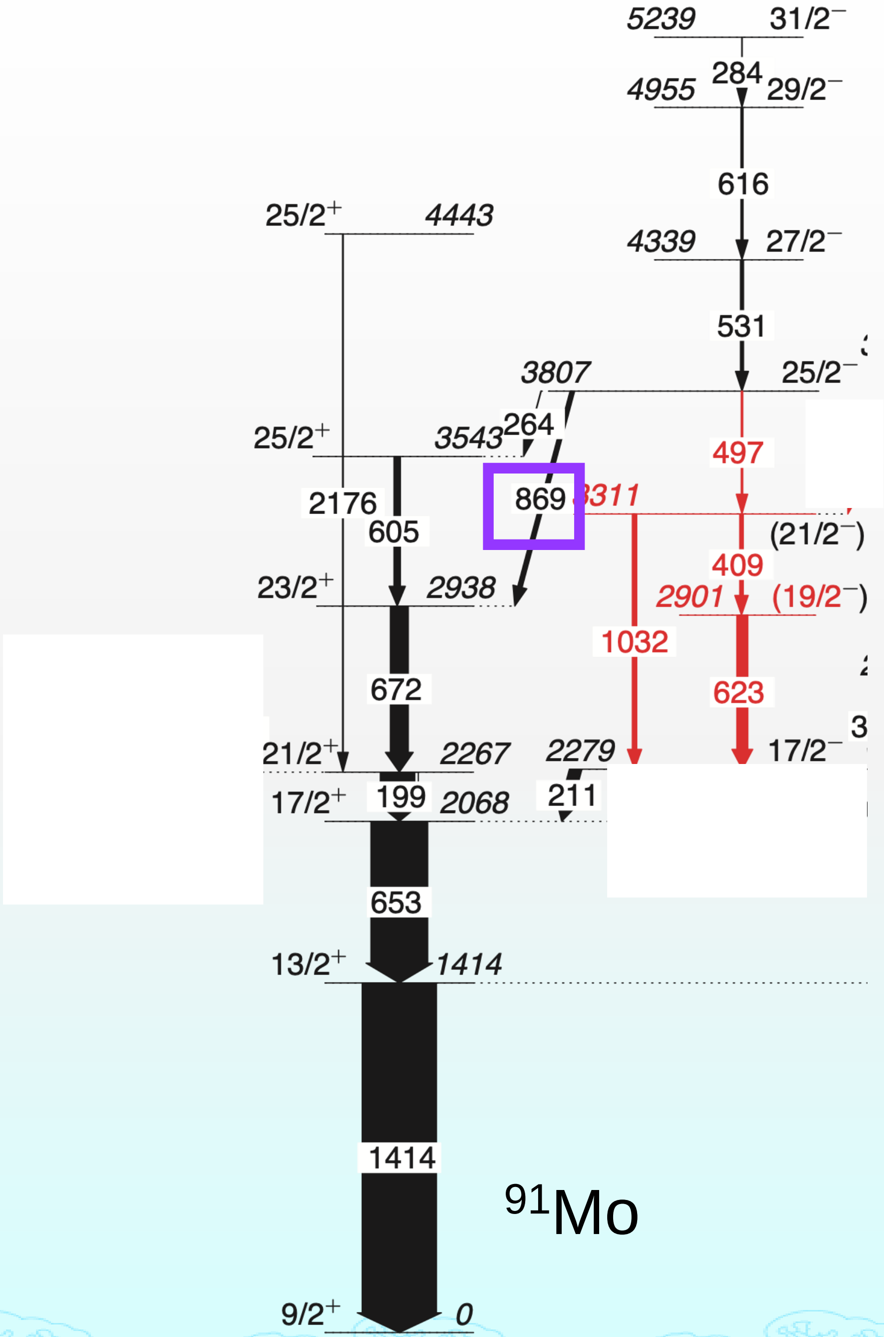

5239 31/2⁻
284
4955 29/2⁻
616
25/2+ 4443
4339 27/2⁻
531
3807 25/2⁻
25/2+ 3543 264
497
2176
605
869
3311
(21/2⁻)
409
23/2+ 2938
2901 (19/2⁻)
1032
672
623
21/2+ 2267
2279
17/2⁻
17/2+ 199 2068
211
653
13/2+ 1414
1414
9/2+ 0
91Mo

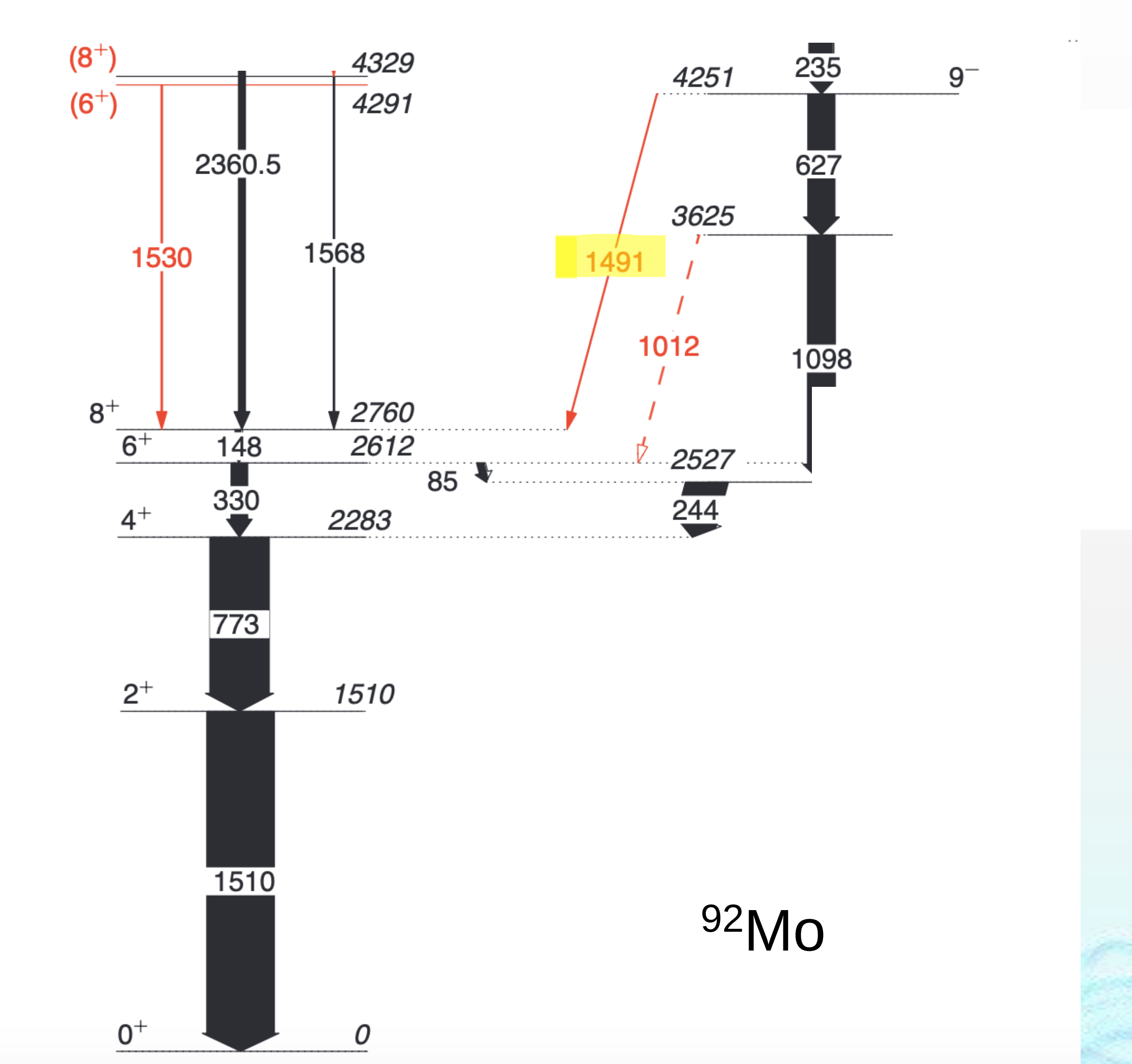

(8+) 4329
(6+) 4291
4251 235 9⁻
2360.5
627
3625
1530
1568
1491
1012
1098
8+ 2760
6+ 148 2612
2527
85
330
244
4+ 2283
773
2+ 1510
1510
0+ 0
92Mo

New energy levels of ^{92,93}Nb

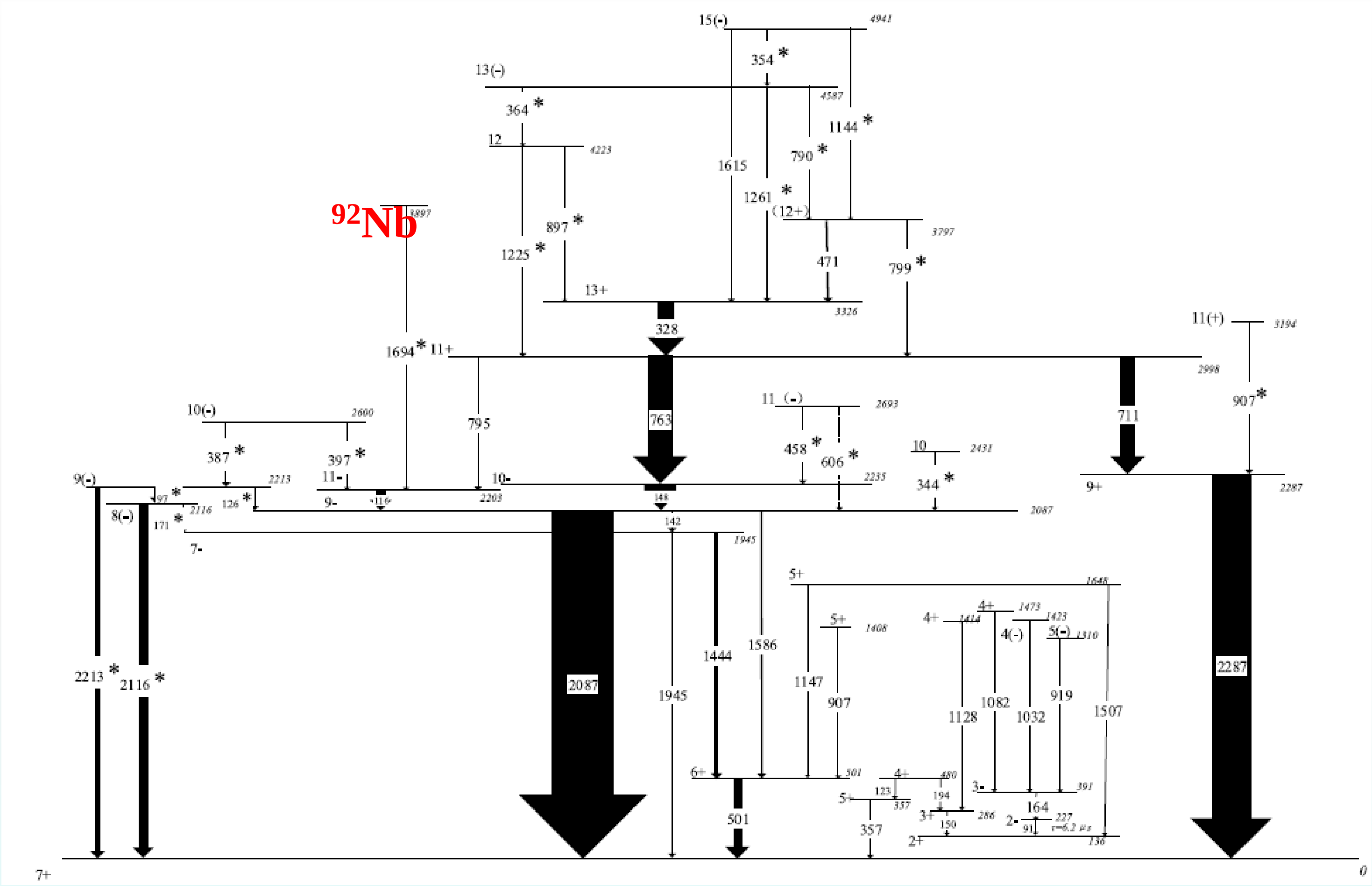

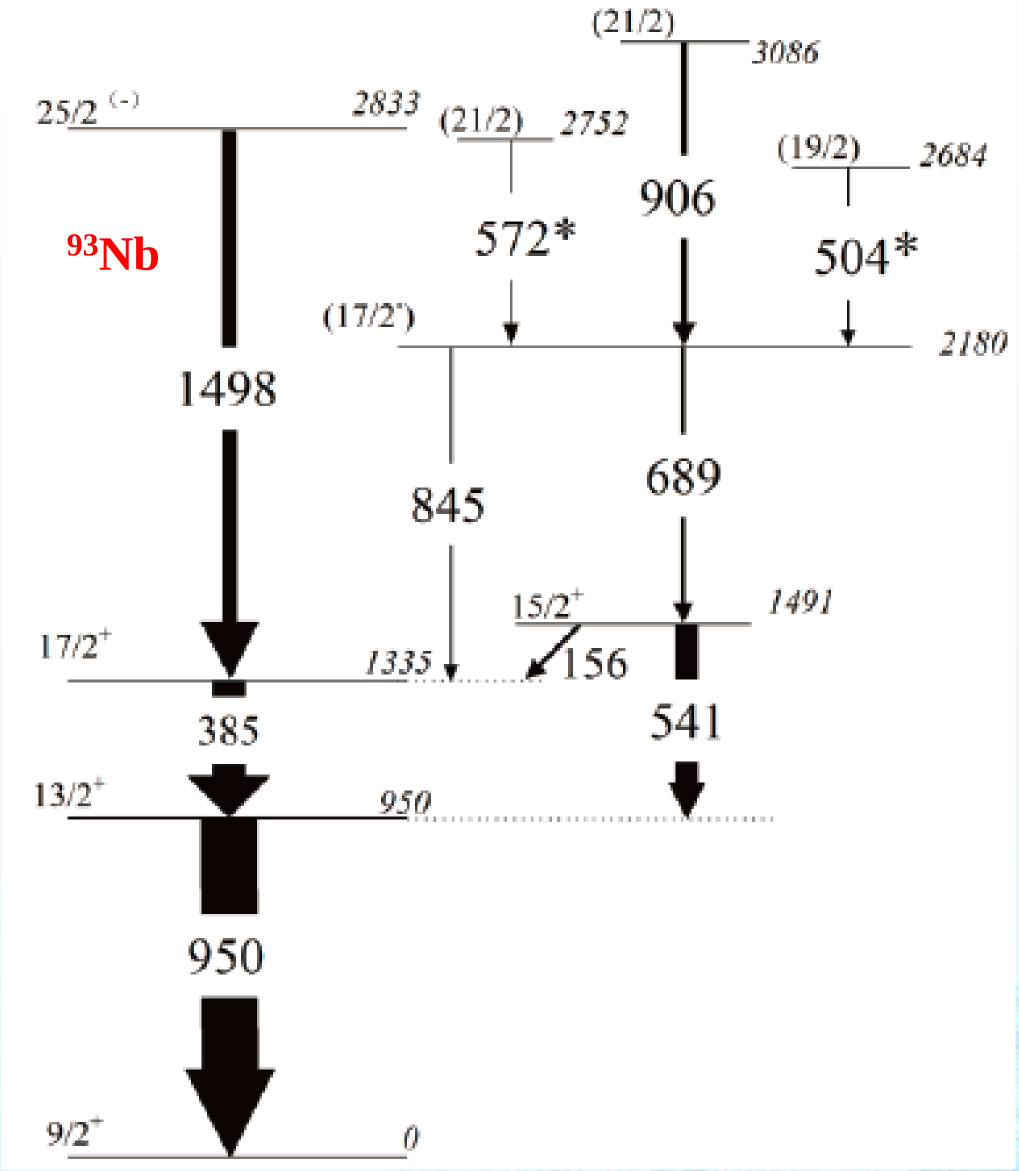

Shell model calculations were performed with the code NushellX to reconstruct the level structure of ^{92}Nb, where SNE valence space and SNET interaction were used. **The results agree well with the experimental data.**

Lv Yifeng et al., Chin. Phys. C43 (2019) 104102

Zhen Ren et al., Phys. Rev. C106 (2022) 024323.

New energy levels of ^{89}Zr, ^{91}Mo

^{89}Zr

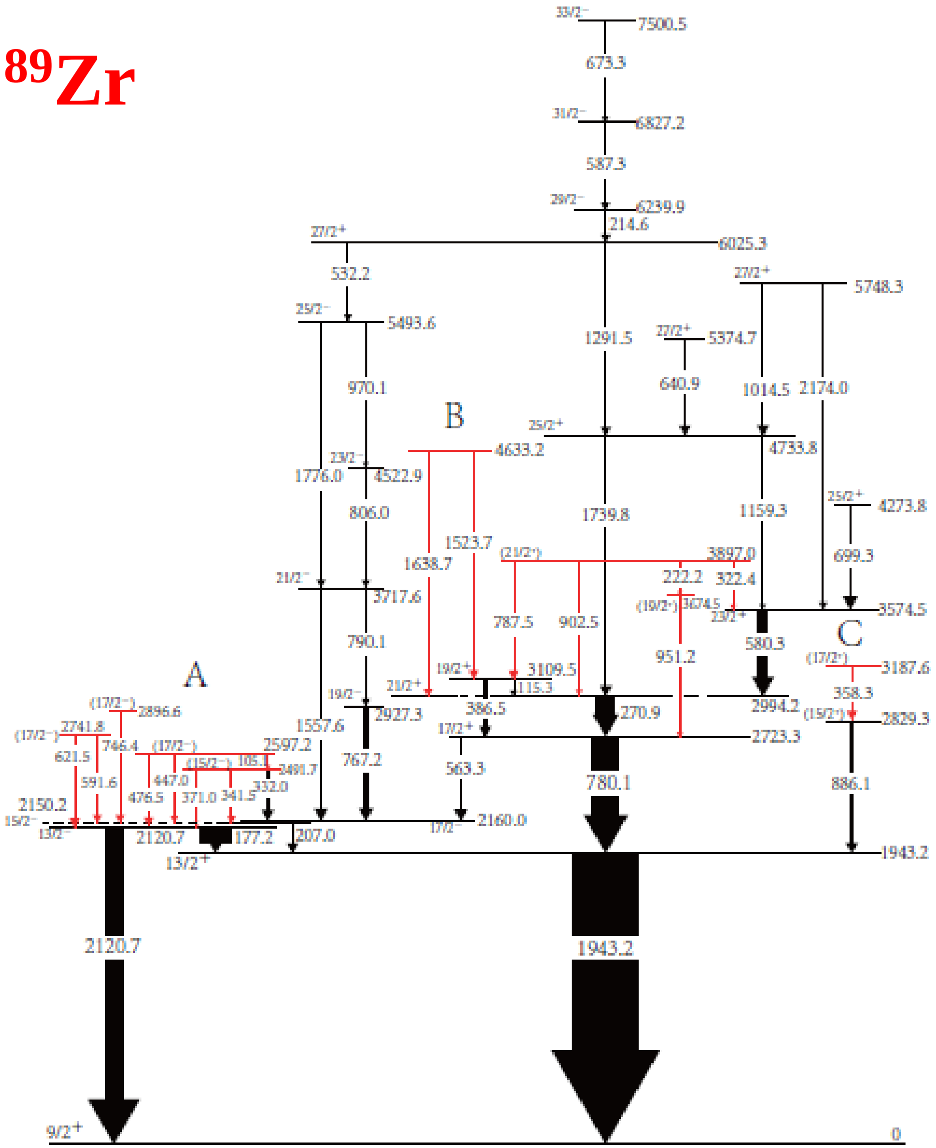

^{91}Mo

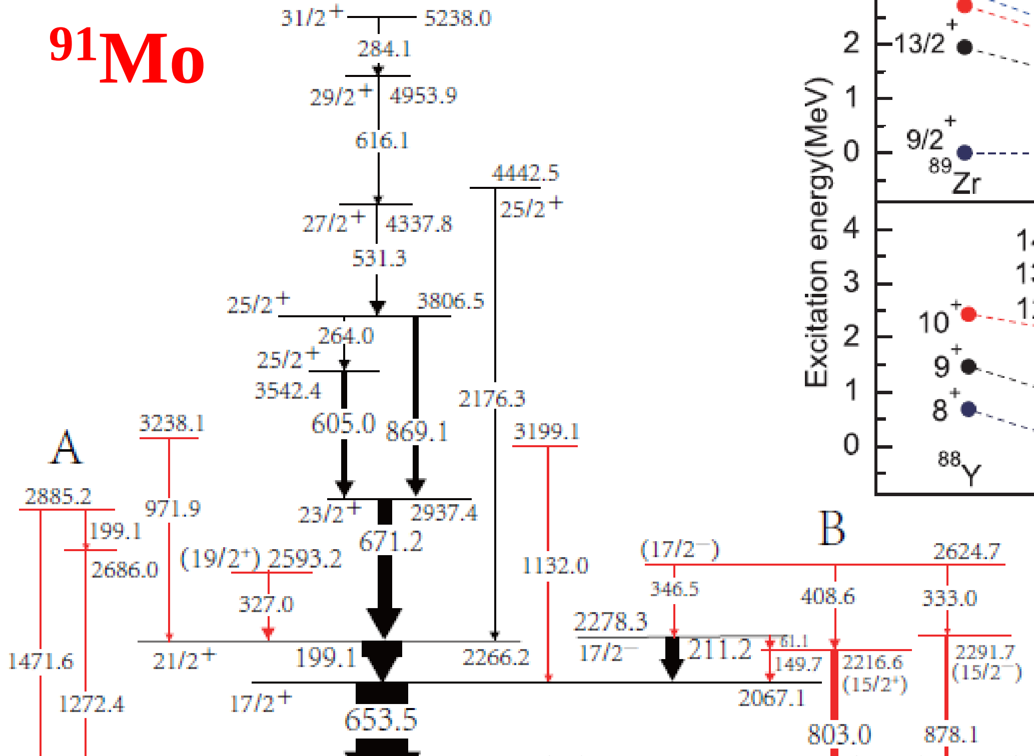

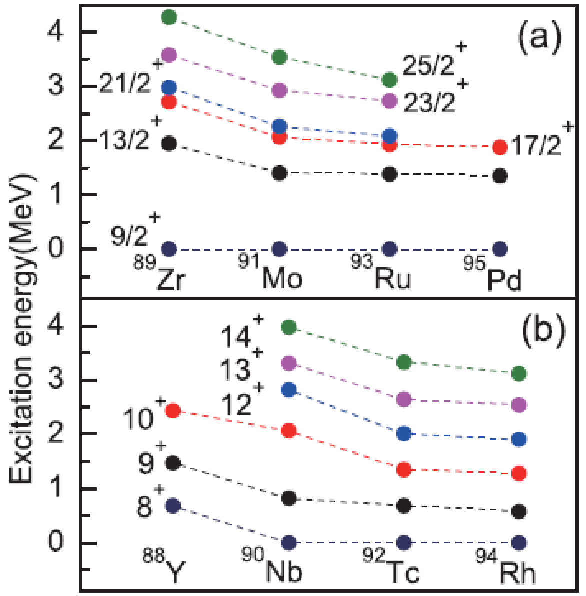

Low lying states are dominated by particle excitations from the $\pi p1/2$ orbit to the $\pi g9/2$ orbit. With the increase of the excitation energy, **the states are well described by proton excitations across the Z = 38 subshell into higher orbits.** Finally, By studying the systematic features of N = 49 isotones, with the increase of proton number, **the valence protons becoming closer to the high- j $\pi g9/2$ causes the decrease of the excitation energies for the same states.**

New energy levels of ^{212}Rn

C. B. Li et al., Phys. Rev. C 101 (2020) 044313

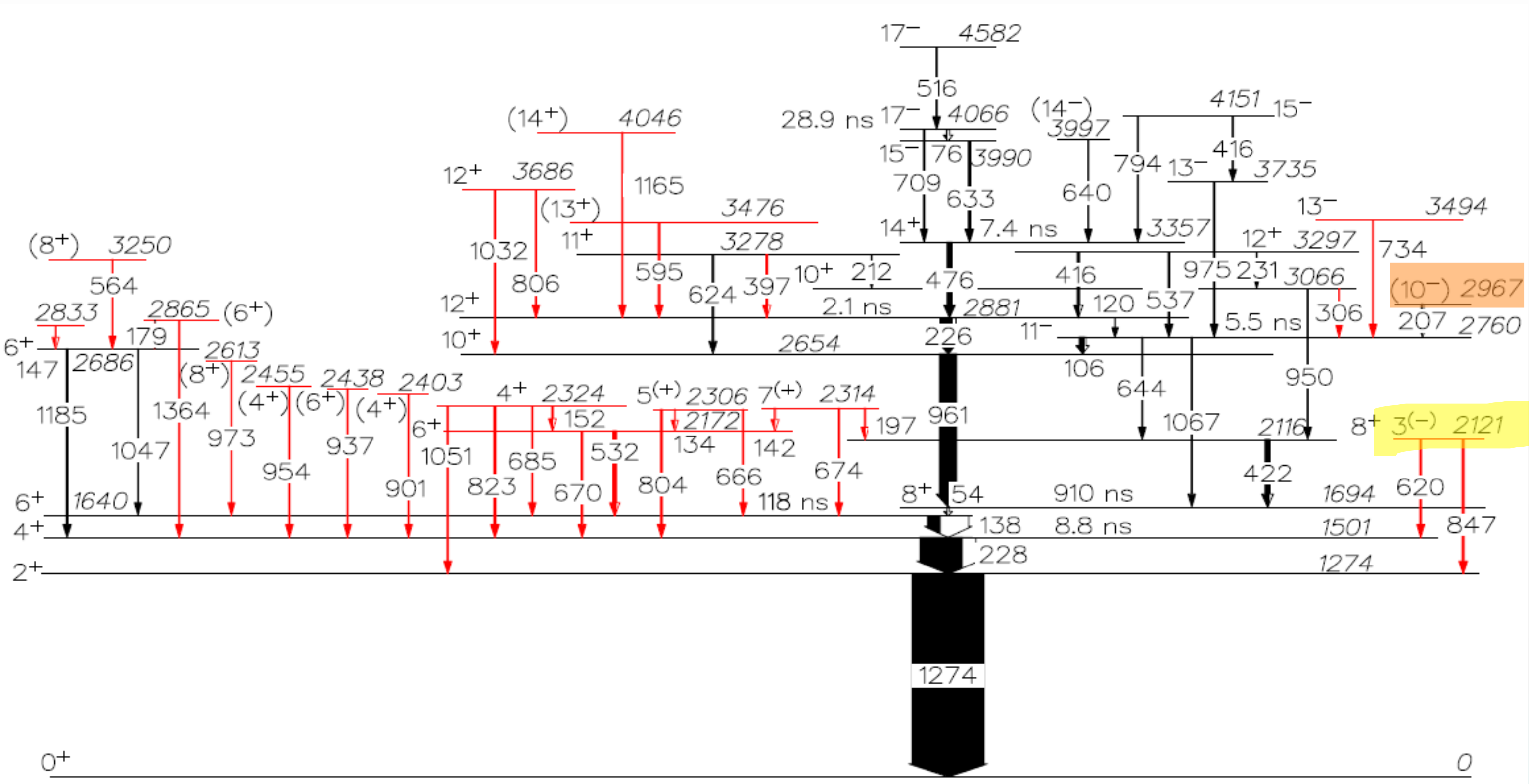

A $3^{(-)}$collective state is also proposed at 2121 keV, which is most likely formed by **mixing the octupole vibration** with the 3_-member of the $\pi h^3_{9/2}i_{13/2}$ multiplet.

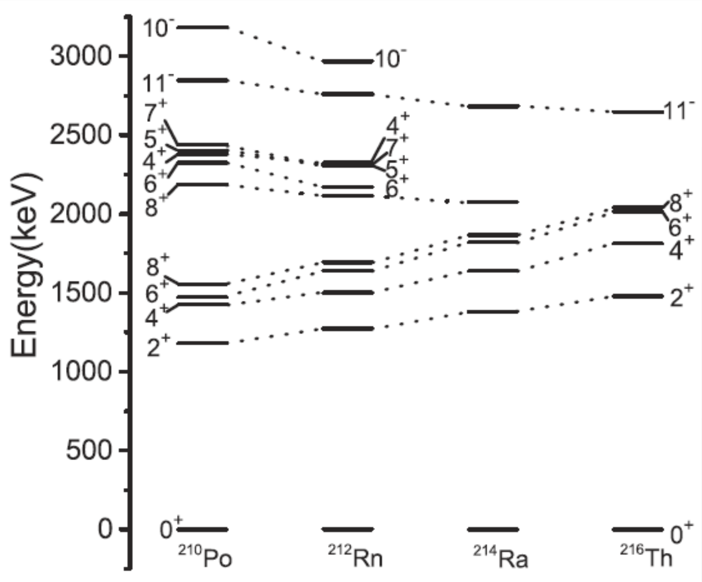

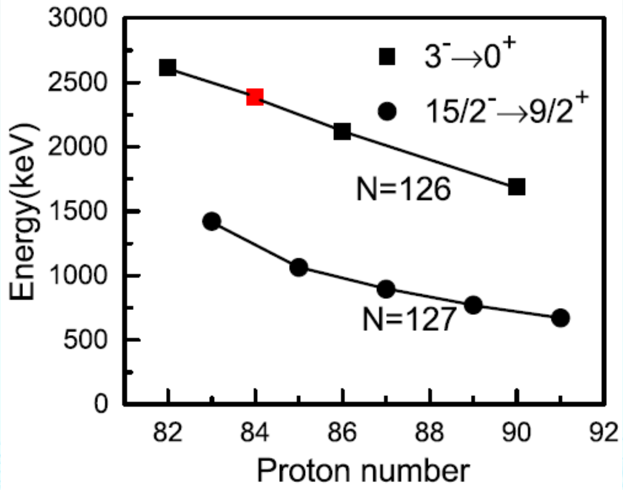

The excitation energy of 3⁻ in ^{212}Rn nicely accord with almost linearity decrease in energy when adding proton pairs similar to the case for N = 127 isotones. However, the calculations of present shell model locate the levels of the $\pi h^3_{9/2}i13/2$ 3⁻ proton multiplet at about 0.8 MeV above the corresponding possible level. **This is more likely the result of some involved mixing the octupole vibration** as in neighboring N = 126 ^{210}Po, ^{214}Ra, and ^{216}Th isotones

The spin-parity assignment for the 2967 keV state, which was tentatively assigned as 12⁺, is instead suggested to be (10⁻). The 2_1^+, 4_1^+, 6_1^+, and 8_1^+ states indicate a steady increase energy as proton number increases, while energies for 8_2^+ and 11_1^- states are observed to decrease gradually. **These evolutional tracks could be analyzed in terms of a pairing approach.**

总结

- ✓ Fusion by induced ^{6}Li on ^{12}C, ^{94,96}Zr, ^{209}Bi targets have been studied. The results have been published and the preliminary results have been obtained. The CF suppression have been observed. **The breakup triggered by transfer plays a main role.**
- ✓ A powerful combination of gamma and light charged particles can **distinguish the various reaction channels and separate the different reaction processes** including CF, ICF and transfer.
- ✓ **The new energy levels** for many nuclei including ^{91,92}Mo, ^{92,93}Nb, ^{89}Zr and ^{212}Rn are obtained. The information of gamma angular distribution can be extracted. The nuclear structure can be studied.

Not only explore the reaction dynamics of weakly bound nuclei at low energies, but also study the nuclear structure!!!

Thank you for your attention